TRAJECTORY TRACKING FOR A PLANAR REDUNDANT MANIPULATOR THROUGH OPTIMAL CONTROL FORMULATION

by

ANIRVAN DASGUPTA

DEPARTMENT OF MECHANICAL ENGINEERING

INDIAN INSTITUTE OF TECHNOLOGY, KANPUR

July, 1993

TRAJECTORY TRACKING FOR A PLANAR REDUNDANT MANIPULATOR THROUGH OPTIMAL CONTROL FORMULATION

A Thesis Submitted

in Partial Fulfilment of the Requirements

for the Degree of

MASTER OF TECHNOLOGY

by

ANIRVAN DASGUPTA

to the

DEPARTMENT OF MECHANICAL ENGINEERING

INDIAN INSTITUTE OF TECHNOLOGY KANPUR

JULY, 1993

CERTIFICATE

This is to certify that the present work titled *TRAJECTORY TRACKING FOR A PLANAR REDUNDANT MANIPULATOR THROUGH OPTIMAL CONTROL FORMULATION* by Mr. Anirvan DasGupta has been carried out under my supervision and that, it has not been submitted elsewhere for a degree.

Dr. Himanshu Hatwal

Professor

Department of Mechanical Engineering

Indian Institute of Technology, Kanpur

Dedicated to

MY PARENTS

ACKNOWLEDGEMENTS

It is my proud priviledge to express my deep sense of gratitude towards my guide, Dr. Himanshu Hatwal, for suggesting this work as well as for his helpful guidance throughout the course of the work. It has been a very educative experience for me to work under him. I am also grateful to him for introducing me to the area of Optimal Control through this work.

I dedicate this thesis to my parents who have given me constant encouragement and supported me in every way throughout my stay at IIT Kanpur.

The helpful suggestions provided by Mr. Soumya Bhattacharya and Mr. Samiran Mandal in this work are gratefully acknowledged. I am also thankful to my all friends, in particular, Surjya Pal, Rajeev Dubey, Ravindra Telang, Manjunath Hegde, Shaligram Tiwari, Arun Garg, Parag Kumar, Y.P. Singh and Shreekant Sharma, who provided me a wonderful company and made my stay at IIT Kanpur a memorable one.

The access to the facilities at the Centre for Robotics has helped me a lot in the preparation of this thesis. I am also grateful to Dr. Gautam Biswas and Mr. Prabodh Maji who provided me the facilities at the Computational Fluid Dynamics Laboratory to prepare the thesis in it's final form.

IIT Kanpur — Anirvan DasGupta

July, 1993

CONTENTS

NOMENCLATURE

e	End-effector trajectory error
k, d	Constraint stiffness and damping
l_i	Length of the i^{th} link of manipulator
m_i, I_i	Mass and moment of inertia of the i^{th} link of manipulator
${}^0r_i$, ${}^0v_i$	Position and velocity vectors of i^{th} link with respect to the world coordinate system
t_f	Time of travel
q	Joint variable vector
q_{lim}	Joint angle limit vector
q′	Joint velocity vector
q″	Joint acceleration vector
u	Joint torque vector
x	State vector
y	End-effector position vector
y_d	Desired end-effector position vector
A, B	System matrices in the linearized state space equations
C(q, q′)	Coriolis and centrepetal force vector
F(q′)	Frictional torque vector
J	Performance index
J, J^+	Jacobian matrix and it's pseudo-inverse

K	Kinetic energy of a system
[M(q)]	Inertia matrix of manipulator
P	Potential energy of a system
Q, Q_f, R, W	Positive definite weighting matrices
${}^{j}T_{i}$	Coordinate transformation matrix from i^{th} to j^{th} frame
θ_i	Joint variable of the i^{th} joint
θ'_i	Joint velocity of the i^{th} joint
θ''_i	Joint acceleration of the i^{th} joint
ρ_i	Position of centre of gravity of the i^{th} link of manipulator
τ_i	Joint torque at the i^{th} Joint

LIST OF FIGURES

ABSTRACT

Kinematic redundancy in robot manipulators has been found to be an advantageous feature from application point of view. Redundant manipulators are versatile and offer a broad spectrum of applicability. They posses useful features like dexterity, ability to avoid obstacles etc.. Presence of redundancy, however, complicates the control problem which is a major issue of research in this area.

This work addresses the problem of control of redundant manipulators in tracking a specified end-effector trajectory. The objective is to determine the joint torques required to track a desired trajectory. A case of a three-link planar manipulator has been considered for the present study.

The problem has been formulated as a fixed time Optimal Tracking Problem with fixed initial states and free terminal states. The redundancy is resolved by minimizing an integral performance index which has been constructed using the weighted norms of the tracking error and the joint torques. The dynamics of the manipulator has been used as the equations of constraint. The optimality conditions, as obtained from the Variational Principle, are used, which leads to a Non-Linear Two Point Boundary Value Problem (NLTPBVP). An iterative numerical algorithm has been used to solve the NLTPBVP.

The efficacy of the scheme has been investigated by considering different performance criteria. The results of the simulations for various examples have been presented and discussed.

CHAPTER 1

INTRODUCTION

1.1 INTRODUCTION

One of the fundamental requirements of a general purpose manipulator is versatility in operation. This in turn implies dexterity and a broad spectrum of applicability of the manipulator. In other words the manipulator should be able to perform a variety of tasks. Introdution of *kinematic redundancy* in a manipulator has been found to be a very useful solution to meet such requirements. This follows from a close observation of the human arm which has a high degree of dexterity and verssatility due to the redundancy it possesses. Kinematic redundancy not only increases the versatility of the manipulator arm but also renders it with certain useful properties which are discussed in this chapter.

A robot manipulator is said to posses *kinematic redundancy* if it has more degrees-of-freedom than is required for performing a specified task. Redundancy, in a more general sense, is defined relative to a particular task. For example, In the three dimensional cartesian space, the general motion of the end-effector is specified by six independent quantities, three for positioning and three for orienting. A spatial manipulator having

more than six degrees-of-freedom is said to posses kinematic redundancy. Likewise, for a three degrees-of-freedom planar manipulator, the position and orientation of the end-effector is specified completely by three independent coordinates. If on the other hand, the task of the manipulator is specified in terms of the position of the end-effector alone, without any reference to its orientation, then, relative to such a task , the manipulator is redundant.

There are many interesting features of redundant manipulators. Detailed analyses presented in the next chapter indicate that infinite sets of joint trajectories can produce the same end-effector trajectory. Redundancy thus offers a tremendous flexibility in selection of a joint trajectory for a specified end-effector trajectory which can be utilized tactfully to satisfy a number of other requirements. This property brings in versatility in operation which is advantageous in a numerous applications. Some of the possible advantages of redundant manipulators are

1. Potential to avoid singular configurations.
2. Ability to avoid obstacles.
3. Ability to negotiate curvatures to reach to a location which are otherwise inaccessible.
4. Ability to avoid structural limitations.
5. Scope for configuration or posture control.

Moreover, redundant manipulators are more reliable in the sense that they can perform certain tasks even in case of joint failures. This is particularly useful in case of deep sea and space applications.

However this richness in the choice of joint trajectories complicates the control problem considerably which has motivated many researchers to propose various algorithms to resolve the problem.

1.2 LITERATURE REVIEW

The significance of redundancy was first pointed out by Whitney [1969, 1972]. He proposed the principle of resolved motion rate control in which the end-effector velocities are related to the joint velocities using the Jacobian matrix. The required instantantaneous joint velocities for a given end-effector velocity can be determined by inverting the Jacobian matrix. For rectangular Jacobian matrix as in the case of redundant manipulators, Whitney proposed to minimize a quadratic function of the instantaneous joint velocities at every knot point on a given Cartesian space trajectory. The solution turned out to be the weighted pseudo-inverse of the full rank Jacobian matrix of the manipulator.

Liegeois [1977] was the first to discuss the active utilization of redundancy of robot manipulators. He used the

generalized inverse of the Jacobian matrix. He proposed the minimization of a scalar function by projecting it's gradient onto the null space of the Jacobian matrix. Using numerical simulation, he demonstrated one such potential function to keep the joint angles within physical limits.

A comprehensive review of the pseudo-inverse approach to control of redundant manipulators had been presented by Klein and Huang [1983]. They had pointed out some problems such as drift in the joint space trajectory with pseudo-inverse control. Drift results in non-conservative joint trajectories i.e., closed trajectories in the cartesian space does not result in closed joint space trajectories. They had demonstrated this effect using a four degrees of freedom planar manipulator tracking a square end-effector trajectory.

Baillieul [1985] proposed an *Extended Jacobian Method* for solving the redundancy problem which optimizes a scalar function. His method requires the initial configuration of the robot to be such that the scalar function assumes an optimal value at the initial point. He also pointed out that using the pseudo-inverse control, the global optimal solution is not guaranteed.

Certain special configurations of a manipulator where the rank of the Jacobian matrix is less than the full rank are termed as *Singular configurations*. In the case of redundant manipulators, the redundancy can be utilized to avoid the singularities. Yoshikawa [1985(a), 1985(b), 1990] defined the manipulability

measure which quantitatively describes the distance of a manipulator configuration from a singular configuration. He proposed to use the generalized inverse of the Jacobian matrix in such a way that a scalar function, defined as the manipulability measure, is maximized as the manipulator moves, thereby avoiding singular configurations.

Local minimization of actuator torques in a least square sense by resolving redundancy at joint acceleration level was proposed by Hollerbach and Suh [1985]. Their scheme exhibited unexpected instability for relatively long cartesian space trajectories.

Maciejewski and Klein [1985] presented an approach to determine the required joint angle rates for a manipulator under constraints of multiple goals. The primary goal was to track a specified end-effector trajectory and the secondary goal, to avoid obstacles. The primary goal was satisfied exactly by the particular solution of the pseudo-inverse of the Jacobian matrix. The homogeneous component of the solution maximized the distance of the manipulator from the obstacles. The implemention was fast enough to work efficiently in a dynamically changing environment. This was similar to the task priority based approach of Hanafusa et al [1987].

The concept of task priority was introduced by Hanafusa et al [1987] into general redundancy control problem. It requires the desired task to be broken up into sub-tasks of different

priorities and the sub-tasks with lower priorities are realized using the redundancies not committed to satisfy the sub-tasks with higher priorities.

Kazerounian and Nedungadi [1987] developed an algorithm to locally minimize the driving torques by resolving redundancy at the joint velocity level. This resulted in high joint acceleration and hence high torques leading to instability. They concluded that there has to be a trade-off between joint driving force optimization and algorithm stability.

Dubey and Luh [1987] suggested the *Manipulator Velocity Ratio* (MVR) as a measure of manipulability. It is defined as the ratio of the norm of end-effector velocity and norm of joint velocity. For redundant manipulators, MVR is not unique for the simple reason that given the end-effector velocity, the joint velocity is not unique. They had proposed a control algorithm which progressively maximized the minor axis of the *Manipulator Velocity Ratio Ellipsoid* (MVRE) which represents the minimum value of the MVR, as the manipulator moves. This ensured uniform manipulability in all directions and hence avoided singular configurations.

Anderson and Angeles [1989] used a constrained non-linear least-square minimization approach in which a positive definite performance index was minimized subjected to the kinematic constraint equations. The resulting non-linear problem was solved as a sequence of linear quadratic problems. The algorithm resulted

in conservative joint motions.

Dubey et al [1988,1991] proposed a gradient projection optimization scheme in the framework of the resolved motion rate control. Their scheme did not require the calculation of the pseudo-inverse of the Jacobian matrix but otherwise similar to that used by Liegeois [1977].

In all the research works cited above, the redundancy resolution was based upon a local optimization of some performance criterion or objective function while carrying out a task. Most of them proposed to use the generalized inverse of the full rank Jacobian matrix, the range space of which is used to track a specified cartesian space trajectory and the null space to carry out the secondary sub-task such as avoidance of collision, obstacles, singularity and joint limits. Though computationally fast and well suited for on-line implementation, these schemes have drawbacks some of which are listed below.

1. They may not result in the "best" joint space trajectory for complete manipulator motion. In other words, they do not guarantee a globally optimal solution.

2. Closed trajectories in cartesian space may not result in closed trajectories in joint space, i.e. non-conservative joint space trajectories may result, which is undesirable in case of repetitive and cyclic tasks.

3. Singularity avoidance in a strict sense may not be achieved by locally maximizing the manipulability measure

(Baillieul [1985]). Moreover, in using certain methods (Yoshikawa [1985(a), 1985(b), 1990]), the manipulability in certain directions may reduce drastically.

4. Local optimization schemes may result in some instabilities as has been observed, for example, by Hollerbach and Suh [1985, 1987(a)] and Kazerounian and Nedungadi [1987].

There is yet another class of research which addresses the redundancy resolution problem and proposes to optimize a performance measure in a global sense, that is, over the entire trajectory of the end-effector.

Whitney [1971] suggested minimization of a global criterion which was in the form of minimization of the kinetic energy of the manipulator over the whole trajectory. He did not propose any computational method.

Nakamura and Hanafusa [1987] solved the global optimal redundancy resolution problem by using the Pontryagin's Maximum Principle. The problem is reduced to a two point boundary value problem (TPBVP) and the solution is obtained by a minimal value search.

Hollerbach and Suh [1987(b)] investigated and compared the local and global optimization schemes for minimizing the torque loading at the joints of a redundant manipulator in a least square sense by resolving the redundancy at joint acceleration level. They observed that local optimization methods may show an unexpected instability for relatively long trajectories for which

global optimization methods always converged.

Kazerounian and Wang [1988] used the Calculus of Variation to solve the problem of redundancy resolution by minimizing the square of the norm of joint velocities over the whole trajectory. They also proved that local minimization of joint accelerations result in a global minimization of the joint velocities.

Sheraji [1989] proposed a configuration control scheme for redundant manipulators over the entire end-effector motion. In his method some kinematic functions in the form of constraints are introduced to reflect the additional task to be performed due to redundancy. The scheme ensured cyclic motion of the manipulator. Based on the *Model Reference Adaptive Control* (MRAC) approach, the algorithm neither requires the complex dynamic model of the manipulator nor the Jacobian matrix inversion. It was found to be computationally fast and suitable for real time implementation.

Martin et al [1989] solved the redundancy control problem by minimizing an integral performance index subject to path constraints in the cartesian space using the Lagrangian approach. The algorithm resulted in conservative trajectories in the joint space for cyclic paths in the catesian space.

More recently Gupta and Luh [1991] proposed a closed loop state feedback motion control scheme for redundant manipulators based on Hamilton-Jacobi-Bellman equation. They defined a quadratic performance criterion which was minimized over the entire trajectory with redundancy being resolved at the joint

acceleration level. The algorithm used the linearized equations of dynamics of the manipulator.

A unified approach to the inverse kinematics solution for redundant manipulators was put forward by Won et al [1993]. They proposed to resolve the redundancy at the joint velocity level irrespective of the performance index chosen. They had demonstrated the validity of their approach by applying it to a three link planar manipulator for various types of performance indices.

1.3 OBJECTIVE AND SCOPE OF THE PRESENT WORK

This work adresses the the problem of tracking a specified end-effector trajectory by a redundant manipuator. The objective of the problem is to determine the required joint torques, considering the dynamics of the manipulator, at all the points over the trajectory in order to track the specified trajectory by the end-effector.

At the most basic level researchers have proposed redundancy resolution methods involving optimized solution of the inverse kinematics problem. All the local and most of the global optimization schemes require the generalized inverse of the full rank Jacobian matrix. Near the singular configurations the Jacobian matrix inversion results in undesirably high joint rates. Moreover dynamics of the manipulator has not been considered in the optimization process by most of the researchers. This might

lead to very high joint torques near the singular configurations.

This work attempts to solve the redundancy control problem following the optimal control approach. The primary objective has been to solve the global optimal control problem and at the same time eliminate the need to resolve redundancy at velocity or acceleration level. This obviates the inversion of the Jacobian matrix thereby avoiding the instability problem due to singularities. The equations of dynamics of the manipulator have been taken into consideration in the optimization process by using them as equations of constraint.

The problem formulation, as has been described later, is very similar to the formulation in the recently reported work by Gupta and Luh [1991] although the solution procedure is different. The present formulation, based on the *Linear Quadratic Problem*, is known as the *Optimal Tracking Problem*. An integral performance index has been defined which involves the tracking error and the joint torques over the entire range of motion of the manipulator. The equations of motion of the manipulator have been considered as the constraint equations. The problem is solved using the Variational Principle which results in a *Non-Linear Two Point Boundary Value Problem* (NLTPBVP). Analytical solution of such a problem is very difficult and calls for numerical solution.

A family of algorithms for solving continuous-time unconstrained non-linear optimal control problems have been proposed by Nedeljkovic [1981]. One of the algorithms has been

found suitable for solving the problem in hand.

The algorithm has been used to study some aspects of redundancy control through optimization. Different forms of performance indices have been constructed, the results analysed and presented. Through the various simulations, a comprehensive understanding of the global optimization approach to redundancy resolution has been sought. Further some of the results have been compared with the solutions obtained using the pseudo-inverse of the Jacobian matrix.

The scope of the present work has been limited to the fixed time optimal control problem. The study has been done for a three degrees-of-freedom planar redundant manipulator and the algorithm has been tested through numerical simulations.

1.4 ORGANIZATION OF THE THESIS

This thesis has been organized into five chapters. The second chapter deals with the analysis of redundant manipulators from the kinematics view-point. The optimal control formulation of the trajectory tracking problem and an iterative numerical solution scheme are presented in chapter three. In chapter four, numerical results for various examples considered have been presented and discussed to highlight some of the aspects of the trajectory tracking problem. The final chapter concludes the present work and suggests scope of future work.

CHAPTER 2

KINEMATICS OF REDUNDANT MANIPULATORS

2.1 INTRODUCTION

Redundant manipulators have a number of advantages over the non-redundant ones. Some of the interesting and advantageous features have been described in the previous chapter. Such special features can be explained on the basis of the kinematics of redundant manipulators. This chapter deals with the basic theory of redundant manipulators from the kinematics view-point. The problem of forward and inverse kinematics of redundant manipulators has been discussed in the second section. Some of the implications of redundancy have been pointed out. In this work, a three degrees-of-freedom planar manipulator has been considered for the study and the equations of kinematics and the motion rate equations of the manipulator have been presented in the third section of the chapter.

2.2 FORWARD AND INVERSE KINEMATICS RELATIONS

The problem of forward kinematics in robotics is concerned with determination of the position and orientation of the end effector of the manipulator in terms of the joint variables. On the contrary, the inverse kinematics problem is concerned with

solving the joint variables when the position and orientation of the end-effector are specified.

2.2.1 The Forward Kinematics Equations

Consider an m degree-of-freedom robot, as shown in Fig. 2.1, having m joint variables as q_1, q_2 . . . q_m. These joint variables can be represented in vector notation as

$$q = [q_1 \quad q_2 \ldots q_m]^T$$

where,

q_i represents the joint variable corresponding to the i^{th} joint.

Let the position and orientation of the end-effector coordinate frame, $O_E X_E Y_E Z_E$, be specified completely by p independent quantities expressed in the World Coordinate System (WCS). Let these variables be represented in the vector notation as

$$y = [y_1 \quad y_2 \ldots y_p]^T$$

where,

y_i is along the i^{th} coordinate direction.

The value of p represents the minimum number of independent quantities required to completely specify a rigid body in the WCS. For example, for a general two-dimensional planar motion, p = 3 as

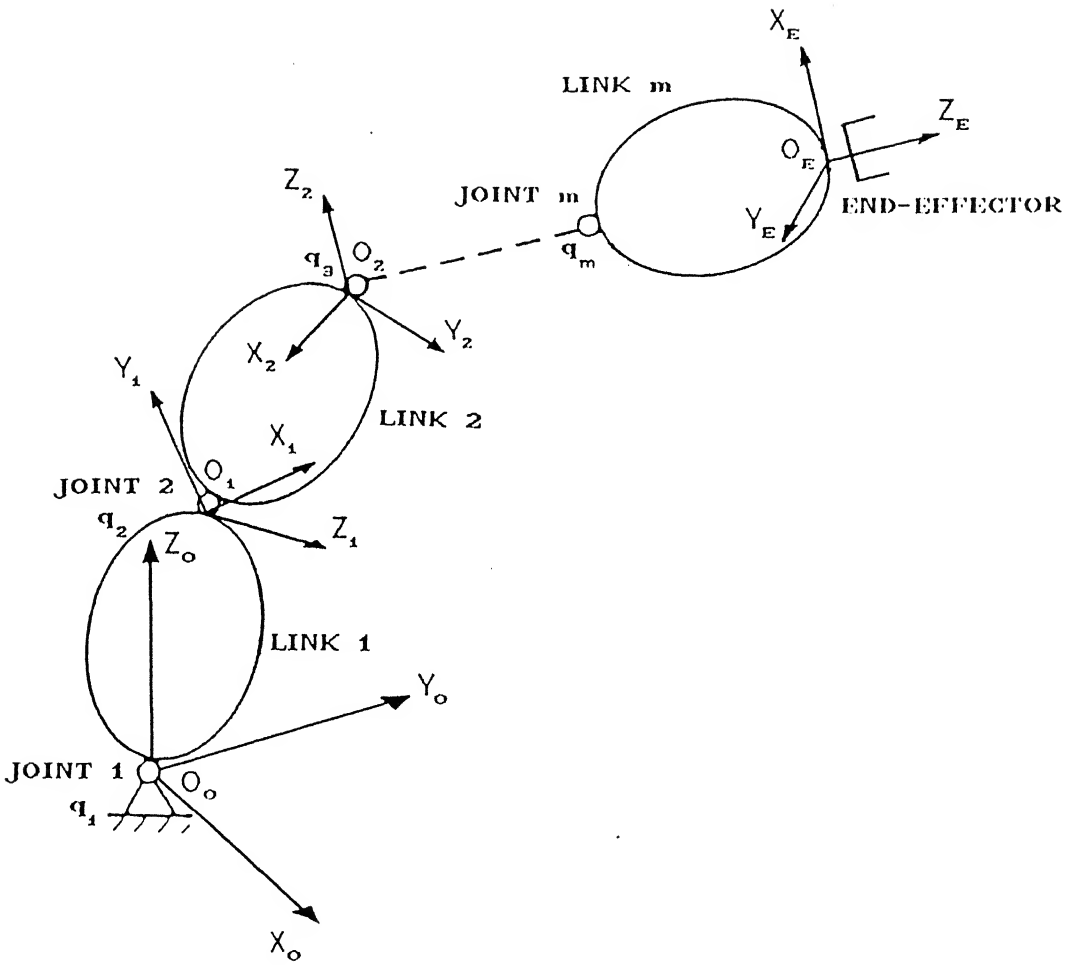

G. 2.1 REPRESENTATION OF A GENERAL m DEGREE-OF-FREEDOM MANIPULATOR

two translational and one rotational coordinates completely specify the rigid body in a plane. Likewise, for a general three-dimensional motion, $p = 6$, since three position and three orientation coordinates completely specify the rigid body as in the case of $O_E X_E Y_E Z_E$ in Fig. 2.1. Each of these p quantities can be expressed as functions of the joint variables. These functions, which are in general non-linear, can be derived purely from geometry and represented in the form

$$\begin{aligned} y_1 &= f_1(q_1, q_2, \ldots q_m) \\ y_1 &= f_2(q_1, q_2, \ldots q_m) \\ &\ldots \\ y_p &= f_p(q_1, q_2, \ldots q_m), \end{aligned} \qquad (2.1(a))$$

or in a more compact form as

$$y = f(q) \qquad (2.1(b))$$

where,

$$f(\cdot) = [f_1(\cdot) \quad f_2(\cdot) \ldots f_p(\cdot)]^T.$$

2.2.2 The Inverse Kinematics Equations

Determination of the joint variables required to attain a specified position and orientation of the end-effector is the problem of inverse kinematics. In other words, given the end-effector position vector y, the problem is to determine the

joint variable vector **q** by solving (2.1). The complicacy of the problem is primarily due to the non-linearities involved in the kinematics relations described above. Another point which needs to be investigated is the solvability in terms of the number of equations and number of unknowns involved.

Consider the system of equations (2.1). In certain situations it may so happen that only n of the p quantities at the end-effector are of significance. Then depending on the values of m, p and n, the manipulator may be termed as redundant or non-redundant as discussed below.

(*i*) *Non-Redundant Case* : If, $m = n = p$, then there are m equations in m unknowns which may be solved for a unique or at most a finite set of solutions of **q** and the robot is said to be non-redundant.

(*ii*) *Redundant Case* : If, ($m = p$, $n < p$) or ($m > p$, $n = p$), the number of unknowns involved are more than the number of equations. An infinite number of solution sets of **q** are possible and the robot is said to posses ($m - n$) or ($m - p$) redundant degrees-of-freedom as the case might be. When ($m = p$, $n < p$), the presence of redundancy is decided by the task the manipulator performs, while in the situation when ($m > p$, $n = p$), the manipulator is redundant irrespective of the task specified.

An end-effector trajectory can be considered as a finite set of points in an n-dimensional real space while a joint trajectory can be considered as finite set of points in an m-dimensional real

space. These points are known as *knot points*. For redundant manipulators, at every knot point in the cartesian space, there exists infinite solutions of the joint variables as the number of unknowns are more than the number of equations. Thus for a redundant manipulator, infinitely many sets of trajectories can exist in the joint space which results in the same end-effector trajectory. This is the most important feature of a redundant manipulator and to exploit it meaningfully has been the subject of research in this area.

2.2.3 Inverse Kinematics of Redundant Manipulators Using Motion Rate Equations

In order to perform a task, a definite solution of the joint variables of the manipulator has to be chosen out of the infinite sets of solutions as mentioned above. The choice of the inverse solution is made either by introduction of secondary tasks to be carried out or by imposing a performance criteria to be satisfied. For example, minimization of the weighted norm of the joint velocities is a possible guideline for the selection of a joint space trajectory as suggested by Whitney [1969, 1972].

The motion rate equations of the manipulator are written by differentiating (2.1) once with respect to time as

$$\mathbf{y}' = \mathbf{J}\,\mathbf{q}' \tag{2.2}$$

where,

$y' = \frac{dy}{dt}$ is a vector of size $n \times 1$,

$q' = \frac{dq}{dt}$ is a vector of size $m \times 1$ and

$J = \frac{\partial f(q)}{\partial q}$ is the Jacobian matrix of the manipulator of size $n \times m$ and $n < m$.

The optimization problem is then formulated as

$$\text{Minimize } (q'^T W q')$$

subject to

$$x' = J q',$$

where,

W is the weight matrix on the joint velocities.

This is a simple constrained optimization problem. The solution obtained from this minimization procedure is represented as q'_1 and is of the form (see Appendix A)

$$q'_1 = J^+ x' \qquad (2.3(a))$$

where,

$J^+ = W^{-1}J^T (J W^{-1}J^T)$ is known as the weighted pseudo-inverse of J.

The solution for joint velocity vector q'_1 obtained from (2.3(a)) is known as the *range space* solution of J. The Jacobian, being a recangular matrix, has yet another solution, the *null*

space solutionas given by (Yoshikawa [1985])

$$q_2' = (I - J^T J)\ k \qquad (2.3(b))$$

where,

q_2' is the null space solution of J,

I is an $m \times m$ identity matrix and

k is an $m \times 1$ arbitrary non-zero vector.

Hence the total solution is given by

$$q' = J^+ x' + (I - J^T J)\ k \qquad (2.4)$$

The joint velocity solution q_1', as given by (2.3(a)), produces the desired end-effector motion, while, q_2', as obtained from (2.3(b)), only contributes to change the arm configuration which might be required for secondary tasks to be performed. There are infinite solutions of q_2' depending on the form of k chosen in (2.3(b)). The choice of k is made on the basis of the secondary task to be carried out.

Since the Jacobian is a function of the joint variables q, there may exist one or more q such that the Jacobian is not of full rank, i.e., Rank (J) $< n$. The configurations corresponding to such values of the joint variables are termed as the *singular configurations* and the corresponding end-effector positions are the *singular points* of the workspace. If the Jacobian matrix is

not of full rank, i.e. at the singular points, the solution of $\dot{q}$ as given by (2.4) does not exist. In the neighbourhood of the singular points, the solution results in impracticably high joint velocities.

2.3 CASE OF A PLANAR THREE-LINK REDUNDANT MANIPULATOR

In this section the special case of a planar three link manipulator with revolute joints. The equations of kinematics and the motion rate equations are also derived.

2.3.1 Forward Kinematic Relations

Consider a three-link planar manipulator with revolute joints, as shown in Fig. 3.1(a). The joint variable vector q, in this case, is defined as

$$q = [\ \theta_1 \quad \theta_2 \quad \theta_3]^T$$

where,

θ_i is the i^{th} joint variable.

The end-effector position is specified by y_1 and y_2, which represent the position coordinates along the X_0 and Y_0 directions of the WCS as was shown in Fig. 3.1(a). The orientation of the end-effector is not considered as a task variable and thus the end-effector is specified by only two variables namely y_1 and y_2 which can be expressed in terms of the joint variables, using

geometry, as

$$y_1 = l_1 \cos \theta_1 + l_2 \cos \theta_{12} + l_3 \cos \theta_{123} \qquad (2.5(a))$$

$$y_2 = l_1 \sin \theta_1 + l_2 \sin \theta_{12} + l_3 \sin \theta_{123} \qquad (2.5(b))$$

where,

l_1, l_2, l_3 are the link lengths and

$\theta_{1\ldots n} = \theta_1 + \theta_2 + \ldots + \theta_n$.

The end-effector of this manipulator is required to trace a planar trajectory. At every point of the trajectory, the coordinate values of the point O_3 is specified with respect to the world coordinate system in terms of y_1 and y_2 without any reference to the orientation of the end-effector coordinate axes. The end-effector position vector y is then represented as

$$y = [y_1 \quad y_2]^T$$

In order to determine the joint motions that result in the specified end-effector trajectory, the equations (2.5(a)) and (2.5(b)) have to be solved simultaneously. There are only two equations involving three unknowns namely θ_1, θ_2 and θ_3 and thus there is one redundant degree-of-freedom in the manipulator

2.3.2 Motion Rate Equations

The motion rate equations of the manipulator can be written by differentiating the equations (2.5(a)) and (2.5(b)) as

$$y'_1 = - l_1 \theta'_1 \sin\theta_1 - l_2 \theta'_{12} \sin\theta_{12} - l_3 \theta'_{123} \sin\theta_{123}$$
$$y'_2 = l_1 \theta'_1 \cos\theta_1 + l_2 \theta'_{12} \cos\theta_{12} + l_3 \theta'_{123} \cos\theta_{123}$$

(2.6(a))

or in a more compact form as

$$y' = J\, q' \qquad (2.6(b))$$

where,

$$J = \begin{bmatrix} -l_1\sin\theta_1 - l_2\sin\theta_{12} - l_3\sin\theta_{123} & l_1\cos\theta_1 + l_2\cos\theta_{12} + l_3\cos\theta_{123} \\ -l_2\sin\theta_{12} - l_3\sin\theta_{123} & l_2\cos\theta_{12} + l_3\cos\theta_{123} \\ -l_3\sin\theta_{123} & l_3\cos\theta_{123} \end{bmatrix}^T$$

(2.7)

is the Jacobian matrix of the manipulator ,

$y' = [y'_1 \quad y'_2]^T$ is the end-effector velocity vector and

$q' = [\theta'_1 \quad \theta'_2 \quad \theta'_3]^T$ is the joint rate vector.

CHAPTER 3

OPTIMAL CONTROL FORMULATION FOR PATH TRACKING

3.1 INTRODUCTION

This chapter deals with the trajectory tracking problem considering the dynamic model of the manipulator. In the second section, the equations of dynamics for the three-link planar manipulator, considered in this study, have been presented. The third section addresses some issues related to the trajectory tracking problem. In the fourth section, the trajectory tracking problem has been posed as a fixed time *Optimal Tracking Problem* with fixed initial states and free terminal states for the three-link planar redundant manipulator. An integral performance index has been defined which is required to be minimized over the trajectory, subject to constraints in the form of the equations of motion of the manipulator. Using the Variational Principle, the problem reduces to a non-linear TPBVP which is very difficult to solve in closed form. An iterative numerical scheme used for the solution purpose has been presented in the last section.

3.2 THE DYNAMICS MODEL

In this section the equations of motion for the three-link planar manipulator with revolute joints, shown in the Fig. 3.1(a),

have been presented. The i^{th} coordinate frame, O_i, is fixed to the i^{th} link and positioned at the $(i+1)^{th}$ joint with Z_i along the axis of the joint as shown in Fig. 3.1(a). The manipulator is considered to be in a horizontal plane and hence the gravity forces are not considered. The equations of motion have been derived using the Lagrange-Euler formulation.

3.2.1 Lagrange-Euler Formulation

The Lagrange-Euler equation of motion is of the form (Fu, Gonzalez and Lee [1987])

$$\frac{d}{dt}\left(\frac{\partial \mathcal{L}}{\partial \dot{q}_i}\right) - \frac{\partial \mathcal{L}}{\partial q_i} = \tau_i \qquad i = 1, 2, 3. \tag{3.1}$$

where,

$\mathcal{L} = K - P$ is the Lagrangian of the system,

K, P represent the total kinetic energy and potential energy of the system respectively,

q_i is the i^{th} generalized coordinate describing the system state and

τ_i is the i^{th} generalized force along the respective coordinate direction.

Consider a differential mass dm_i on the i^{th} link as shown in Fig. 3.1(b). The kinetic energy, dK_i, due to this mass can be expressed as

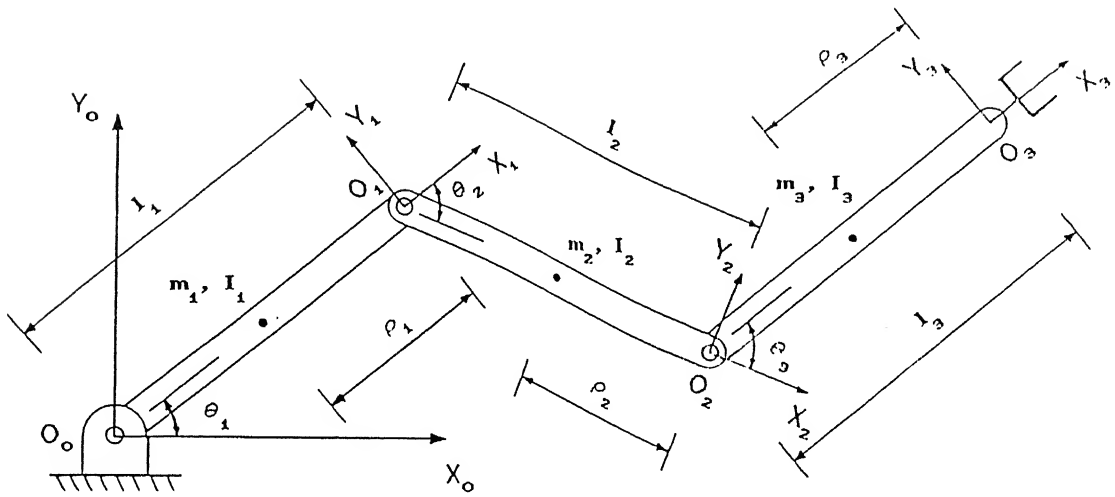

FIG. 3.1(a) REPRESENTATION OF A THREE-LINK PLANAR MANIPULATOR

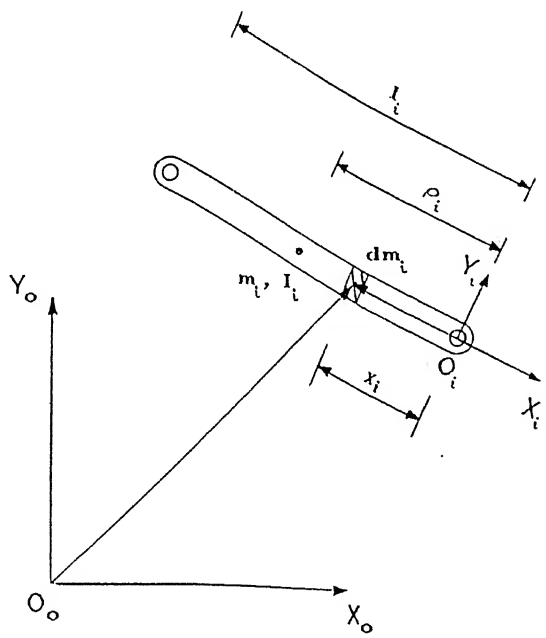

FIG. 3.1(b) REPRESENTATION OF THE i^{th} LINK OF THE THREE-LINK PLANAR MANIPULATOR

$$dK_i = \frac{1}{2} \text{Trace} \left({}^0v_i \, {}^0v_i^T \right) dm_i \tag{3.2}$$

where,

${}^0v_i$ is the velocity of the differential mass dm_i expressed in the WCS.

The velocity vector is expressed as

$${}^0v_i = \frac{d}{dt}({}^0r_i) \tag{3.3}$$

where,

${}^0r_i$ is the position vector, in homogeneous coordinates, of the differential mass dm_i expressed in the WCS as shown in Fig. 3.1(b).

Let ${}^ir_i$ be the position vector, in homogeneous coordinates, of the differential mass dm_i, expressed in it's own coordinate frame O_i as

$${}^ir_i = [\, x_i \;\; 0 \;\; 0 \;\; 1 \,]^T \tag{3.4}$$

where,

x_i is the coordinate value along the X_i direction as shown in Fig. 3.1(b).

The position vector ${}^0r_i$ can be represented in terms of ${}^ir_i$ using the *homogeneous transformation* matrix as

$$^{0}r_{i} = {}^{0}T_{i}\ {}^{i}r_{i} \tag{3.5}$$

where,

$^{0}T_{i} = {}^{0}T_{1}\ {}^{1}T_{2} \ldots {}^{i-1}T_{i}$ is the homogeneous transformation matrix relating the i^{th} and the world coordinate frames.

For the planar manipulator in Fig. 3.1(a), the homogeneous transformation matrix relating the i^{th} coordinate frame and the $(i-1)^{th}$ coordinate frame is given by

$$^{i-1}T_{i} = \begin{bmatrix} \cos\theta_i & -\sin\theta_i & 0 & l_i\cos\theta_i \\ \sin\theta_i & \cos\theta_i & 0 & l_i\sin\theta_i \\ 0 & 0 & 1 & 0 \\ 0 & 0 & 0 & 1 \end{bmatrix}$$

where,

l_i is the link length of the i^{th} link and

θ_i is the i^{th} joint variable.

Now from (3.3) and (3.5) one obtains

$$^{0}v_{i} = \frac{d}{dt}({}^{0}T_{i}\ {}^{i}r_{i})$$

$$= \left[\sum_{j=1}^{i} \frac{\partial}{\partial q_j} ({}^0T_i)\ \theta'_j \right]\ {}^i r_i$$

$$= \left[\sum_{j=1}^{i} U_{ij}\ \theta'_j \right]\ {}^i r_i \qquad (3.6)$$

where,

q'_j is the time derivative of the j^{th} joint variable and

$U_{ij} = \frac{\partial}{\partial q_j} ({}^0T_i)$.

Substituting the expression for ${}^0v_i$ from (3.6) in (3.2) and simplifying yields

$$dK_i = \frac{1}{2} \text{ Trace } \left[\sum_{p=1}^{i} \sum_{r=1}^{i} U_{ip} ({}^i r_i\ dm_i\ {}^i r_i^T)\ U_{ir}^T\ \theta'_p\ \theta'_r \right]$$

Hence the total kinetic energy of the link i is obtained by

$$K_i = \int dK_i$$

or, $$K_i = \frac{1}{2} \text{ Trace } \left[\sum_{p=1}^{i} \sum_{r=1}^{i} U_{ip} \left(\int {}^i r_i\ {}^i r_i^T\ dm_i \right)\ U_{ir}^T\ \theta'_p\ \theta'_r \right]$$

$$= \frac{1}{2} \text{ Trace } \left[\sum_{p=1}^{i} \sum_{r=1}^{i} U_{ip}\ I_i\ U_{ir}^T\ \theta'_p\ \theta'_r \right] \qquad (3.7)$$

where,

$$I_i = \int {}^i r_i \; {}^i r_i^T \, dm_i$$

Substituting the expression for ${}^i r_i$ from (3.4) yields

$$I_i = \int \begin{bmatrix} x_i^2 & 0 & 0 & x_i \\ 0 & 0 & 0 & 0 \\ 0 & 0 & 0 & 0 \\ x_i & 0 & 0 & 1 \end{bmatrix} dm_i$$

Using the inertia tensor notation, the above integration reduces to

$$I_i = \begin{bmatrix} I_{zz_i} & 0 & 0 & -m_i \rho_i \\ 0 & 0 & 0 & 0 \\ 0 & 0 & 0 & 0 \\ -m_i \rho_i & 0 & 0 & m_i \end{bmatrix}$$

where,

ρ_i is the position of the center of mass of the i^{th} link expressed in the i^{th} coordinate frame and

I_{zz_i} is the moment of inertia of the link i about the Z_i-axis

Using parallel axis theorem for the moment of inertia, I_{zz_i} can be

expressed as

$$I_{zz_i} = I_i + m_i \rho_i^2$$

where,

I_i is the moment of inertia of link i about the centre of gravity.

The total kinetic energy of the manipulator, with all the links taken togather, can now be written using (3.7) as

$$K = \sum_{i=1}^{3} K_i$$

or, $$K = \frac{1}{2} \text{Trace} \left[\sum_{i=1}^{3} \sum_{p=1}^{i} \sum_{r=1}^{i} U_{ip} I_i U_{ir}^T \theta'_p \theta'_r \right]$$

Expanding the summation, the expression for the total kinetic energy is obtained as

$$\begin{aligned} K = \frac{1}{2} \text{Trace} \Big(& U_{11} I_1 U_{11}^T \theta_1'^2 + U_{21} I_2 U_{21}^T \theta_1'^2 + U_{21} I_2 U_{22}^T \theta'_1 \theta'_2 + \\ & U_{22} I_2 U_{21}^T \theta'_2 \theta'_1 + U_{22} I_2 U_{22}^T \theta_2'^2 + U_{31} I_3 U_{31}^T \theta_1'^2 + \\ & U_{31} I_3 U_{32}^T \theta'_1 \theta'_2 + U_{31} I_3 U_{33}^T \theta'_1 \theta'_3 + U_{32} I_3 U_{31}^T \theta'_2 \theta'_1 + \\ & U_{32} I_3 U_{32}^T \theta_2'^2 + U_{32} I_3 U_{33}^T \theta'_2 \theta'_3 + U_{33} I_3 U_{31}^T \theta'_3 \theta'_1 + \\ & U_{33} I_3 U_{32}^T \theta'_3 \theta'_2 + U_{33} I_3 U_{33}^T \theta_3'^2 \Big) \end{aligned}$$

Substituting the expressions for various terms and simplifying one obtains

$$
\begin{aligned}
K = \; & \frac{1}{2}\Big(I_1 + I_2 + I_3 + m_1(\rho_1^2 - 2l_1\rho_1 + l_1^2) \\
& + m_2(\rho_2^2 - 2l_2\rho_2 + 2l_1\rho_2 C_2 + l_1^2 + l_2^2 + m_3(\rho_3^2 - 2\rho_3 l_3 \\
& - 2l_2\rho_3 C_3 - 2l_1\rho_3 C_{23} + l_3^2 + l_2^2 + l_1^2 + 2l_3 l_2 C_3 + 2l_3 l_1 C_{23} \\
& + 2l_2 l_1 C_2)\Big)\,\theta_1'^2 + \Big(I_2 + m_2(\rho_2 - 2\rho_2 l_2 + 2l_1\bar{\rho}_2 C_2 + l_2^2) \\
& + I_3 + m_3(\rho_3 - 2l_3\rho_3 + l_3^2 + l_2^2 + 2\bar{\rho}_3 l_2 C_3 + \bar{\rho}_3 l_1 C_{23} \\
& + l_1 l_2 C_2)\Big)\,\theta_1'\,\theta_2' + \frac{1}{2}\Big(I_2 + m_2(\rho_2 - l_2\rho_2 + l_2\bar{\rho}_2 C_2) \\
& + I3 + m3(\rho_3 - 2\rho_3 l_3 + l_2 + l_3)\Big)\,\theta_2'^2 + \\
& \Big(I_3 + m_3(-2\rho_3 l_3 + l_3 + l_3 l_2 C_3 + l_3 l_1 C_{23})\Big)\,\theta_1'\,\theta_3' \\
& + \Big(I_3 + m_3(\rho_3^2 - 2\rho_3 l_3 + l_3 l_2 C_3 + l_3^2)\Big)\,\theta_2'\,\theta_3' \\
& + \frac{1}{2}\Big(I_3 - 2m_3\rho_3 l_3 + m_3 l_3\Big)\,\theta_3'^2
\end{aligned}
$$

where,

$$\bar{\rho}_i = l_i - \rho_i.$$

Since the manipulator is considered to be in the horizontal plane, the gravitational potential energy, P, is put to zero.

Substituting the expressions of K and P in (3.1) and simplifying, the equations of motion of the three-link manipulator are expressed as

$$\Big(I_1 + I_2 + I_3 + m_3 l_1 \rho_3 \cos(\theta_{23}) + 2m_3 l_2 \rho_3 \cos(\theta_3) + m_3 \rho_3^2 + m_3 l_1 l_2 \cos(\theta_2) + m_2 l_1 \rho_2 \cos(\theta_2) + m_3 l_2^2 + m_2 \rho_2^2 + m_{23} l_1^2 + m_3 l_2 l_1 \cos(\theta_2) + m_2 \rho_2 l_1 \cos(\theta_2) + m_3 \rho_3 l_1 \cos(\theta_{23}) + m_1 \rho_1^2 \Big) \theta_1'' + \Big(I_2 + I_3 + 2m_3 l_2 \rho_3 \cos(\theta_3) + m_3 \rho_3^2 + m_3 l_2^2 + m_2 \rho_2^2 + m_3 l_2 l_1 \cos(\theta_2) + m_2 \rho_2 l_1 \cos(\theta_2) + m_3 \rho_3 l_1 \cos(\theta_{23}) \Big) \theta_2'' + \Big(I_3 + m_3 \rho_3^2 + m_3 \rho_3 l_2 \cos(\theta_3) + m_3 \rho_3 l_1 \cos(\theta_{23}) \Big) \theta_3'' + \Big(m_3 l_1 \rho_3 \theta_1'^2 \sin(\theta_{23}) + m_3 l_2 l_3 \theta_{12}'^2 \sin(\theta_3) + m_{23} l_1 l_2 \theta_1'^2 \sin(\theta_2) - m_3 \rho_3 l_2 \theta_{123}'^2 \sin(\theta_3) - m_2 l_1 \bar{\rho}_2 \theta_1'^2 \sin(\theta_2) - m_3 l_2 l_1 \theta_{12}'^2 \sin(\theta_2) - m_2 \rho_2 l_1 \theta_{12}'^2 \sin(\theta_2) - m_3 \rho_3 l_1 \theta_{123}'^2 \sin(\theta_{23}) + c_1 \theta_1' \Big) = \tau_1$$

$$\Big(I_2 + I_3 + m_3 l_1 \rho_3' \cos(\theta_{23}) + 2m_3 l_2 \rho_3 \cos(\theta_3) + m_3 \rho_3^2 + m_3 l_1 l_2 \cos(\theta_2) + m_2 l_1 \rho_2 \cos(\theta_2) + m_3 l_2^2 + m_2 \rho_2^2 \Big) \theta_1'' + \Big(I_2 + I_3 + 2m_3 l_2 \rho_3 \cos(\theta_3) + m_3 \rho_3^2 + m_3 l_2^2 + m_2 \rho_2^2 \Big) \theta_2'' + \Big(I_3 + m_3 \rho_3^2 + m_3 \rho_3 l_2 \cos(\theta_3) \Big) \theta_3'' + \Big(m_3 l_1 \rho_3 \theta_1'^2 \sin(\theta_{23}) + m_3 l_2 \rho_3 \theta_{12}'^2 \sin(\theta_3) + m_{23} l_1 l_2 \theta_1'^2 \sin(\theta_2) - m_3 \rho_3 l_2 \theta_{123}'^2 \sin(\theta_3) - m_2 l_1 \bar{\rho}_2 \theta_1'^2 \sin(\theta_2) + c_2 \theta_2' \Big) = \tau_2$$

$$\Big(I_3 + m_3 l_1 \rho_3 \cos(\theta_{23}) + 2m_3 l_2 \rho_3 \cos(\theta_3) + m_3 \rho_3^2 \Big) \theta_1'' + \Big(I_3 + m_3 l_2 \rho_3 \cos(\theta_3) + m_3 \rho_3^2 \Big) \theta_2'' + \Big(I_3 + m_3 \rho_3^2 \Big) \theta_3'' + \Big(m_3 l_1 \rho_3 \theta_1'^2 \sin(\theta_{23}) + m_3 l_2 \rho_3 \theta_{12}'^2 \sin(\theta_3) + c_3 \theta_3' \Big) = \tau_3$$

where,

$$\theta_{1..n} = \theta_1 + \theta_2 + \ldots + \theta_n ,$$

$$\theta_{1..n} = \theta_1 + \theta_2 + \ldots + \theta_n ,$$

$$m_{1..n} = m_1 + m_2 + \ldots + m_n ,$$

$$\theta'_i = \frac{d\theta_i}{dt} ,$$

$$\theta''_i = \frac{d^2\theta_i}{dt^2} ,$$

$$\bar{\rho}_i = l_i - \rho_i ,$$

c_i is the coefficient of viscous friction in the i^{th} joint.

The frictional forces at the joints have been included in the equations of motion above as generalized joint forces and represented by

$$F_i = c_i \theta'_i$$

where,

F_i is the viscous frictional torque on the i^{th} joint.

The above equations of dynamics can be represented in a general form as

$$[M(q)]q'' + C(q,q') + F(q') = u \qquad (3.8)$$

where,

$q = [\ \theta_1 \quad \theta_2 \quad \theta_3\ ]^T$, is the joint variable vector,

$q' = [\ \theta'_1 \quad \theta'_2 \quad \theta'_3\ ]^T$, is the joint velocity vector,

$q'' = [\ \theta''_1 \quad \theta''_2 \quad \theta''_3\ ]^T$, is the joint acceleration vector,

$u = [\ \tau_1 \quad \tau_2 \quad \tau_3\ ]^T$, is the joint torque vector,

$M(q)$ is the inertia matrix of size 3×3,

$C(q,q')$ is the Coriolis and centrepetal force vector of size 3×1 and

$F(q')$ if the friction force vector of size 3×1.

The detailed expressions for the matrix elements are presented in Appendix B.

3.3 TRAJECTORY PLANNING PROBLEM

The trajectory planning problem, for a general manipulator, is concerned with determination of the joint torque vector u, when, the end-effector trajectory is specified. Here, the problem is discussed with reference to redundant manipulators. If, the time of travel, t_f, is also specified, then, any of the following approaches may be adopted as discussed below.

One approach is through motion rate control. The Jacobian of the manipulator is obtained from the motion rate equations which is inverted to obtain the joint rates at each knot point required to track the specified end-effector trajectory. In case of redundant manipulators the pseudo-inverse of the Jacobian is used as was discussed in Sec. 2.2. Once the joint velocities are

obtained, the joint acceleration and joint angle trajectories can be determined using finite difference methods. The inverse dynamics equations are then used to calculate the required joint torques.

The motion rate control is a local optimization scheme in the sense that it resolves the redundancy by minimizing the norm of the joint velocities locally at each knot point. There is another approach in which a global performance criterion in the form of an integral performance index is minimized. The problem can be posed as an Optimal Tracking Problem based on the Linear Quadratic Problem. This approach has been discussed below in detail.

3.4 TRAJECTORY TRACKING THROUGH OPTIMAL CONTROL FORMULATION

3.4.1 Performance Criterion and the Tracking Problem Formulation

In order to formulate the problem as an *Optimal Tracking Problem*, the stringency on the requirement of exactly tracking a specified end-effector trajectory is relaxed. An error vector function is defined which represents the deviation of the actual trajectory from the desired trajectory of the end-effector at every knot point as

$$e = y - y_d$$

where,

e represents the end-effector trajectory error

y represents the generated end-effctor trajectory and

y_d represents the desired trajectory.

Now, a positive definite scalar function is defined in the form of weighted quadratic function of the error vector which is required to be minimized over the entire trajectory and this minimization criterion is the primary performance requirement. The above requirement of tracking a workspace trajectory provides only a kinematic constraint without considering the dynamics of the manipulator. So minimization of just the trajectory error may result in high torque requirement at the joints. In order to keep a bound on the joint torques, the performance index is modified by appending a weighted quadratic function of the torque vector. Hence, the performance index, J, for a fixed time problem is written in the following form.

$$J = \frac{1}{2}\int_0^{t_f} (e^T Q_1 e + u^T R\ u)\ dt \qquad (3.9)$$

where,

Q_1 is a positive definite symmetric weighting matrix on the tracking error,

R is a positive definite symmetric weighting matrix on the joint torques,

u is the joint torque vector and

t_f is the specified final time.

Secondary performance objectives such as global minimization of joint velocity norm or kinetic energy can also be specified. An additional requirement on achieveing a final state in terms of position and/or velocity can be imposed by putting a penalty on the error from the desired state at the final time. The augmented performance index can then be expressed as

$$J = \frac{1}{2} z_f^T Q_f z_f + \frac{1}{2} \int_0^{t_f} (z^T Q\, z + u^T R\, u)\, dt \qquad (3.10)$$

where,

$z = [e \quad q']^T$,

$z_f = z\Big|_{t=t_f}$,

$Q = \text{diag}\,[Q_1 \quad Q_2]$ and

$Q_f = Q\Big|_{t=t_f}$.

The sub-matrix Q_2 of Q decides the secondary performance criterion which has been discussed in chapter four.

The joint torque vector, u, is related to the joint variables and their derivatives through the equations of dynamics of the manipulator as given by (3.8). For the solution purpose,

(3.8) is converted to state equation form as given below.

Let

$$q_1 = q$$

$$q_2 = q'$$

Then, the state space representation of (3.8) is,

$$\begin{aligned} q_1' &= q_2 \\ q_2' &= -\,[M(q_1)]^{-1}\,\{\, C(q_1,q_2) + F(q_2) - u \,\} \end{aligned} \tag{3.11}$$

Or in a more compact form

$$x' = f(x,u)$$

where,

$x = [q_1 \quad q_2]^T$ is the state vector,

$x' = [q_1' \quad q_2']^T$ is the derivative of the state vector and

$f[x,u] = [q_2 \quad -[M(q_1)]^{-1}\,\{\, C(q_1,q_2) + G(q_1) + F(q_2) - u \,\}]^T$

The vector z in the performance index may not be directly observable from the state equations. So the observer equation

$$z = g(x) \tag{3.12}$$

is used which constructs the vector z from the state vector x. The

form of the function $g(\cdot)$ is different for the different cases considered in chapter four and hence is discussed in detail in that chapter.

Having defined the performance criterion, the tracking problem can now be mathematically stated as

$$\text{Minimize } J = \frac{1}{2} z_f^T Q_f z_f + \frac{1}{2} \int_0^{t_f} (z^T Q\, z + u^T R\, u)\, dt \qquad (3.13(a))$$

subject to,

$$x' - f(x,u) = 0 \qquad (3.13(b))$$

$$z = g(x). \qquad (3.13(c))$$

This is termed as the Optimal Tracking Problem in control literature. The above problem is a simple fixed time non-linear constrained optimization problem because of the non-linear constraint equations (3.13(b)). It can be converted to an unconstrained optimization problem using the Lagrange undetermined multipliers as

$$\text{Minimize } J = \frac{1}{2} z_f^T Q_f z_f + \int_0^{t_f} [\frac{1}{2} (z^T Q\, z + u^T R\, u) + \lambda^T (f(x,u) - x')]\, dt \qquad (3.14)$$

where,

λ is the Lagrange undetermined multiplier.

3.4.2 The Variational Approach

The fixed time unconstrained optimization problem (3.14) can be solved using the Variational Principle. The necessary conditions for optimality are obtained in the following manner (Kirk [1967]).

First define the Hamiltonian of the system as

$$\mathcal{H} = (z^T Q\, z + u^T R\, u) + \lambda^T f(x,u).$$

The necessary conditions of optimality can then be expressed conveniently in terms of the Hamiltonian as

$$\frac{\partial \mathcal{H}}{\partial u} = 0 \qquad (3.15(a))$$

$$\frac{\partial \mathcal{H}}{\partial x} = -\lambda' \qquad (3.15(b))$$

$$\frac{\partial \mathcal{H}}{\partial \lambda} = x' \qquad (3.15(c))$$

for all time $t \in [0, t_f]$

The boundary condition are

$$x\Big|_{t=0} = x_0 \qquad (3.16(a))$$

and

$$\left(\frac{\partial h_f}{\partial u} - \lambda_f \right)^T \delta x_f = 0. \qquad (3.16(b))$$

where,

$$h_f = h\Big|_{t=t_f} = z_f^T Q_f z_f \ ,$$

$$z_f = z\Big|_{t=t_f} \ ,$$

$$Q_f = Q\Big|_{t=t_f}$$

δx_f is the variation on x at the terminal time ,

$\lambda_f = \lambda\Big|_{t=t_f}$ and

$$\lambda' = \frac{\partial \lambda}{\partial t} \ .$$

The set of non-linear differential and algebraic equations (3.15) with the split boundary conditions (3.16) form the Non-Linear Two Point Boundary Value Problem (NLTPBVP). In general, the analytical solution for such a problem is not possible and even the numerical solution is very involved. An iterative numerical scheme used in this work is presented in the next section.

3.5 NUMERICAL ALGORITHM FOR OPTIMAL SOLUTION

Nedeljkovic [1981] proposed a family of first-order iterative algorithms for solving continuous-time unconstrained non-linear optimal control problems. He has also presented the

proof of improvement at each iterative step. The method is essentially as used for the class of *Linear Quadratic Problem*. The algorithm used in the present work is discussed below.

Since the algorithm is based on the Linear Quadratic Problem, it requires the linearized form of the state and observer equations (3.11) and (3.12). The iterative nature of the scheme allows the linearization based on the state vector and the input vector of the previous trajectory. For the trajectory at the i^{th} iteration, the state equations are,

$$x'^{(i)} = f(x^{(i)},u^{(i)})$$
$$z^{(i)} = g(x^{(i)})$$

Then the trajectory at the $(i+1)^{th}$ iteration is written by expanding it in Taylor series upto the first order terms to get

$$x'^{(i+1)} = f(x^{(i)},u^{(i)}) + \left.\frac{\partial f}{\partial x}\right|_i (x^{(i+1)} - x^{(i)}) + \left.\frac{\partial f}{\partial u}\right|_i (u^{(i+1)} - u^{(i)})$$

$$\text{or,} \quad x'^{(i+1)} = \left.\frac{\partial f}{\partial x}\right|_i x^{(i+1)} + \left.\frac{\partial f}{\partial u}\right|_i u^{(i+1)} + \left(f(x^{(i)},u^{(i)}) - \left.\frac{\partial f}{\partial x}\right|_i x^{(i)} - \left.\frac{\partial f}{\partial u}\right|_i u^{(i)} \right)$$

$$\text{or,} \quad x'^{(i+1)} = A\, x^{(i)} + B\, u^{(i)} + e^{(i)} \qquad (3.17)$$

where

$$A = \left.\frac{\partial f}{\partial x}\right|_i \tag{3.18(a)}$$

$$B = \left.\frac{\partial f}{\partial u}\right|_i \tag{3.18(b)}$$

$$e^{(i)} = f(x^{(i)},u^{(i)}) - \left.\frac{\partial f}{\partial x}\right|_i x^{(i)} - \left.\frac{\partial f}{\partial u}\right|_i u^{(i)} \tag{3.18(c)}$$

Similarly for the observer equation,

$$z^{(i+1)} = g(x^{(i)}) + \left.\frac{\partial g}{\partial x}\right|_i (x^{(i+1)} - x^{(i)})$$

$$\text{or,} \quad z^{(i+1)} = \left.\frac{\partial g}{\partial x}\right|_i x^{(i+1)} + \left(g(x^{(i)}) - \left.\frac{\partial g}{\partial x}\right|_i x^{(i)} \right)$$

$$\text{or,} \quad z^{(i+1)} = C\, x^{(i+1)} + w^{(i)} \tag{3.19}$$

where,

$$C = \left.\frac{\partial g}{\partial x}\right|_i \quad \text{and} \tag{3.20(a)}$$

$$w = g(x^{(i)}) - \left.\frac{\partial g}{\partial x}\right|_i x^{(i)}. \tag{3.20(b)}$$

For notational convenience, (3.17) and (3.19) are rewritten after dropping out the superscripts as

$$x' = A\,x + B\,u + e \qquad (3.21(a))$$

$$z = C\,x + w \qquad (3.21(b))$$

where,

A is a square matrix,

B is a rectangular matrix,

C is a rectangular matrix,

u is the joint torque vector or input vector and

e, w are the linearization error vectors.

The detailed expressions of the matrices A and B have been presented in Appendix B.

The algorithm can now be stated as follows.

Step 1

For iteration index i = 0, assume nominal control $u^{(0)}$ and numerically integrate the non-linear equations of motion (3.11) to get $x^{(0)}$.

Evaluate $J^{(0)}$ from (3.10).

Step 2

Solve the following equations backwards from t_f to 0

$$P' + A^T P + PA + C^T Q C - PBR^{-1}B^T P = 0 \qquad (3.22(a))$$

$$s' - PBR^{-1}B^T s + A^T s + C^T Q(w - y_d) + Pe = 0. \qquad (3.22(b))$$

with the boundary conditions,

$$P\Big|_{t=t_f} = C^T Q_f C x_f \qquad \text{and}$$

$$s\Big|_{t=t_f} = C^T Q_f (w_f - y_{d_f}).$$

Step 3

Define

$$b^{(i)} = u^{(i)} + R^{-1}B^T(Px^{(i)} + s)$$

and

$$\Delta u = \int_0^{t_f} {b^{(i)}}^T R\, b^{(i)}\, dt$$

Set $\varepsilon = 1.0$.

If $\Delta u = 0$ then stop.

Step 4

Set

$$u^{(i+1)} = u^{(i)} - \varepsilon b^{(i)} - R^{-1}B^T P(x^{(i+1)} + x^{(i)})$$

and integrate the non-linear equations of motion (3.10).

Evaluate $J^{(i+1)}$.

Step 5

If $J^{(i+1)} - J^{(i)} + - \varepsilon \Delta u^{(i)} < 0$,

then {

Set

$x^{(i+1)} = x^{(i)}$,

$u^{(i+1)} = u^{(i)}$ and

$J^{(i+1)} = J^{(i)}$.

Goto *Step 2.* }

else {

$\varepsilon = \frac{\varepsilon}{2}$

Goto *Step 4* }

The equation (3.22(a)) in the above algorithm is known as the *Matrix Riccati Differential Equation*. It is a non-linear first order matrix differential equation.

This algorithm has been used for solving the present problem. Different perfomance criteria have been constructed under the framework of Linear Quadratic Problem. The simulation results and their analyses are presented in the next chapter.

MTech Oral Examination

Mr. Anirvan DasGupta (Roll No. 9110502) will defend his Mtech thesis titled TRAJECTORY TRACKING FOR A PLANAR REDUNDANT MANIPULATOR USING OPTIMAL CONTROL FORMULATION on 3rd Aug. 1993 at 9.00 AM in the Mechanical Engg. Conference room. All interested are welcome.

Prof. Himanshu Hatwal

Thesis Supervisor

CC: SPGC Chairman

DPGC Convener

Prof. S. S. Prabhu

Dr. S. Mukherjee

CHAPTER 4

NUMERICAL SIMULATION, RESULTS AND DISCUSSIONS

4.1 INTRODUCTION

In this chapter, various numerical examples of the trajectory tracking problem for a three-link planar manipulator have been presented. The algorithm outlined in Sec. 3.5 has been used to solve the optimal tracking problem. For the purpose of comparison, the pseudo-inverse solution was obtained using (2.3(a)) in Sec. 2.2. The results of the numerical experiments performed have been presented. The computer implementation of the algorithm has been in the C language and the program was executed on the HP9000/850S machines. The Starbase graphics library was used to generate the plots of the results.

4.2 ROBOT PARAMETERS AND TRAJECTORY SPECIFICATIONS

The various parameters values assumed for the manipulator shown in Fig. 3.1(a) are tabulated below.

i	m_i (kg.)	l_i (m)	ρ_i (m)	I_i (kgm^2)
1	5.0	1.0	0.5	0.41667
2	3.0	1.0	0.5	0.250
3	2.0	1.0	0.5	0.16667

Type A :

Radius of the circle = 0.50 m

Position of the center : (1.50, 1.50) m

Type B :

Radius of the circle = 1.0 m

Position of the center : (1.0, 1.50) m

The time of travel for both the trajectories were fixed at 10.0 seconds. The initial configuration of the manipulator for both the trajectories were taken as

θ_1 = 1.43047 rad θ_2 = -0.89521 rad θ_3 = -0.535492 rad

Case 2 : Linear trajectory

Starting point : (1.6, 1.0) m

End point : (-1.6, 1.0) m

The time of travel was fixed at 8.0 seconds. The initial configuration for this case was

θ_1 = 2.214296 rad θ_2 = -1.287 rad θ_3 = -0.927294 rad

For the purpose of numerical simulation, the trajectories were specified as a set of closely spaced points in the workspace. For numerical computation purpose, in each case, 2000 equispaced points were considered over the trajectory.

4.3 RESULTS AND DISCUSSIONS

In this section the various numerical experiments performed have been discussed. Different types of performance indices were constructed to investigate the efficacy and versatility of the algorithm in solving the optimal control problem. In each case the nominal input, required at the start of the algorithm, was assumed to be zero, i.e.

$$u^{(0)} = 0.0.$$

The numerical integration of the differential equations involved in the algorithm, as outlined in Sec. 3.5, were performed using fourth order Runge-Kutta integration scheme with fixed step size. Results of the experiments have been presented in the form of plots and the various observations discussed.

4.3.1 Circular Trajectory Tracking with no Bounds on Joint Torques and Joint Velocities

In this sub-section, four cases are presented as follows.

CASE 1

In this case, simple tracking of the trajectory is considered. No limits are imposed on the range of joint motion. The performance index was of the form

$$J = \frac{1}{2} z_f^T Q_f z_f + \frac{1}{2} \int_0^{t_f} (z^T Q z + u^T R u) dt \qquad (4.1)$$

where,

$z = [e \quad q']^T$,

e is the trajectory error vector,

$z_f = z\Big|_{t=t_f}$,

u is the joint torque vector,

t_f = 10.0 sec, is the time of travel,

Q_f, Q, R are the positive definite weighting matrices,

Q = diag $[Q_1 \quad Q_2]$ and

$Q_f = Q\Big|_{t=t_f}$.

The sub-matrix, Q_1 is of dimension 2 × 2 while, Q_2 is of dimension 3 × 3.

The observer equation (3.6) mentioned in Sec. 3.4 in this case was defined as

$$\begin{aligned} z_1 &= l_1\cos(\theta_1) + l_2\cos(\theta_{12}) + l_3\cos(\theta_{123}) \\ z_2 &= l_1\sin(\theta_1) + l_2\sin(\theta_{12}) + l_3\sin(\theta_{123}) \\ z_3 &= \theta'_1 \\ z_4 &= \theta'_2 \\ z_5 &= \theta'_3 \end{aligned} \qquad (4.2)$$

where,

l_i is the ith link length and

θ_i, θ_i' are the i^{th} joint variable and joint velocity respectively.

The weighting matrices chosen were

Q_f = diag [6.0E3 6.0E3 8.0 8.0 8.0]

Q = diag [2.0E4 2.0E4 0.0 0.0 0.0]

R = diag [1.0 1.0 1.0]

The sub-matix Q_2 of Q was chosen with all elements as zero implying thereby that there is no penalty on the joint velocities along the trajectory. Whereas, in order to reduce the joint motion at the end of the trajectory, penalty has been imposed on the joint velocities at the final time through Q_f.

The simulation runs for type A circular trajectory was taken. The results are presented in form of plots in Figs. 4.1(a)-(f). The configurations at six instants are shown in Fig. 4.1(a) along with the generated end-effector trajectory. With 2000 points taken on the end-effector trajectory, each configuration in the figure is taken at an interval of 400 points and numbered sequentially. A comparison of the generated and the desired trajectory is presented in Fig. 4.1(b). The variation of joint angles, joint velocities, end-effector velocity and joint torques with time are plotted in Figs. 4.1(c)-(f) respectively.

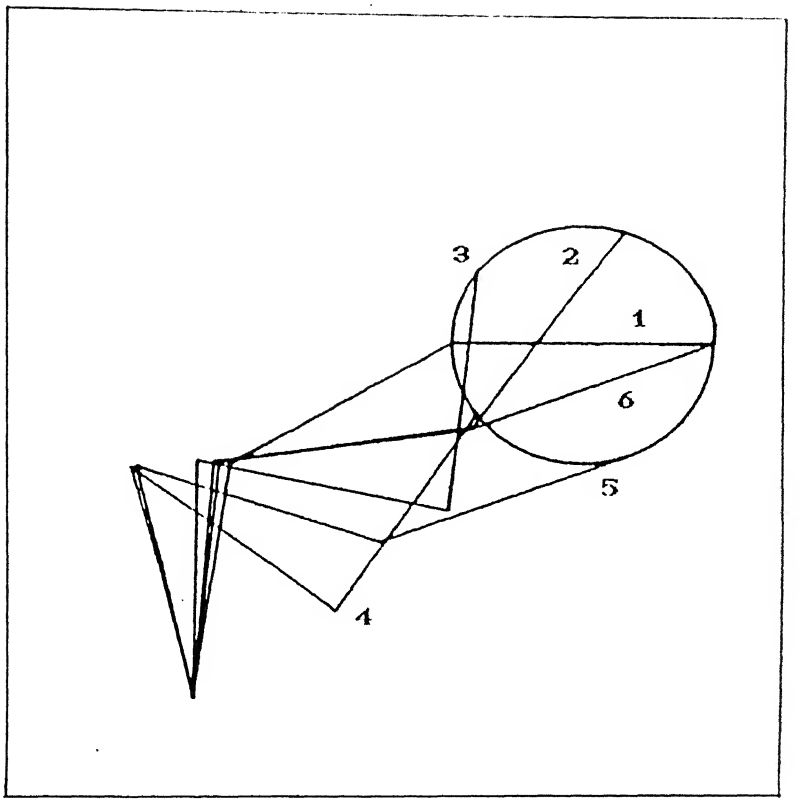

FIG. 4.1(a) MANIPULATOR CONFIGURATIONS IN OPTIMAL TRACKING WITHOUT BOUNDS ON JOINT VELOCITIES AND JOINT TORQUES

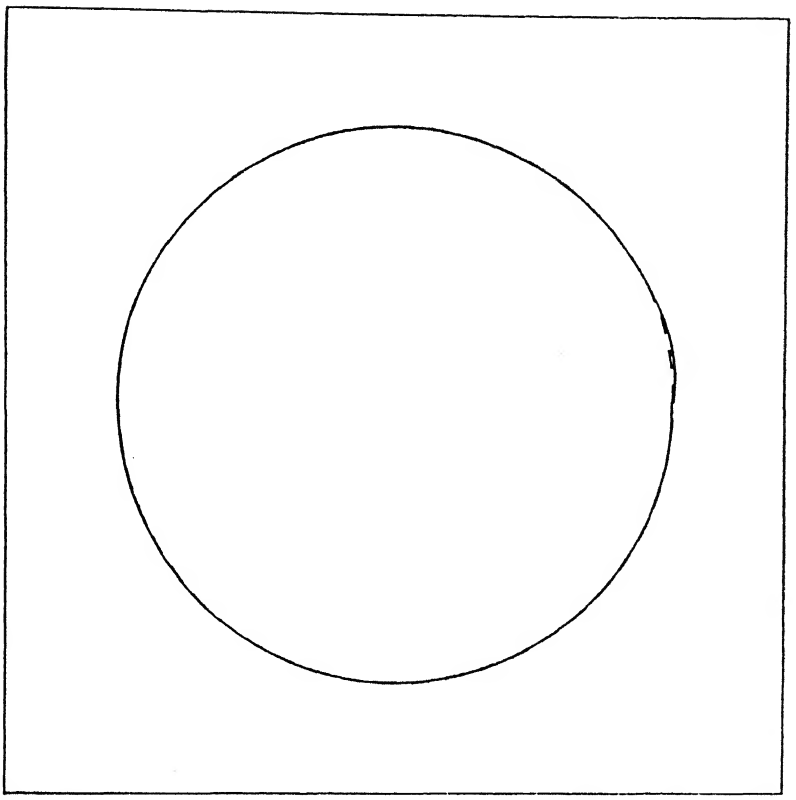

FIG. 4.1(b) COMPARISON OF GENERATED AND DESIRED END-EFFECTOR TRAJECTORIES IN OPTIMAL TRACKING WITHOUT BOUNDS ON JOINT VELOCITIES AND JOINT TORQUES

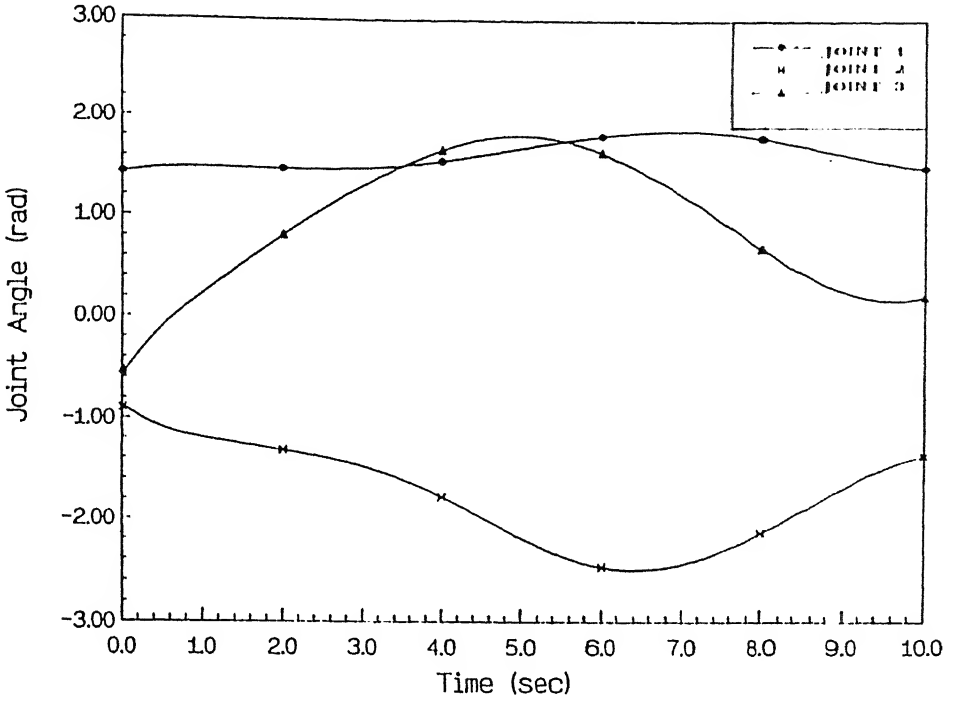

FIG. 4.1(c) VARIATION OF JOINT ANGLES WITH TIME IN OPTIMAL TRACKING WITHOUT BOUNDS ON JOINT VELOCITIES AND JOINT TORQUES

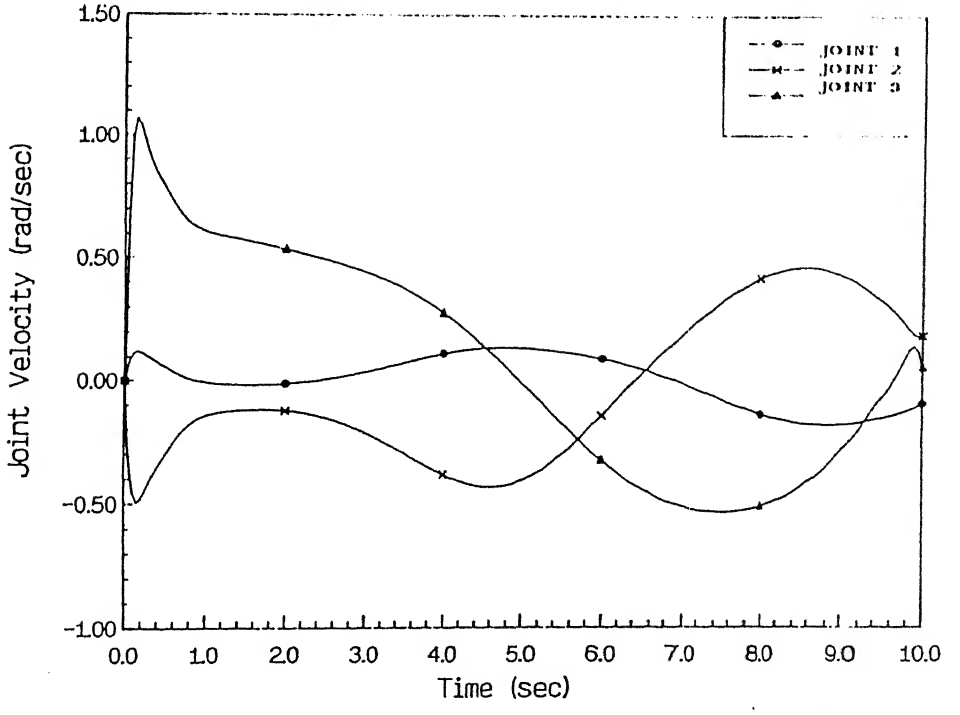

FIG. 4.1(d) VARIATION OF JOINT VELOCITIES WITH TIME IN OPTIMAL TRACKING WITHOUT BOUNDS ON JOINT VELOCITIES AND JOINT TORQUES

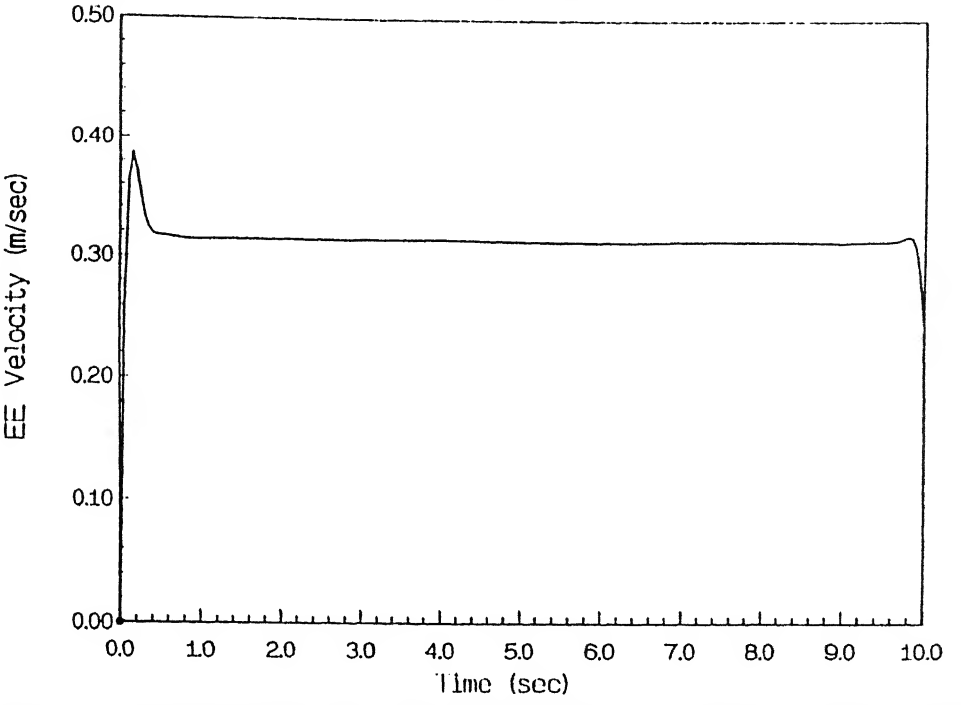

FIG. 4.1(e) VARIATION OF END-EFFECTOR VELOCITY WITH TIME IN OPTIMAL TRACKING WITHOUT BOUNDS ON JOINT VELOCITIES AND JOINT TORQUES

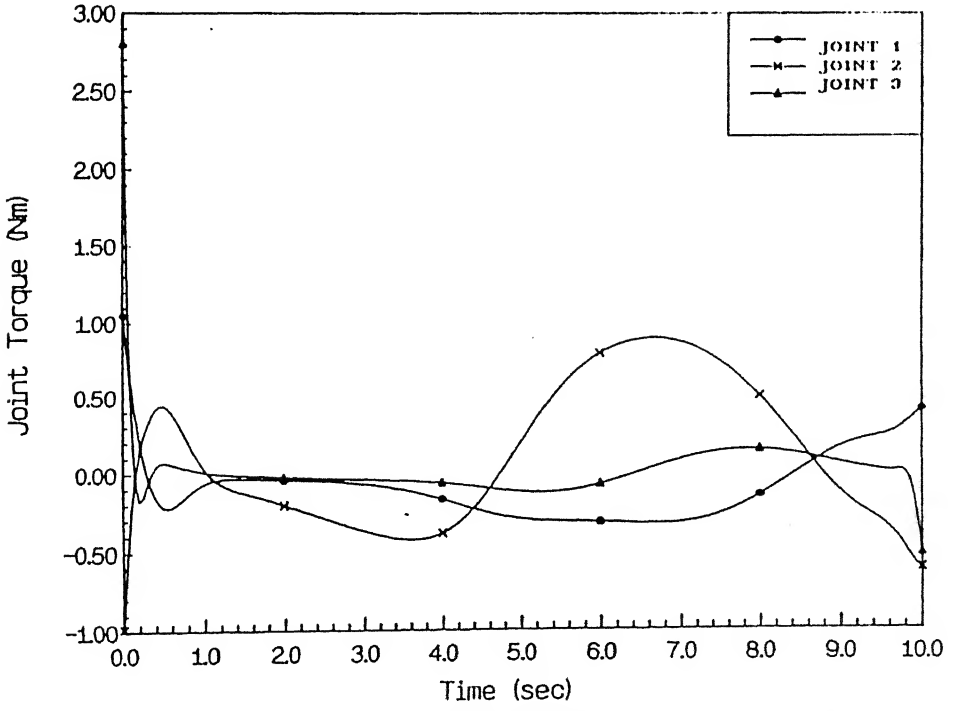

FIG. 4.1(f) VARIATION OF JOINT TORQUES WITH TIME IN OPTIMAL TRACKING WITHOUT BOUNDS ON JOINT VELOCITIES AND JOINT TORQUES

It is observed from the joint velocity plot (Fig. 4.1(d)) that there is an initial surge in the joint velocity implying a high initial acceleration. This is very prominent in the third joint of the manipulator. The joint torque plot (Figs. 4.1(f)) also exhibits a high initial joint torque for the third joint. The initial configuration is such that the third joint is most effective in producing the initial end-effector motion which is vertically upwards. As a result of this, the third joint flips position from negative to positive joint angle. The end-effector also attains a high initial velocity as reflected by the initial surge in the end-effector velocity plot in Fig. 4.1(e), which is otherwise uniform over the rest of the motion.

It is also observed from the joint velocity plot (Fig. 4.1(d)) and end-effector velocity plot (Fig. 4.1(e)) that at the terminal time, a small but finite velocity persists. This is due to the fact that the problem has been solved considering free terminal states while putting weightage on the terminal states. Hence by increasing the weightage on the joint velocities at the terminal time, terminal velocities can be reduced. It has been observed though, that the weights cannot be increased arbitrarily as it tends to make the backward numerical integration of the Riccati equation (3.22(a)) unstable. In order to arrest the motion of the manipulator completely at the final time, brakes may be applied which is done often in practice.

It is observed from Fig. 4.1(a) that the final configuration

is different from the initial configuration. This phenomenon is referred to as drift in configuration or non-conservative motion of the manipulator. This is particularly observed in case of control schemes based on local optimization in redundant manipulator (Klein and Huang [1983]). While performing cyclic tasks, configuration drift may result in collision with obstacles in the robot workspace and hence is an undesirable feature.

In order to compare the problem of drift, the inverse kinematic solution was obtained using the pseudo-inverse of the Jacobian matrix of the manipulator as was outlined in Sec 3.3. In this case, the circular trajectory of type B was considered. The manipulator configuration at six instants over the trajectory, obtained through the pseudo-inverse solution, is shown in Fig. 4.2(a) and the joint angle and joint velocity variation are plotted against time in Figs. 4.2(b) and (c) respectively. It has been conclusively proved (Klein and Huang [1983]) that in planar redundant manipulators, involved in tracking a cyclic trajectory, drift is unavoidable using the pseudo-inverse solution. Figures 4.2(d) and (e) show the configurations as obtained by the pseudo-inverse solution and the optimal control solution respectively, at the end of each cycle of the circular trajectory.

It is clear from Fig. 4.2(d) that the drift in the end-effector configuration through pseudo-inverse solution is unstable in nature that is, the configuration keeps drifting from cycle to cycle without settling down on a definite configuration.

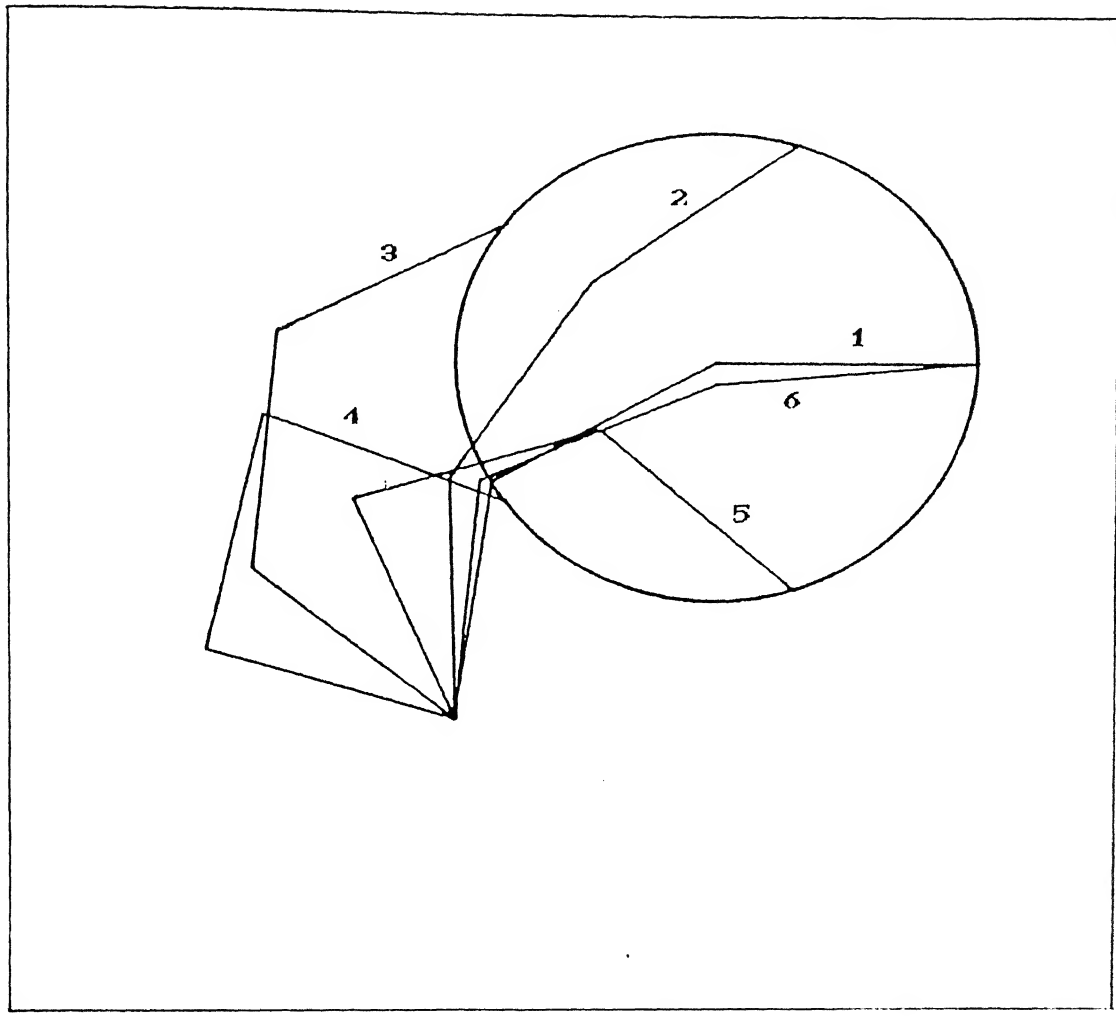

FIG. 4.2(a) MANIPULATOR CONFIGURATIONS IN TRACKING USING PSEUDO-INVERSE SOLUTION

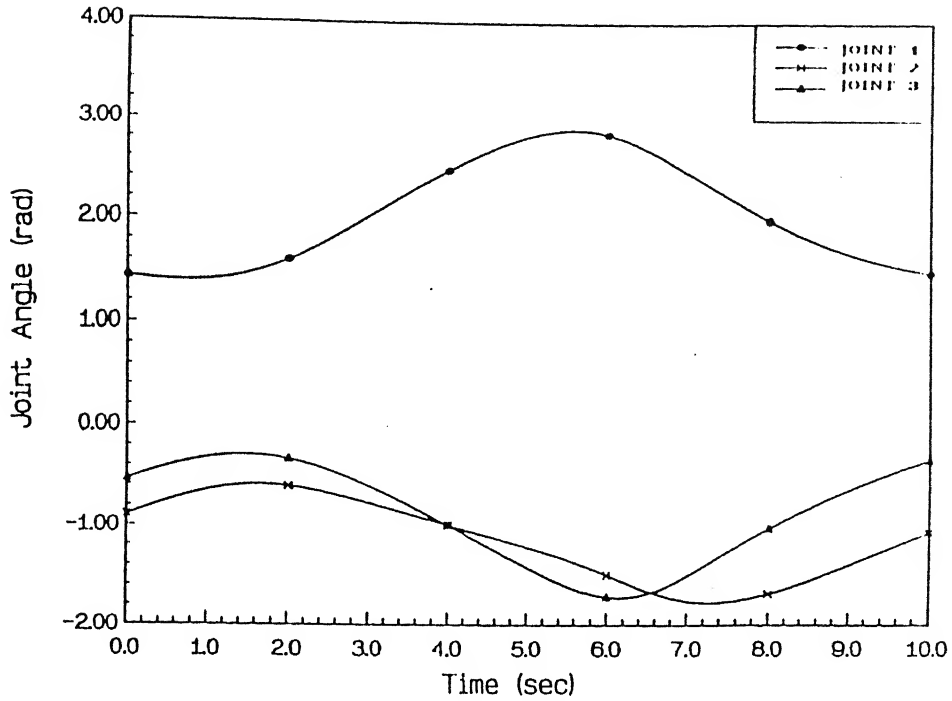

FIG. 4.2(b) VARIATION OF JOINT ANGLES WITH TIME IN TRACKING USING PSEUDO-INVERSE SOLUTION

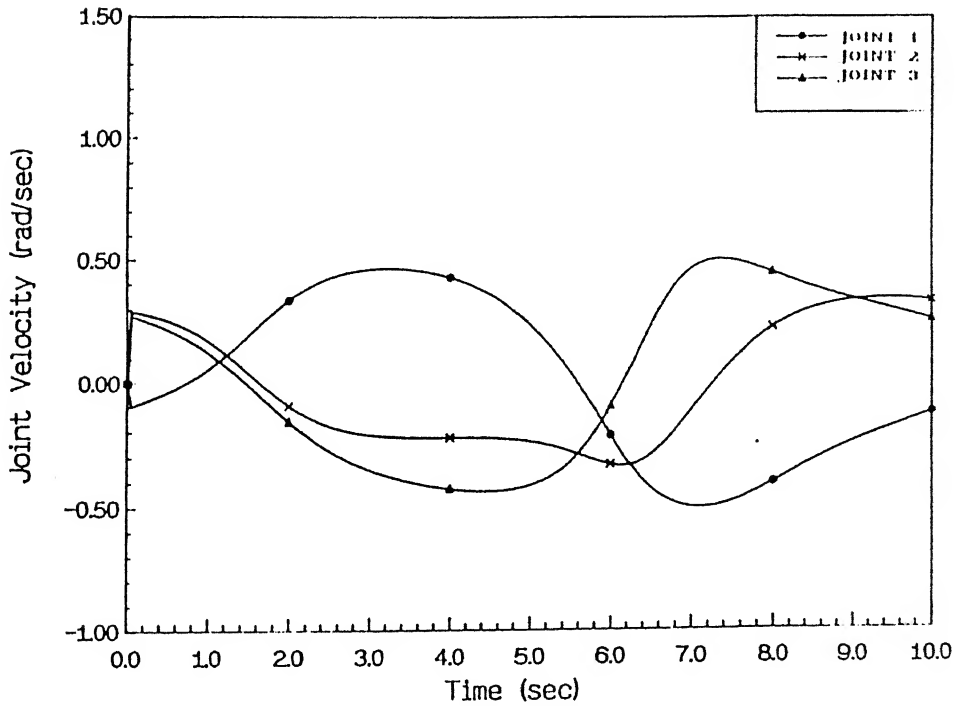

FIG. 4.2(c) VARIATION OF JOINT VELOCITIES WITH TIME IN TRACK USING PSEUDO-INVERSE SOLUTION

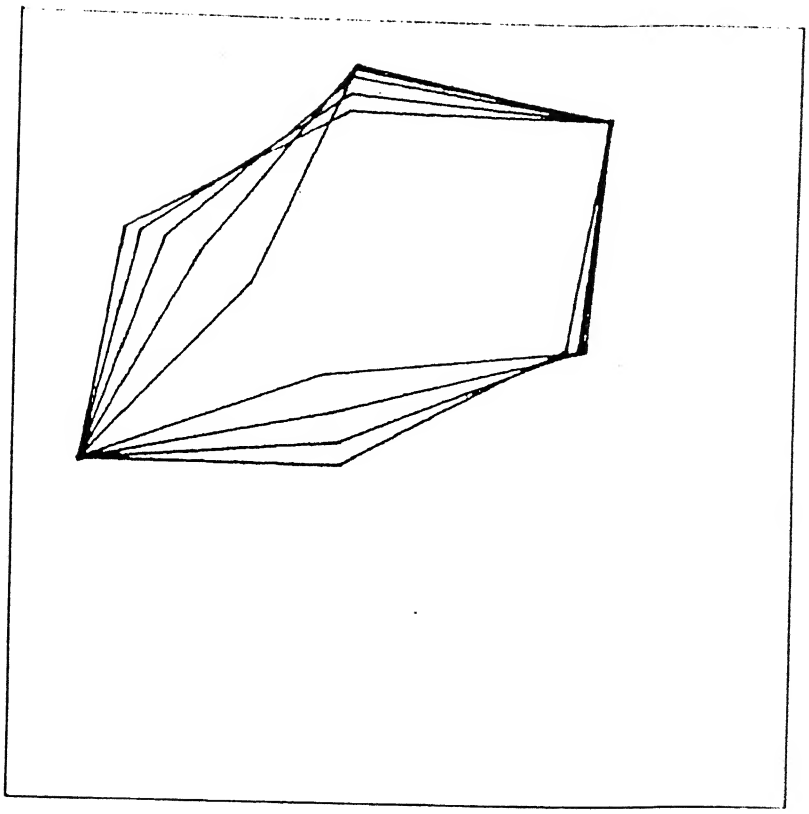

FIG. 4.2(d) MANIPULATOR CONFIGURATIONS AT THE END OF TRAJECTORY AFTER EVERY CYCLE USING PSEUDO-INVERSE SOLUTION

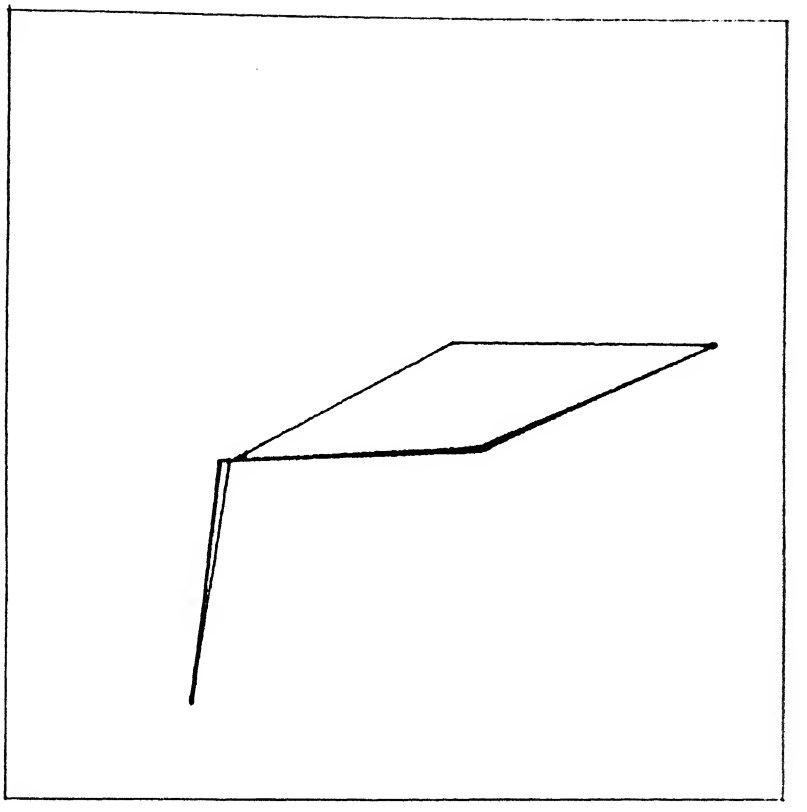

FIG. 4.2(e) MANIPULATOR CONFIGURATIONS AT THE END OF TRAJECTORY AFTER EVERY CYCLE USING OPTIMAL TRACKING ALGORITHM

On the other hand, for the present algorithm it approaches a limiting configuration after only two cycles as seen in Fig 4.2(e). So an initial configuration can be determined which will result in a conservative motion of the manipulator.

The stability of drift in configuration was also observed in case of the circular trajectory of type A. The results, when the limiting configuration was reached, are presented in Figs. 4.3(a)-(f). The configurations of the manipulator at six instants over the trajectory are shown in Fig. 4.3(a). A comparison of the generated and desired trajectories is presented in Fig. 4.3(b). The joint angle plot against time is presented in Fig. 4.3(c). Variation of joint velocities, end-effector velocity and joint torques are presented in Figs. 4.3(d)-(f) respectively. Starting from this configuration it is observed from Fig. 4.3(a) that the flipping of the third joint is absent. Moreover the initial surge in joint velocities (Fig. 4.3(d)) and the end-effector velocity (Fig. 4.3(e)) is comparitively low as observed respectively in Figs. 4.1(d) and (e). It is however to be noted that this initial configuration which results in conservative manipulator motion may not be unique as is evident from Fig. 4.3(g) which is a plot of the stable configuration obtained using the present algorithm, for the circular trajectory of type A, starting from an initial configuration different from the that in Fig. 4.1(a).

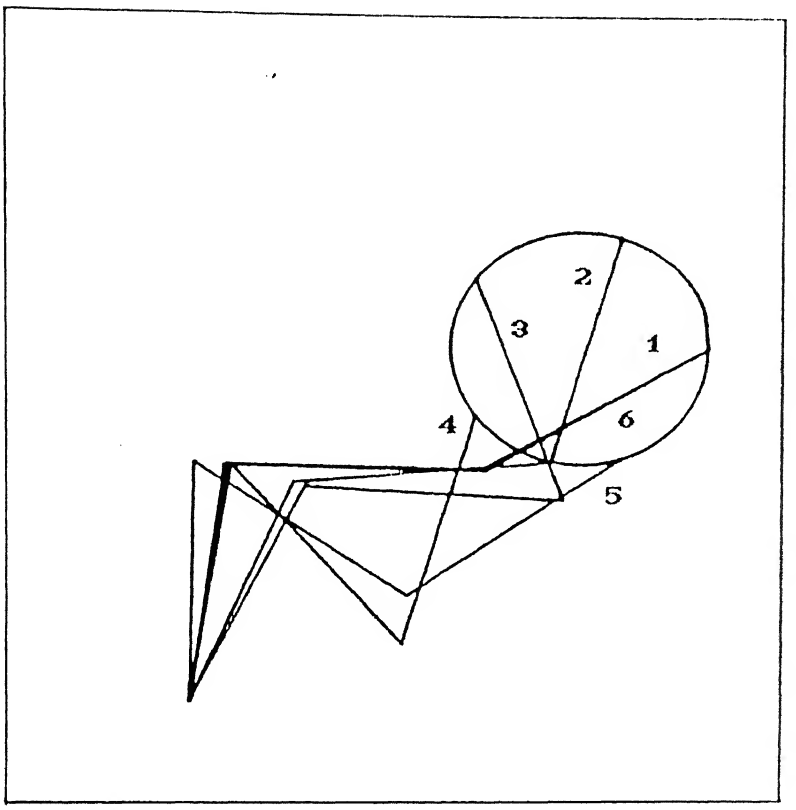

FIG. 4.3(a) MANIPULATOR CONFIGURATIONS IN OPTIMAL TRACKING STARTING FROM A LIMITING CONFIGURATION

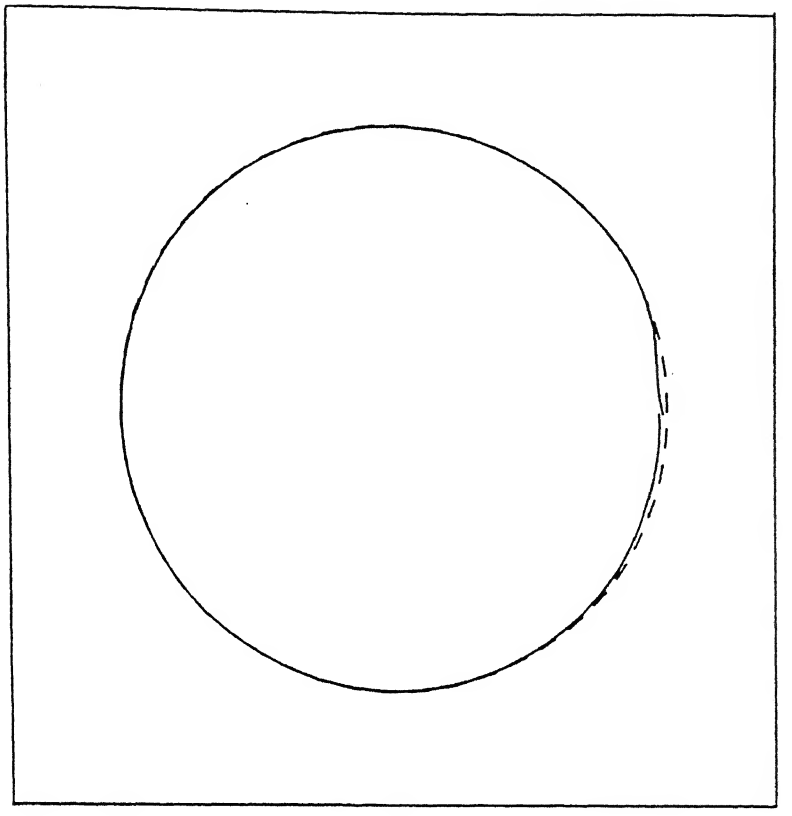

FIG. 4.3(b) COMPARISON OF GENERATED AND DESIRED END-EFFECTOR TRAJECTORIES IN OPTIMAL TRACKING STARTING FROM A LIMITING CONFIGURATION

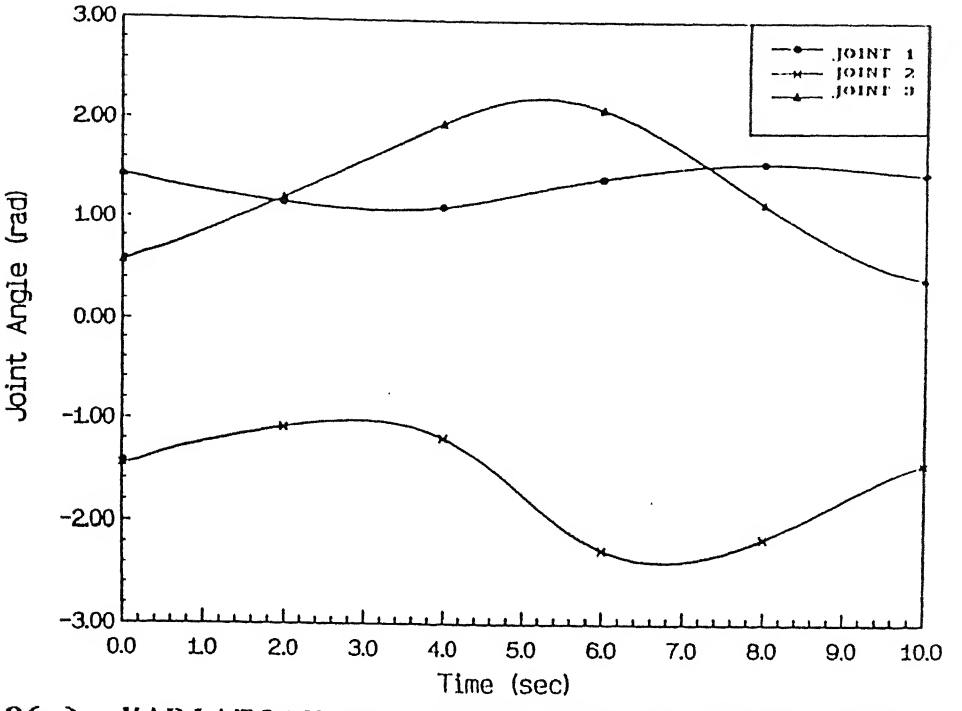

FIG. 4.3(c) VARIATION OF JOINT ANGLES WITH TIME IN OPTIMAL TRACKING STARTING FROM A LIMITING CONFIGURATION

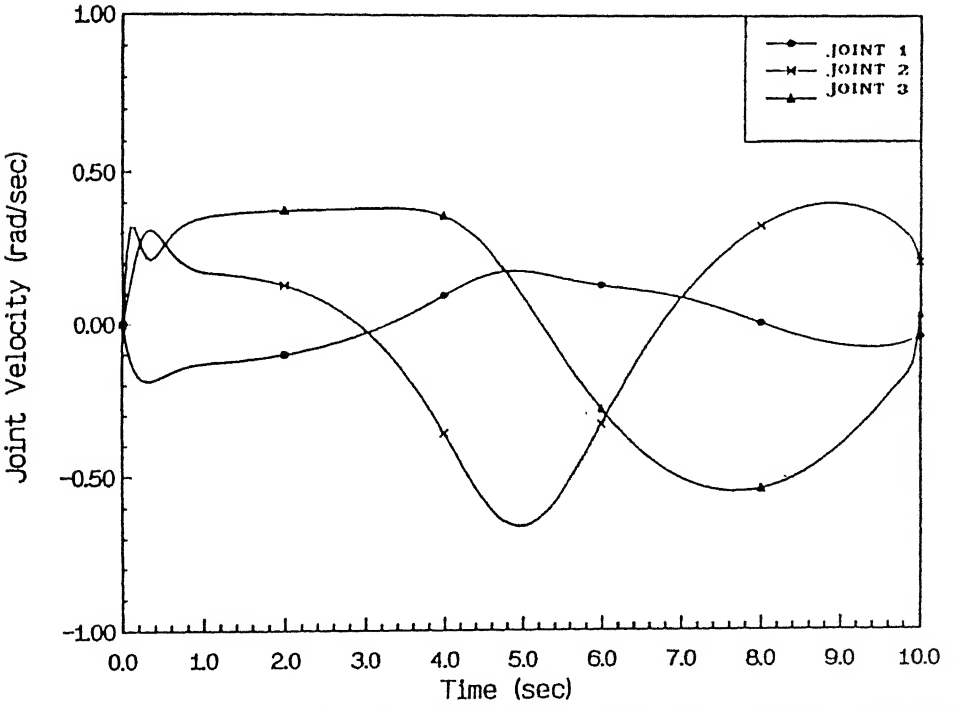

FIG. 4.3(d) VARIATION OF JOINT VELOCITIES WITH TIME IN OPTIMAL TRACKING STARTING FROM A LIMITING CONFIGURATION

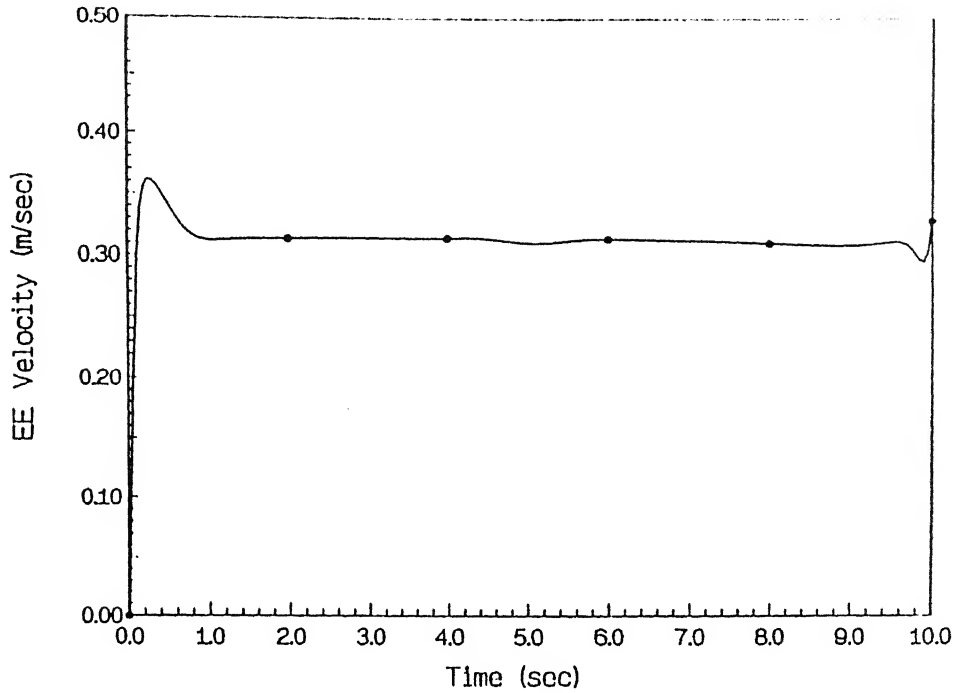

FIG. 4.3(e) VARIATION OF END-EFFECTOR VELOCITY WITH TIME IN OPTIMAL TRACKING STARTING FROM A LIMITING CONFIGURATION

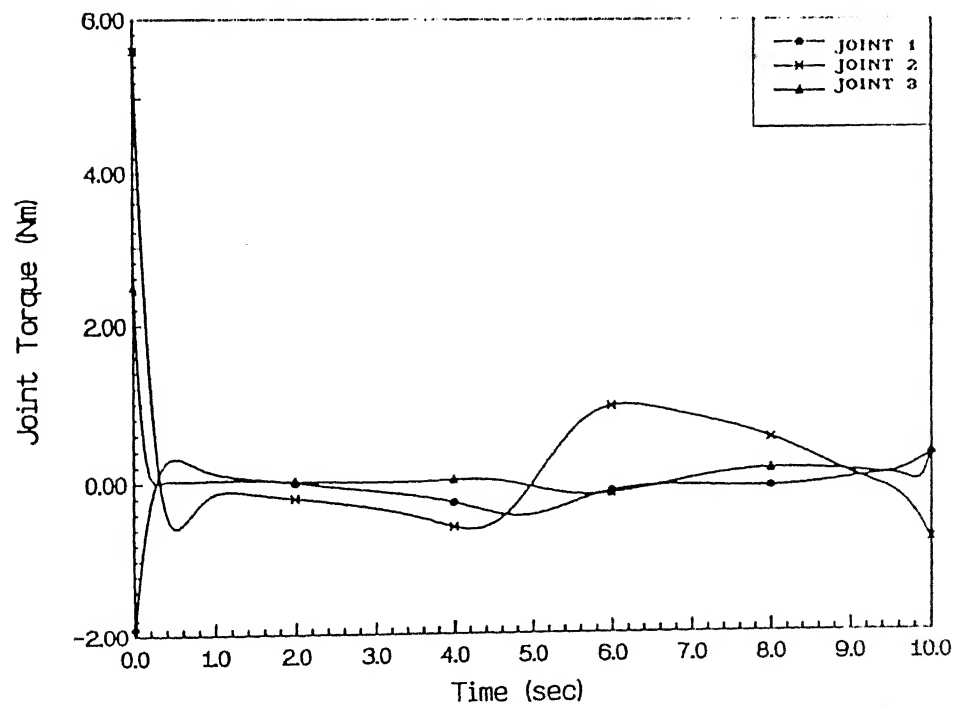

FIG. 4.3(f) VARIATION OF JOINT TORQUES WITH TIME IN OPTIMAL TRACKING STARTING FROM A LIMITING CONFIGURATION

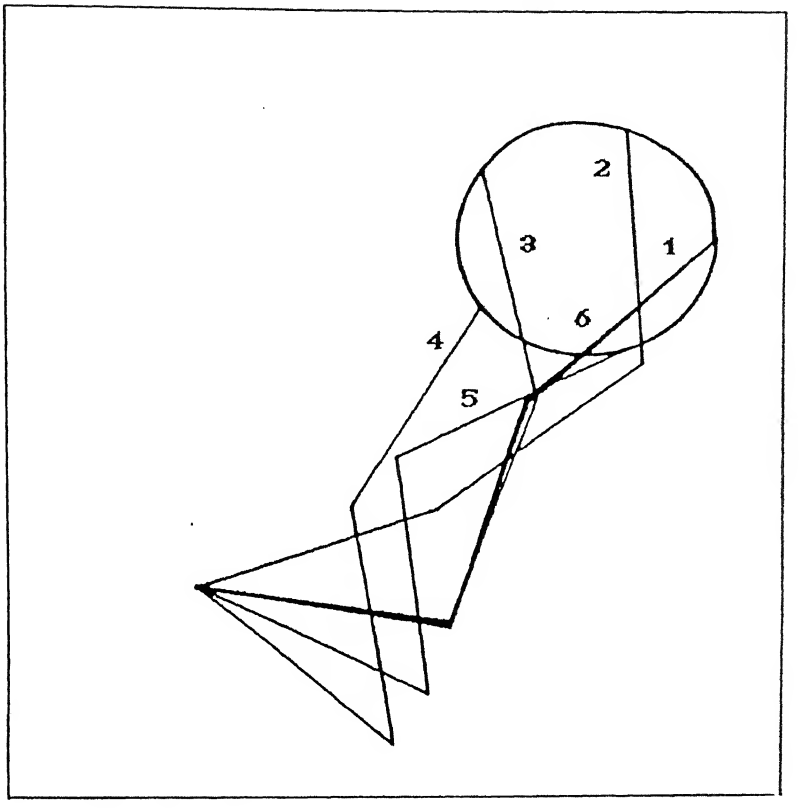

FIG. 4.3(g) MANIPULATOR CONFIGURATIONS IN OPTIMAL TRACKING STARTING FROM A DIFFERENT LIMITING CONFIGURATION

CASE 2

In this case, the problem of trajectory tracking with a specified terminal configuration of the manipulator, has been considered. The terminal configuration was assumed to be same as the initial configuration in order to generate a conservative manipulator motion over the circular trajectory of type A.

The performance index was restated in the form

$$J = \frac{1}{2} z_f^T Q_f z_f + \frac{1}{2} \int_0^{t_f} (z^T Q\, z + u^T R\, u)\, dt \qquad (4.3)$$

where,

$z = [\, e \quad (q - q_d) \quad q' \,]^T$,

e is the trajectory error vector,

$q = [\theta_1 \quad \theta_2 \quad \theta_3]^T$ is the joint variable vector,

q_d is the desired joint variable vector,

$z_f = z\Big|_{t=t_f}$,

u is the joint torque vector,

t_f = 10.0 sec, is the time of travel,

Q_f, Q, R are the positive definite weighting matrices and

$Q_f = Q\Big|_{t=t_f}$.

The condition imposed on the joint variable vector at the terminal time was

$$q_d \Big|_{t=t_f} = q \Big|_{t=0}$$

The observer equation (3.6) mentioned in Sec. 3.4 in this case was defined as

$$z_1 = l_1\cos(\theta_1) + l_2\cos(\theta_{12}) + l_3\cos(\theta_{123})$$
$$z_2 = l_1\sin(\theta_1) + l_2\sin(\theta_{12}) + l_3\sin(\theta_{123})$$
$$z_3 = \theta_1 - \theta_{1d}$$
$$z_4 = \theta_2 - \theta_{2d}$$
$$z_5 = \theta_3 - \theta_{3d}$$
$$z_6 = \theta'_1$$
$$z_7 = \theta'_2$$
$$z_8 = \theta'_3$$

where,

l_i is the i^{th} link length and

θ_i, θ'_i are the i^{th} joint variable and joint velocity respectively.

The weight matrices in this case were chosen as

Q_f = diag [20.0 20.0 2.0E2 2.0E2 2.0E2 8.0 8.0 8.0]

Q = diag [2.0E4 2.0E4 0.0 0.0 0.0 0.0 0.0 0.0]

$$R = \text{diag}\ [1.0 \quad 1.0 \quad 1.0]$$

The third, fourth and the fifth diagonal elements in Q_f impose the penalty on the error of the actual and desired terminal configurations.

The results of the simulation are presented in Figs. 4.4(a)-(e). The configurations at six different instants over the trajectory are presented in Fig. 4.4(a). The plots of joint angles, joint velocities, end-ffector velocities and the joint torques against time are shown in Figs. 4.4(b)-(e) respectively. It can be seen from Fig. 4.4(a) that the final configuration matches exactly with the initial configuration. The joint velocities at the terminal time are also quite low.

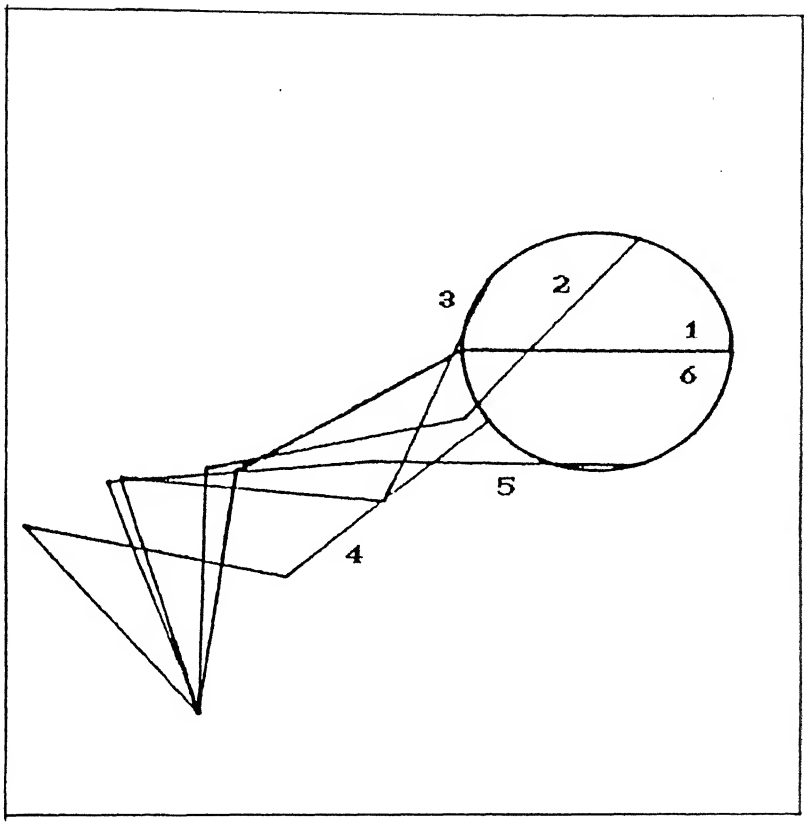

IG. 4.4(a) MANIPULATOR CONFIGURATIONS IN OPTIMAL TRACKING WITH SPECIFIED TERMINAL CONFIGURATION

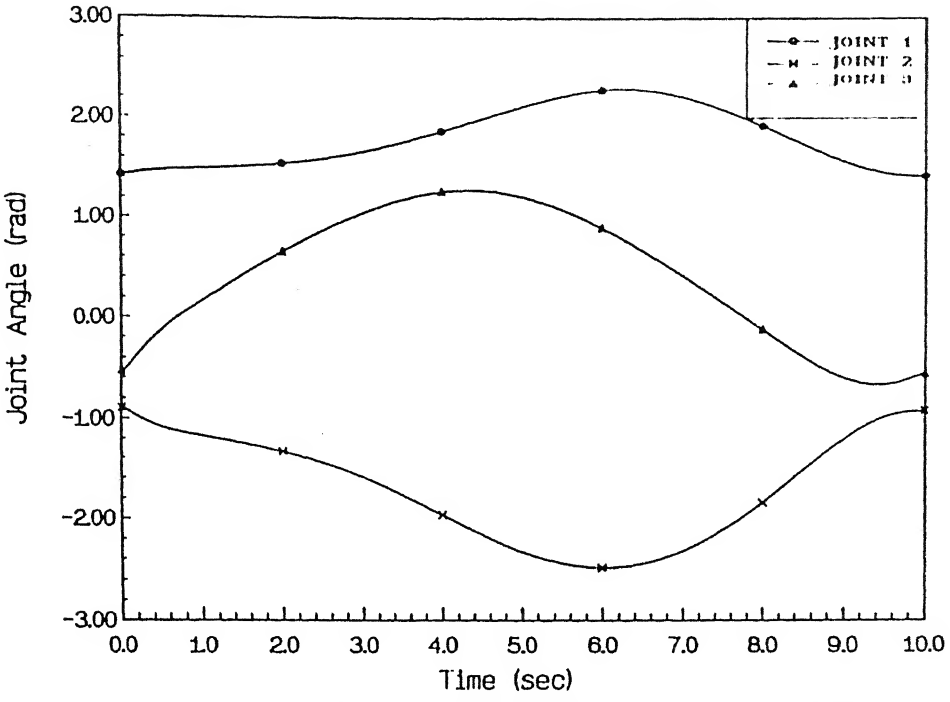

FIG. 4.4(b) VARIATION OF JOINT ANGLES WITH TIME IN OPTIMAL TRACKING WITH SPECIFIED TERMINAL CONFIGURATION

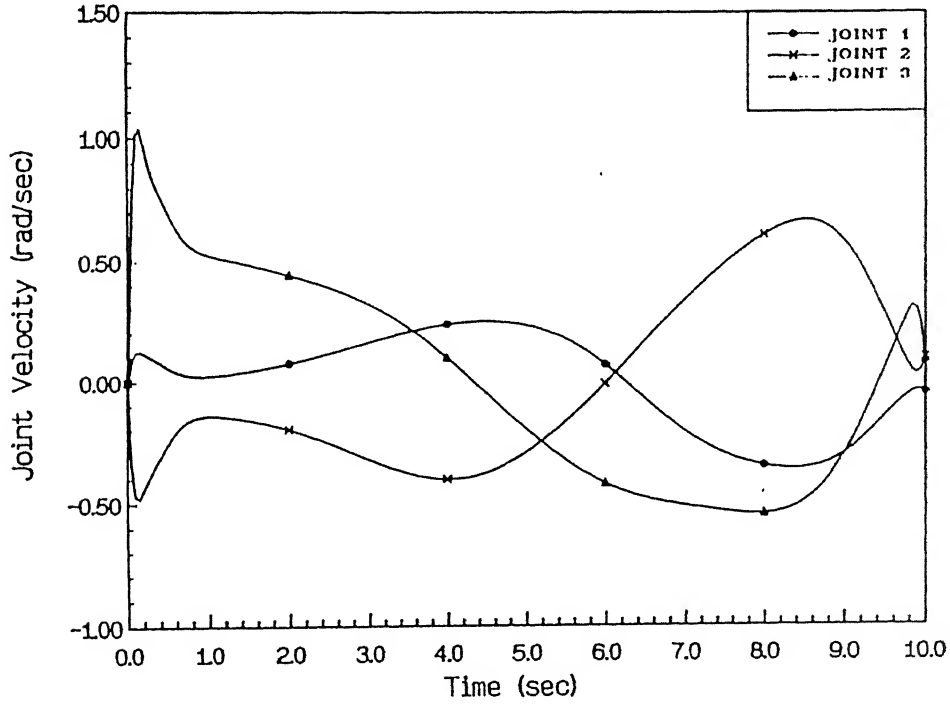

FIG. 4.4(c) VARIATION OF JOINT VELOCITIES WITH TIME IN OPTIMAL TRACKING WITH SPECIFIED TERMINAL CONFIGURATION

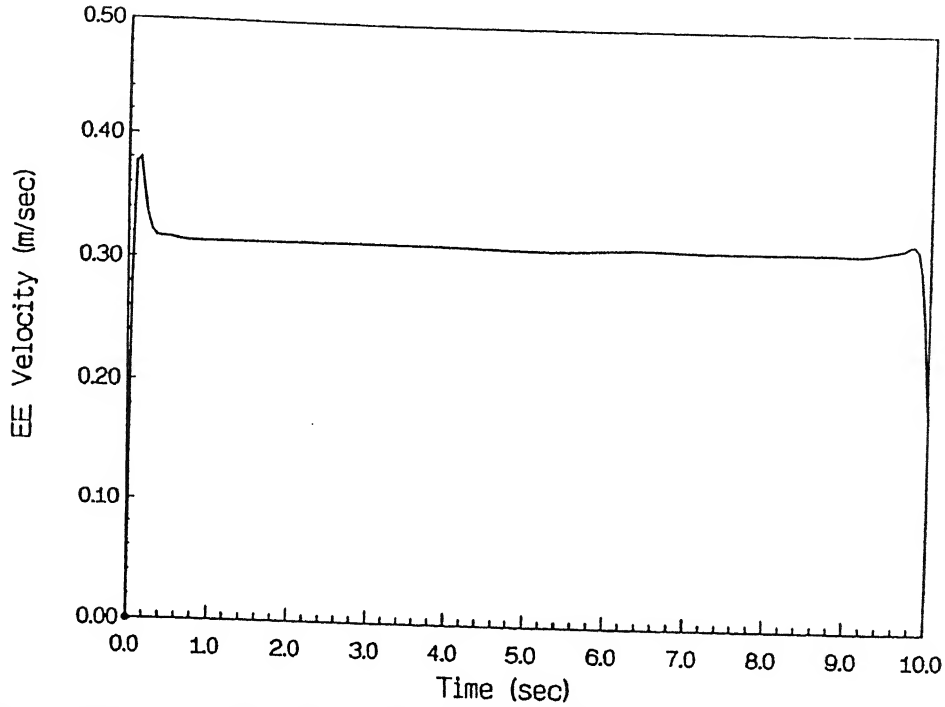

FIG. 4.4(d) VARIATION OF END-EFFECTOR VELOCITY WITH TIME IN OPTIMAL TRACKING WITH SPECIFIED TERMINAL CONFIGURATION

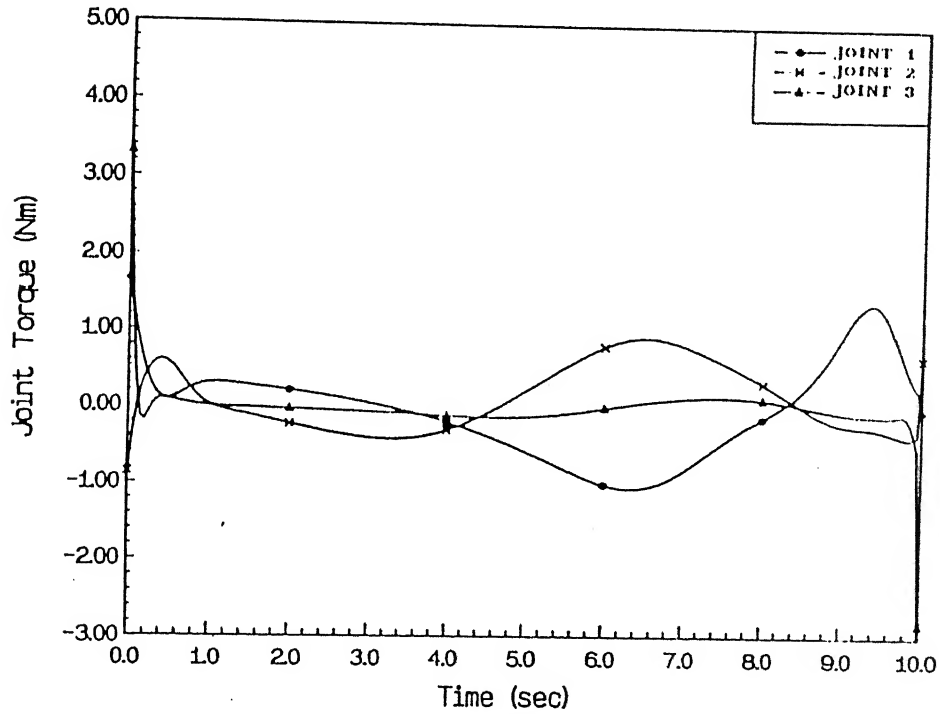

FIG 4.4(e) VARIATION OF JOINT TORQUES WITH TIME IN OPTIMAL TRACKING WITH SPECIFIED TERMINAL CONFIGURATION

CASE 3

In this case, the trajectory tracking problem with the minimization of kinetic energy of the manipulator has been solved. The performance index in this case is the same as given by (4.1) and the observer equation (3.6), as mentioned in Sec. 3.4, is defined to be same as given by (4.2) in Case 1 above

The weighting matrices in the performance index in this case are chosen as follows.

R = diag [1.0 1.0 1.0]

Q_f = diag [6.0E3 6.0E3 8.0 8.0 8.0]

Q_1 = diag [2.0E4 2.0E4]

Q_2 = [M(q)]

where,

M(q) is the inertia matrix of the manipulator.

The term of the form $q'^{T}[M(q)]q'$, obtained on simplifying the performance index (4.1), minimizes the kinetic energy over the trajectory.

The results of the simulation for the circular trajectory of type A are presented in Figs. 4.5(a)-(e). The Fig. 4.5(a) shows the manipulator configuration at six different time instants over the trajectory and the joint angle variation with time is shown in Fig. 4.5(b). The joint velocity, end-effector velocity and joint torque profiles over the trajectory is plotted against time and presented in Figs. 4.5(c)-(e) respectively.

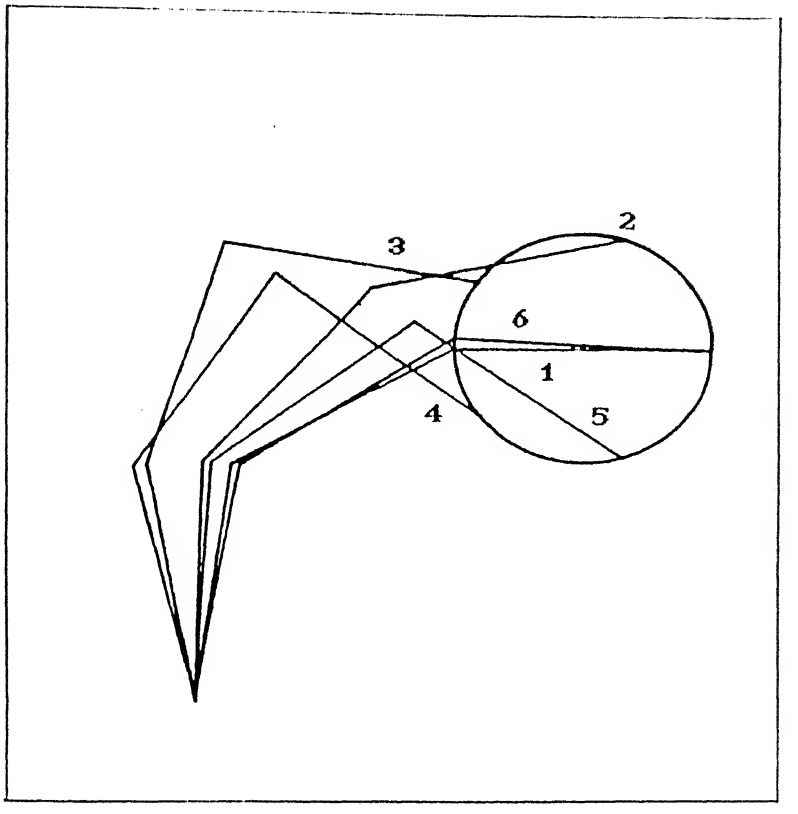

4.5(a) MANIPULATOR CONFIGURATIONS IN OPTIMAL TRACKING WITH MINIMIZATION OF KINETIC ENERGY

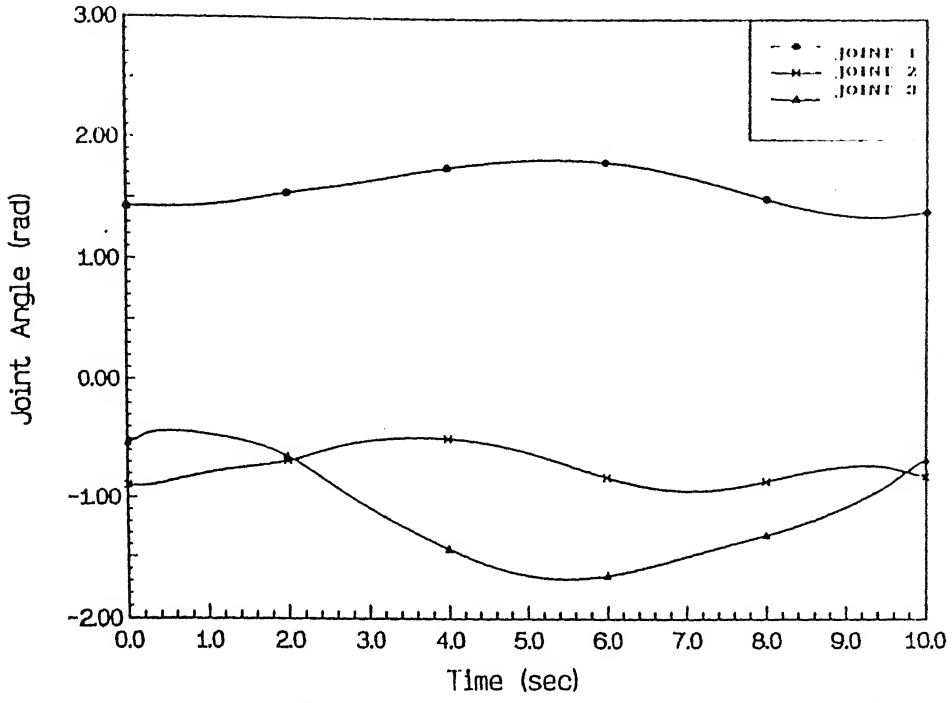

FIG. 4.5(b) VARIATION OF JOINT ANGLES WITH TIME IN OPTIMAL TRACKING WITH MINIMIZATION OF KINETIC ENERGY

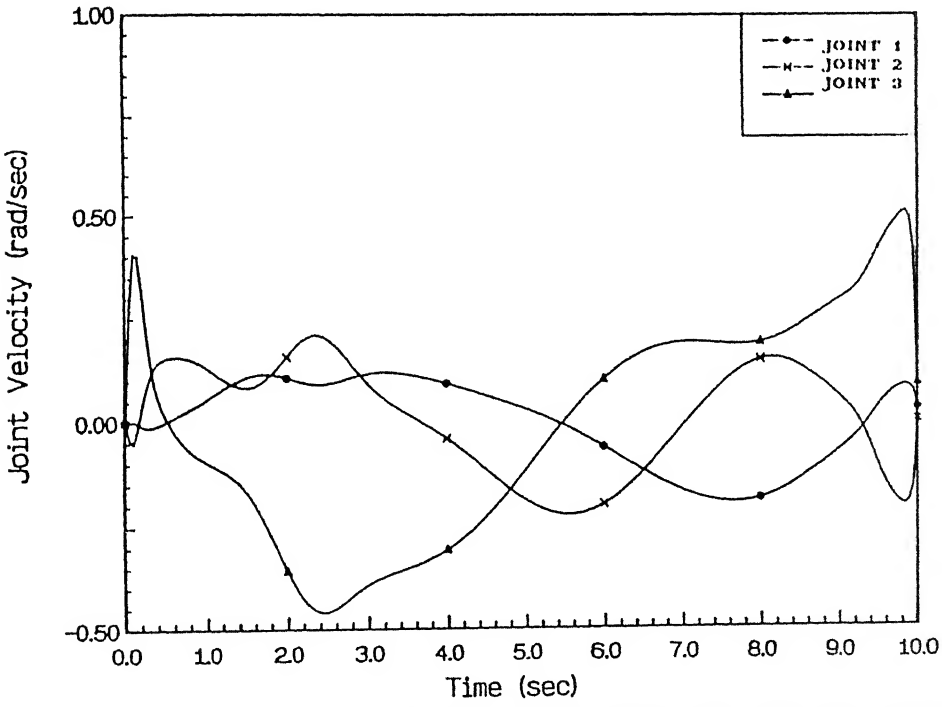

3. 4.5(c) VARIATION OF JOINT VELOCITIES WITH TIME IN OPTIMAL TRACKING WITH MINIMIZATION OF KINETIC ENERGY

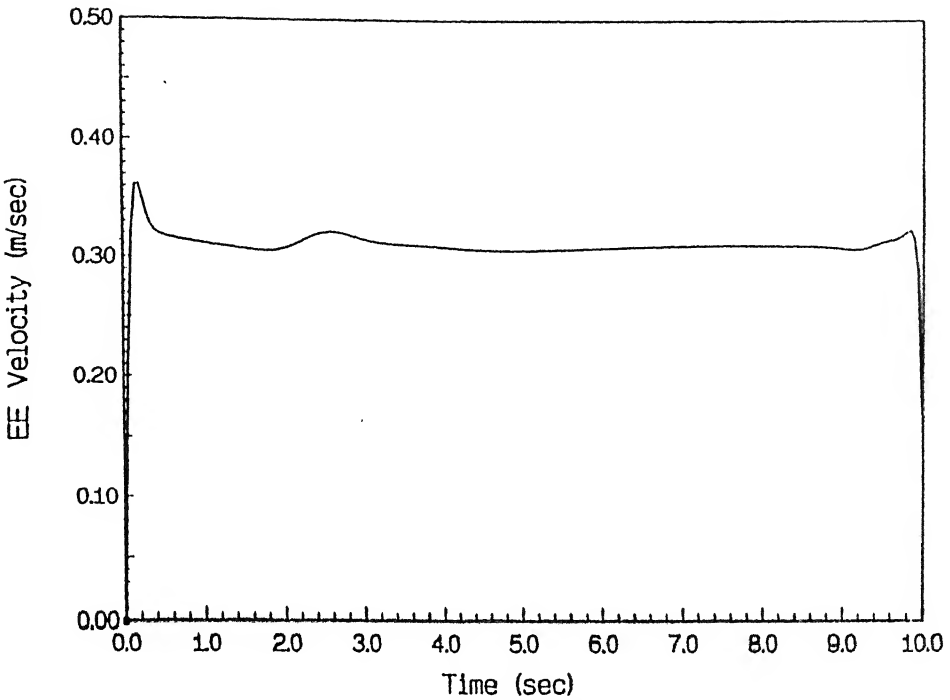

4.5(d) VARIATION OF END-EFFECTOR VELOCITY WITH TIME IN OPTIMAL TRACKING WITH MINIMIZATION OF KINETIC ENERGY

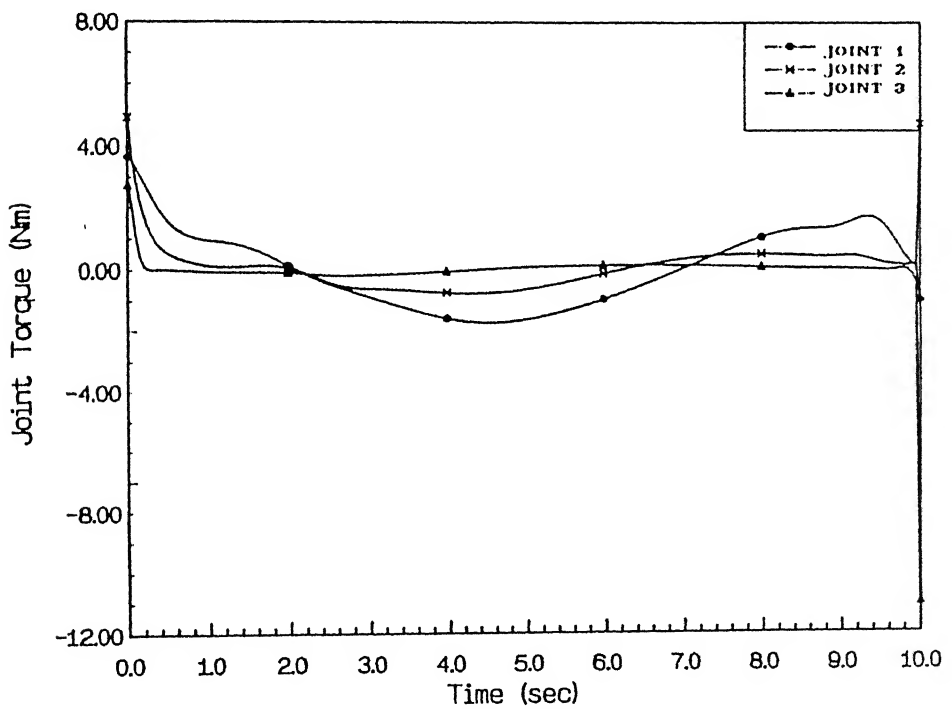

. 4.5(e) VARIATION OF JOINT TORQUES WITH TIME IN OPTIMAL TRACKING WITH MINIMIZATION OF KINETIC ENERGY

Comparing with the joint velocity plot in Figs. 4.1(d) for simple path tracking, it is observed that in this case level of the joint velocities (Fig. 4.5(c)) over the trajectory are low but fluctuating. At the end of the trajectory the joint torques, as shown in Fig. 4.5(e), are comparatively higher and are such, that the terminal motion of the manipulator is almost stopped. The results are reasonable considering that the kinetic energy is minimized.

CASE 4

In this case, the tracking of the specified trajectory with constraint on the range of motion of the joints has been considered. In most practical situations, the joints of a manipulator cannot rotate beyond a certain range because of design considerations. This constraint has been incorporated into the tracking problem not as a mathematical constraint in the optimization process but as an external constraint on the dynamics of the system. The external physical constraint is imposed at the joint limit in such a way that when the joint reaches its limit, it comes in contact with a torsional spring and a dashpot as shown in Fig. 4.6. The equations of dynamics of the manipulator, as presented in Sec. 3.2, are modified by introducing a function $v(q, q', q_{lim})$ which has been defined below. The modified equations of motion are expressed in the standard notations as

$$[M(q)]\, q'' + C(q, q') + F(q') + v(q, q', q_{lim}) = u \qquad (4.4)$$

where,

$$v(q, q', q_{lim}) = \left(k\, |(q - q_{lim})| + d\, q' \right) f(q, q_{lim}),$$

$$f(q, q_{lim}) = 1.0 \qquad |q| > |q_{lim}|$$

$$= 0.0 \qquad \text{otherwise.},$$

q_{lim} is the joint angle limit, upper or lower as the case might be,

k, d are termed as the constraint stiffness and damping respectively.

The performance index in this case was the same as given by (4.1). The observer equations (3.6), as mentioned in Sec. 3.4, are also defined to the same as given by (4.2). The weight matrices chosen case were

$$Q_f = \text{diag } [6.0E3 \quad 6.0E3 \quad 8.0 \quad 8.0 \quad 8.0]$$

$$Q = \text{diag } [2.0E4 \quad 2.0E4 \quad 6.0 \quad 6.0 \quad 6.0]$$

$$R = \text{diag } [1.0 \quad 1.0 \quad 1.0]$$

The last three diagonal elements of the Q matrix imposed certain weights on the norm of the joint velocities. This was found to be necessary in order to stabilize the numerical integration procedure of the differential equations involved in the algorithm as outlined in Sec. 3.5 when the joint reached its limit and came in contact with the torsional stiffness and dashpot.

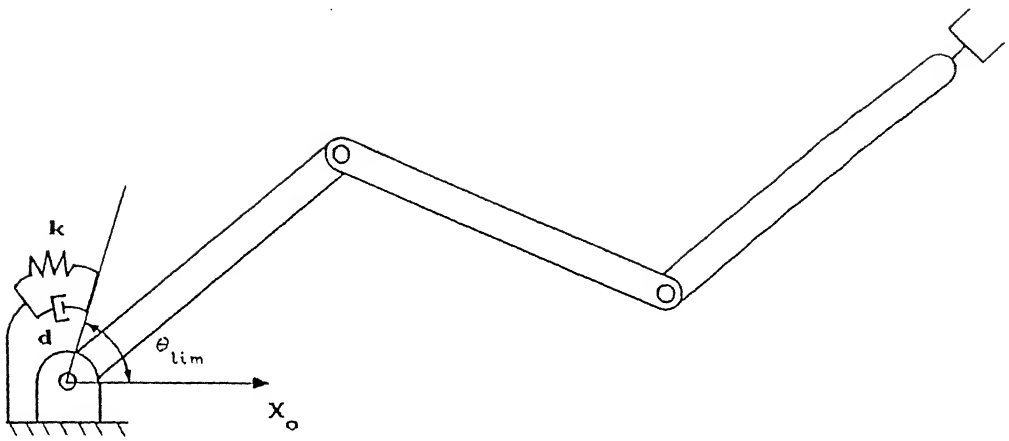

FIG. 4.6 SCHEMATIC DIAGRAM OF SPRING-DASHPOT SYSTEM FOR JOINT CONSTRAINT

The joint limit was imposed on first joint of the manipulator tracking the circular trajectory of type A. From Fig. 4.1(c), it is observed that the first joint makes a maximum angle of about 1.84 radians (105.42°). So the joint upper limit was put at 1.65 radians (94.53°). The constraint stiffness and damping were taken as

$$k = 100 \text{ N/rad}$$

$$d = 200 \text{ Ns/rad}$$

The plots of the results are presented in Fig. 4.7(a)-(e). The configurations at six different instants over the trajectory is shown in Fig 4.7(a). The joint angle variation with time is plotted in Fig. 4.7(b). The joint velocity, end-effector velocity and the joint torque variation with time is presented in Figs. 4.7(c)-(e).

The joint angle plot (Fig. 4.7(b)) and the joint velocity plot (Fig. 4.7(c))indicate that the first joint reached its upper limit of 1.65 radians (94.53°) and remained stationary over a period. There is a discontinuity in the slope of joint velocity curves of all the joints implying a jerk at the joints. This is due to the fact that the joint constraint imposed on the dynamics of the manipulator becomes active in a sudden manner. At that point of time, the motion of the other two joints are readjusted to maintain the tracking. There are clear signs of control torque

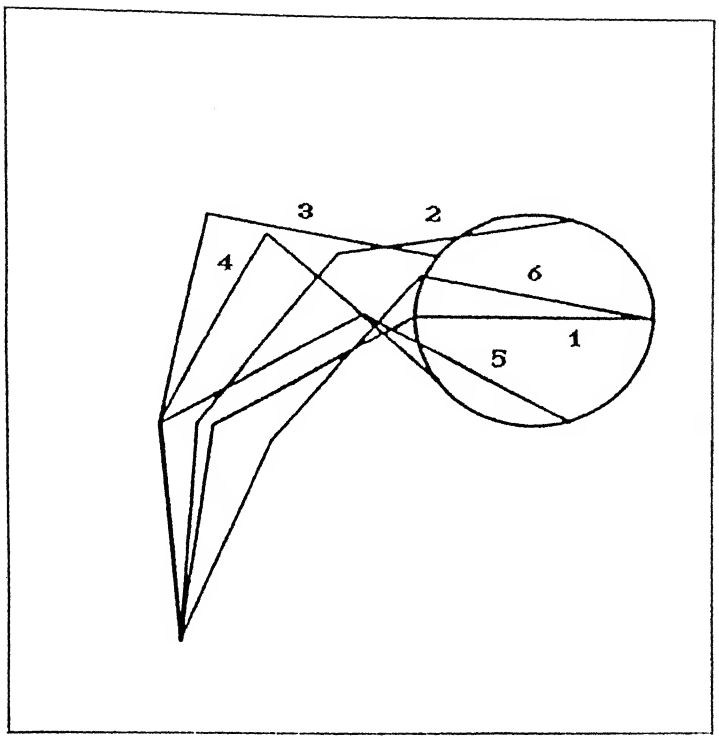

FIG. 4.7(a) MANIPULATOR CONFIGURATIONS IN OPTIMAL TRACKING WITH JOINT CONSTRAINT

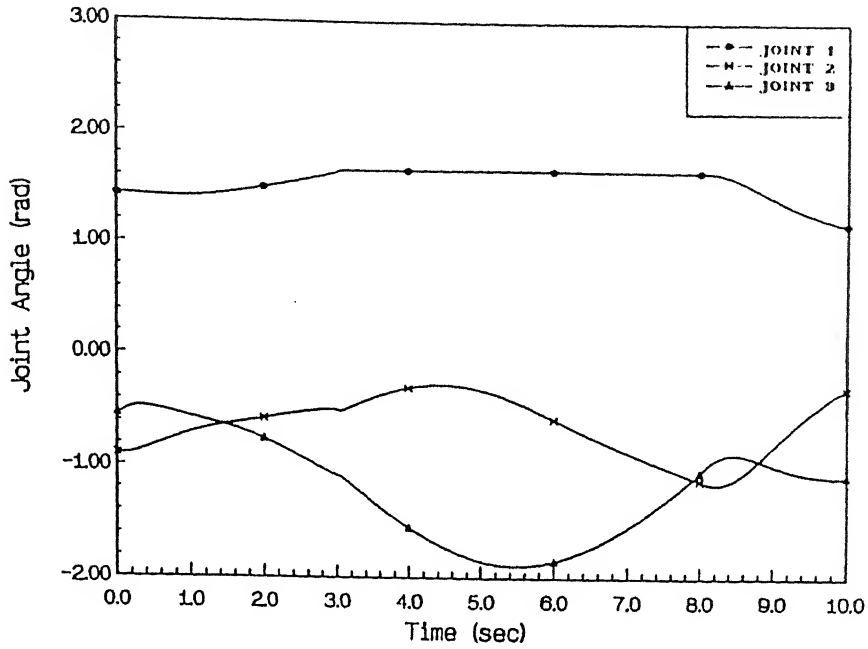

FIG. 4.7(b) VARIATION OF JOINT ANGLES WITH TIME IN OPTIMAL TRACKING WITH JOINT CONSTRAINT

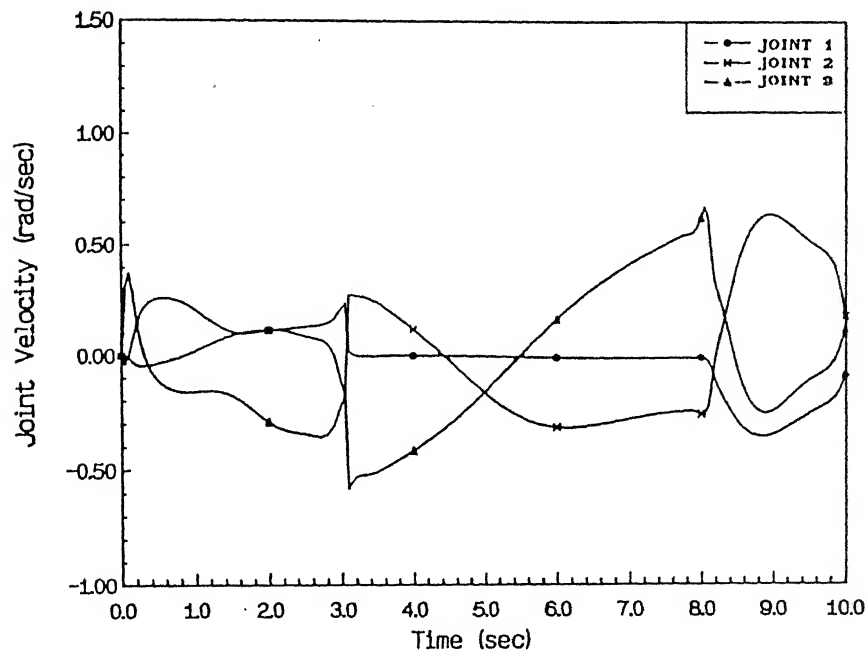

FIG. 4.7(c) VARIATION OF JOINT VELOCITIES WITH TIME IN OPTIMAL TRACKING WITH JOINT CONSTRAINT

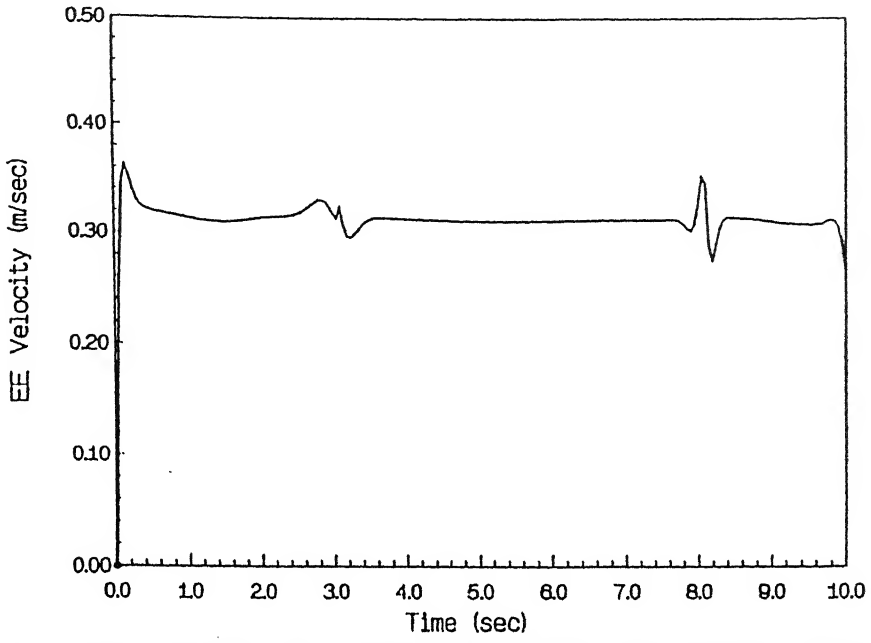

FIG. 4.7(d) VARIATION OF END-EFFECTOR VELOCITY WITH TIME IN OPTIMAL TRACKING WITH JOINT CONSTRAINT

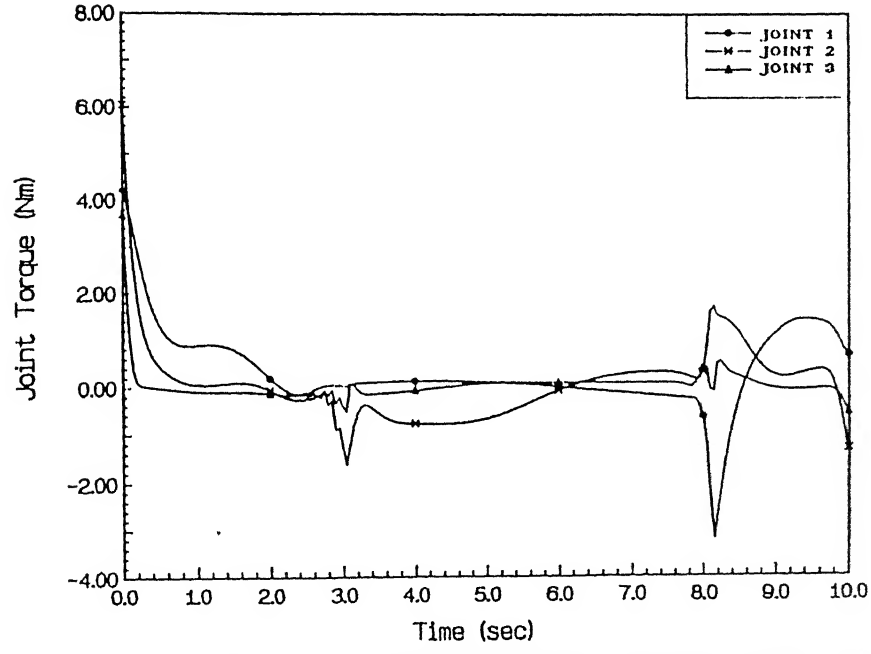

FIG. 4.7(e) VARIATION OF JOINT TORQUES WITH TIME IN OPTIMAL TRACKING WITH JOINT CONSTRAINT

chatter in the joint torque plot (Fig. 4.7(e)) at the point of contact of the joint with the constraint. This is possibly to prevent oscillations because of the stiffness of the constraint.

4.3.2 Linear Trajectory Tracking with no Bounds on Joint Torques and Joint Velocities

In this sub-section, two cases are presented as discussed below.

CASE 1

In this case, a simple trajectory tracking example, with no joint constraint, over a linear trajectory has been considered. The specification of the trajectory is presented in Sec. 4.2. The performance index was defined in the form

$$J = \frac{1}{2}\, z_f^T Q_f z_f + \frac{1}{2} \int_0^{t_f} (z^T Q\, z + u^T R\, u)\, dt \qquad (4.5)$$

where,

$z = [\, e \quad q' \,]^T$,

e is the trajectory error vector,

$z_f = z\Big|_{t=t_f}$,

u is the joint torque vector,

t_f = 8.0 sec, is the time of travel,

Q_f, Q, R are the positive definite weighting matrices,

$Q = \text{diag}\ [Q_1 \quad Q_2]$ and

$Q_f = Q\Big|_{t=t_f}$.

The sub-matrix, Q_1 is of dimension 2×2 while, Q_2 is of dimension 3×3.

The observer equation (3.6), as mentioned in Sec. 3.4, in this case was defined to be same as given by (4.2).

The weight matrices considered in this case were

Q_f = diag [6.0E3 6.0E3 8.0 8.0 8.0]

Q = diag [2.0E4 2.0E4 0.0 0.0 0.0]

R = diag [1.0 1.0 1.0].

The results of the simulation are presented in Figs. 4.8(a)-(e). The manipulator configurations at six instants over the trajectory are plotted in Fig. 4.8(a). The joint angle variation with time is presented in Fig.4.8(b). The joint velocity, end-effector velocity and joint torque variation with time are plotted in Figs. 4.8(c)-(e).

In case of the linear trajectory, the high initial joint velocity (Fig. 4.8(c)) and joint torque (Fig. 4.8(e)) of the third joint is observed. The initial trend is similar to that seen in case of circular trajectory (Figs. 4.1(c) and (e) respectively). It is however observed that the joint torques (Fig. 4.8(e)) are

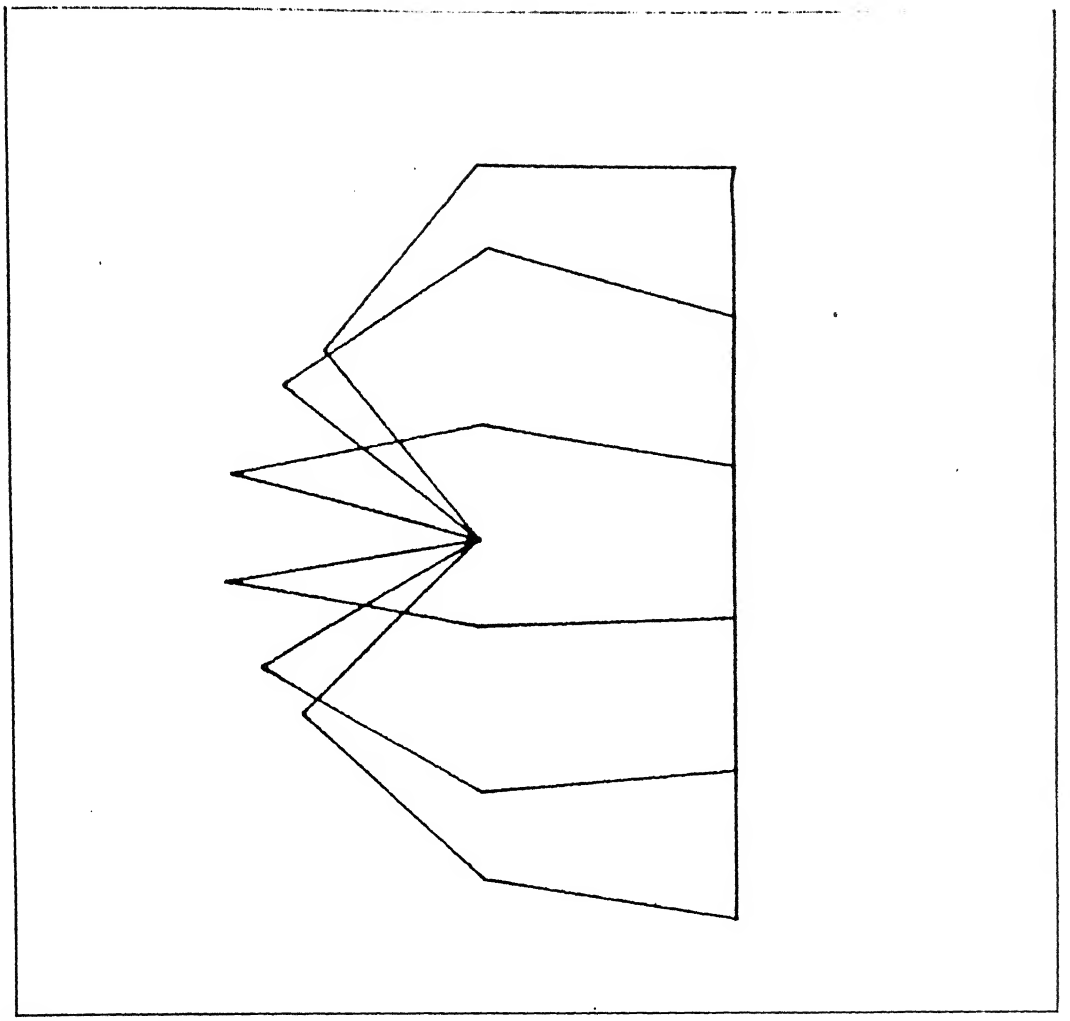

FIG 4.8(a) MANIPULATOR CONFIGURATIONS IN OPTIMAL TRACKING WITHOUT BOUNDS ON JOINT VELOCITIES AND TORQUES

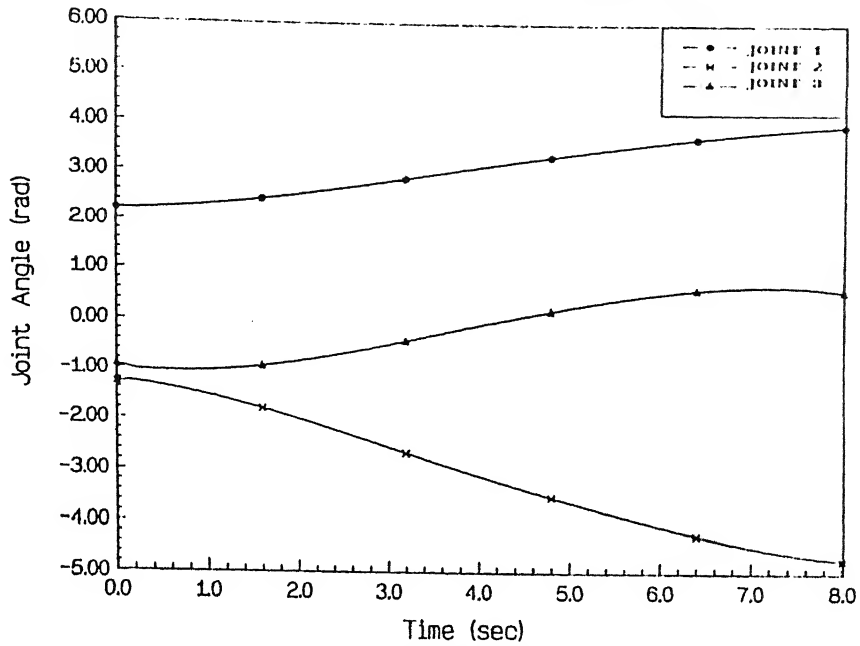

FIG. 4.8(b) VARIATION OF JOINT ANGLES WITH TIME IN OPTIMAL TRACKING WITHOUT BOUNDS ON JOINT VELOCITIES AND TORQUES

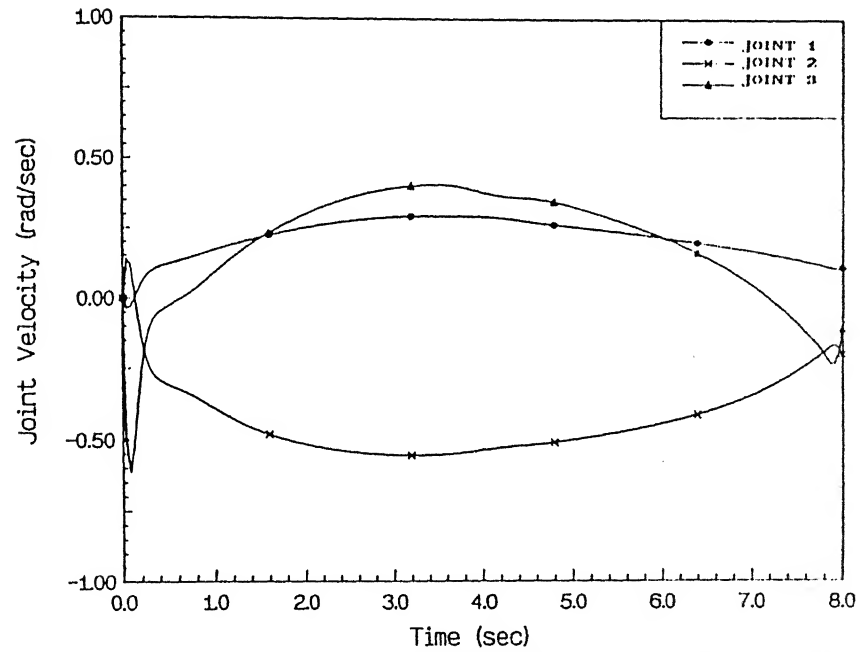

FIG. 4.8(c) VARIATION OF JOINT VELOCITIES WITH TIME IN OPTIMAL TRACKING WITHOUT BOUNDS ON JOINT VELOCITIES AND TORQUES

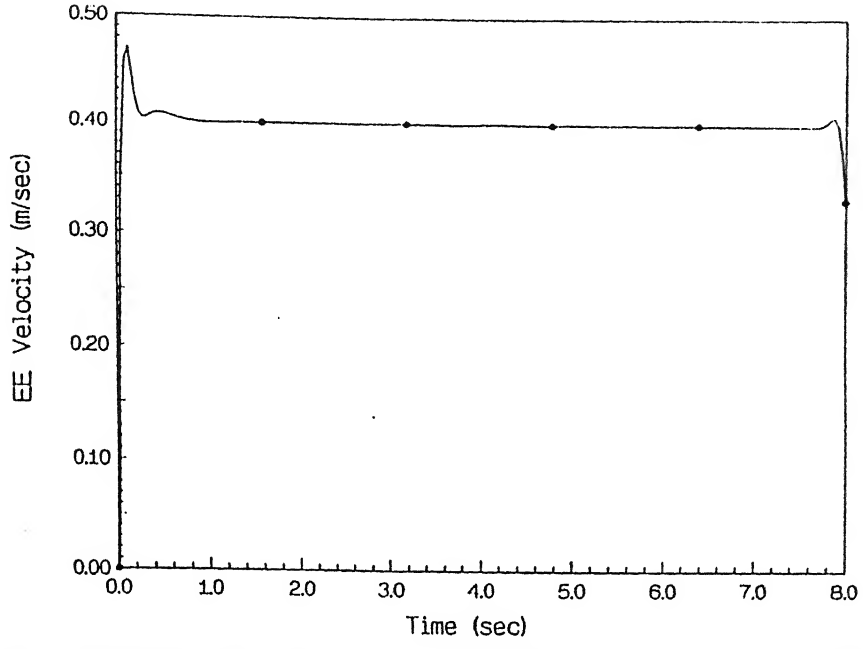

FIG. 4.8(d) VARIATION OF END-EFFECTOR VELOCITY WITH TIME IN OPTIMAL TRACKING WITHOUT BOUNDS ON JOINT VELOCITIES AND TORQUES

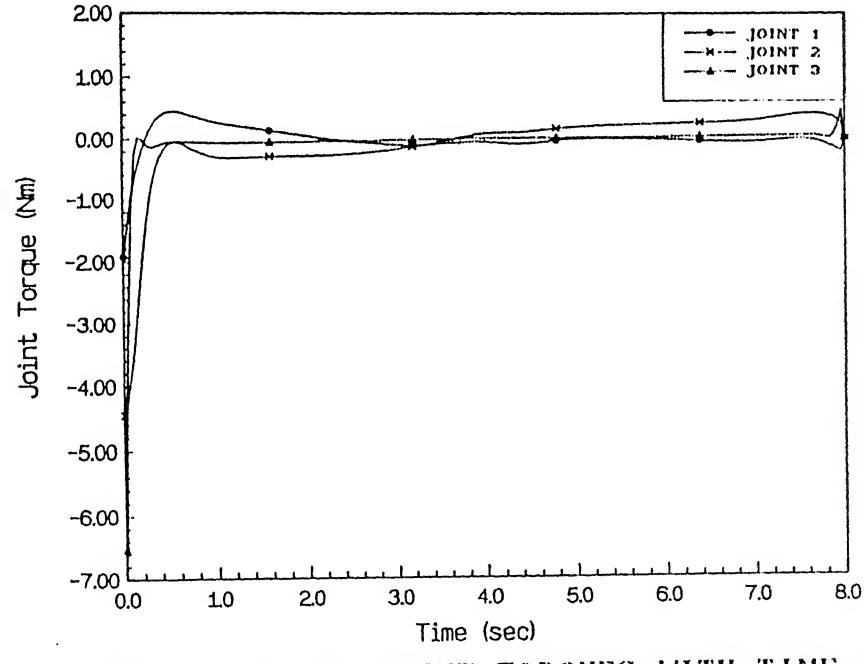

FIG. 4.8(e) VARIATION OF JOINT TORQUES WITH TIME IN OPTIMAL TRACKING WITHOUT BOUNDS ON JOINT VELOCITIES AND TORQUES

low compared to those for the circular trajectory (Fig. 4.1(e)). This is possibly due to the linearity of the trajectory which is free from any change in direction of the end-effector motion unlike that in the case of the circular trajectory.

The simulation results for the linear trajectory tracking using the pseudo-inverse solution is presented in Figs. 4.9(a)-(c). The configurations at different instants over the trajectory are presented in Fig. 4.9(a). The joint angle and joint velocity variation with time are presented in Figs. 4.9(b) and (c) respectively.

The manipulator configurations obtained using the pseudo-inverse solution (Fig. 4.9(a)) is markedly differrent than those obtained using the optimal control algorithm (Fig. 4.8(a)). For the pseudo-inverse solution, it was found that for repetative motion over the linear trajectory (that is for to and fro motion), the configurations for the forward and reverse motions are exactly repeated. Using the present algorithm, it was observed that after two cycles of repeatation of the tracking, a limiting configuration was reached which had no further drift. The results for this observation have not been presented though.

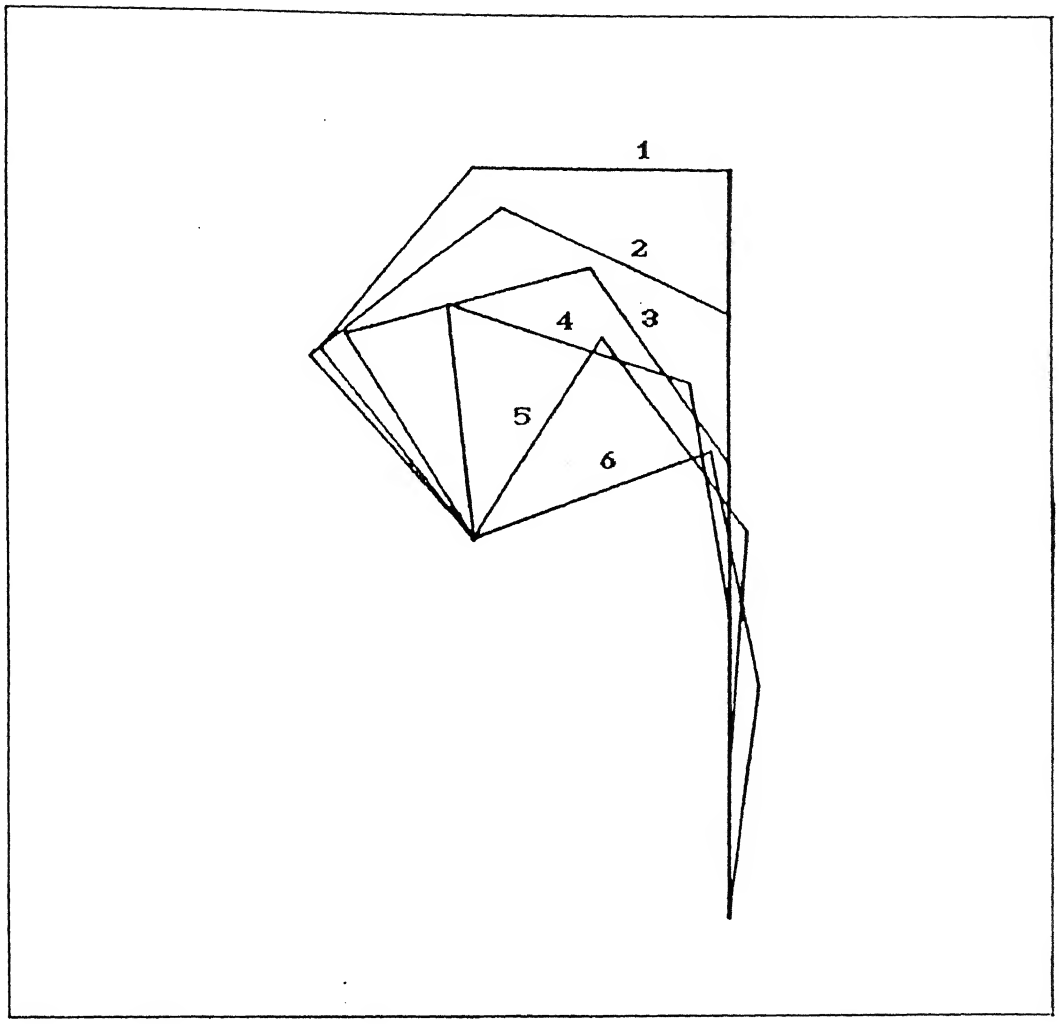

FIG 4.9(a) MANIPULATOR CONFIGURATIONS IN TRACKING USING PSEUDO-INVERSE SOLUTION

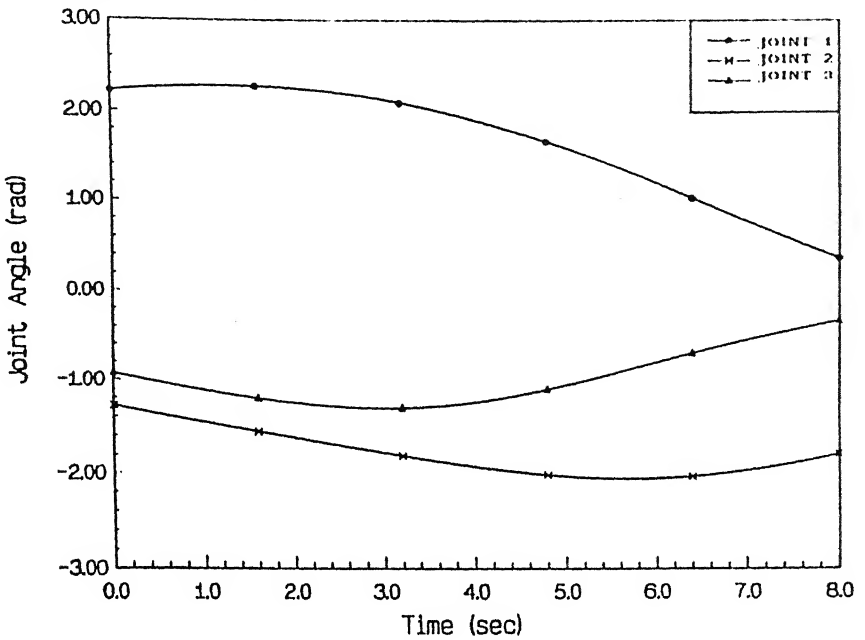

FIG. 4.9(b) VARIATION OF JOINT ANGLES WITH TIME IN TRACKING USING PSEUDO-INVERSE SOLUTION

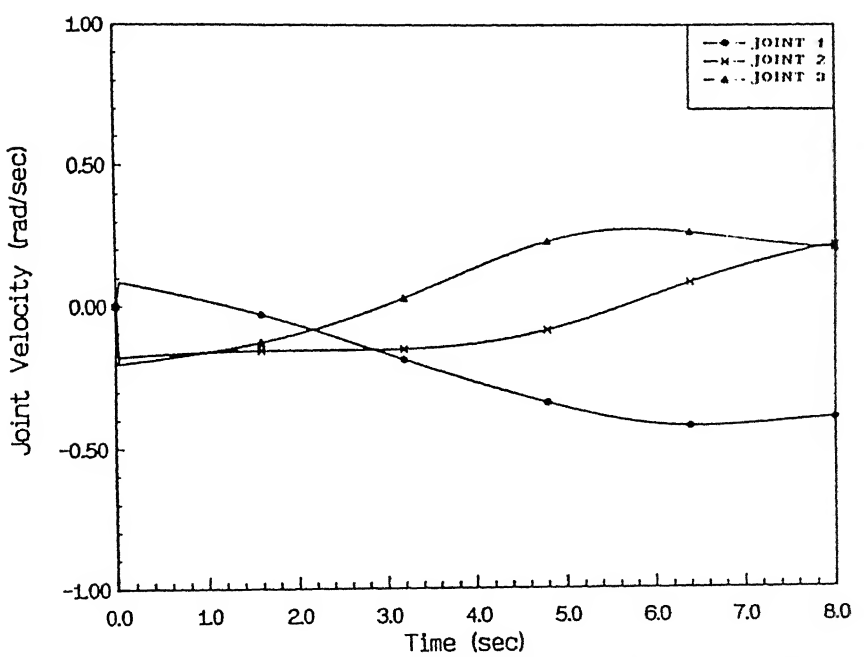

FIG. 4.9(c) VARIATION OF JOINT VELOCITIES WITH TIME IN TRACKING USING PSEUDO-INVERSE SOLUTION

CASE 2

The linear trajectory tracking example with limits on the range of motion of the joints has been considered in this case. It was mentioned earlier that because of the design considerations, the joints of the manipulator can execute only limited motion range. This condition was imposed using an external constraint on the dynamics of the manipulator as was mentioned in Case 3 of Sec. 4.3.1. The equations of motion of the manipulator are therefore the same as given by (4.4).

The observer equation (3.6),as mentioned in Sec. 3.4, in this case was defined to be same as in (4.2). The weight matrices were chosen as

$$Q_f = \text{diag}\ [6.0E3 \quad 6.0E3 \quad 8.0 \quad 8.0 \quad 8.0]$$

$$Q = \text{diag}\ [2.0E4 \quad 2.0E4 \quad 6.0 \quad 6.0 \quad 6.0]$$

$$R = \text{diag}\ [1.0 \quad 1.0 \quad 1.0]$$

The last three diagonal elements of the Q matrix imposed certain weights on the norm of the joint velocities. This was found to be necessary in order to stabilize the numerical integration procedure of the differential equations involved in the algorithm as outlined in Sec. 3.5 when the joint reached its limit and came in contact with the torsional stiffness and dashpot.

In the simple tracking of a linear trajectory, it is observed from Fig. 4.8(a) that the second link folds onto the

first link during the travel. In order to prevent this, a lower joint angle limit for joint two was set at -1.65 radians (-94.53°) on the second joint. The constraint stiffness and damping in this case were taken as

$$k = 600 \text{ N/rad}$$

$$d = 800 \text{ Ns/rad}$$

The results are presented in Figs. 4.10(a)-(e). The manipulator configurations at six instants over the trajectoy are presented in Fig. 4.10(a). The joint angle variation over the trajectory is shown in Fig. 4.10(b). The joint velocity, plotted against time is shown in Fig. 4.10(c) while Figs. 4.10(d) and (e) are the plots of the end-effector velocity and joint torque variation with time.

The joint angle plot in Fig. 4.10(b) shows that the second joint just reaches its lower limit. At that instant the joint velocity reverses direction as observed in Fig. 4.10(c). Since, in this case, the second link could not fold onto the first, the manipulator configurations over the trajectory (Fig. 4.10(a)) are quite different that those observed in Case 1 (Fig. 4.8(a)). The manipulator motion in this case is smooth as compared to those observed in the case of the circular trajectory with joint constraint as in Fig 4.7(b)-(e).

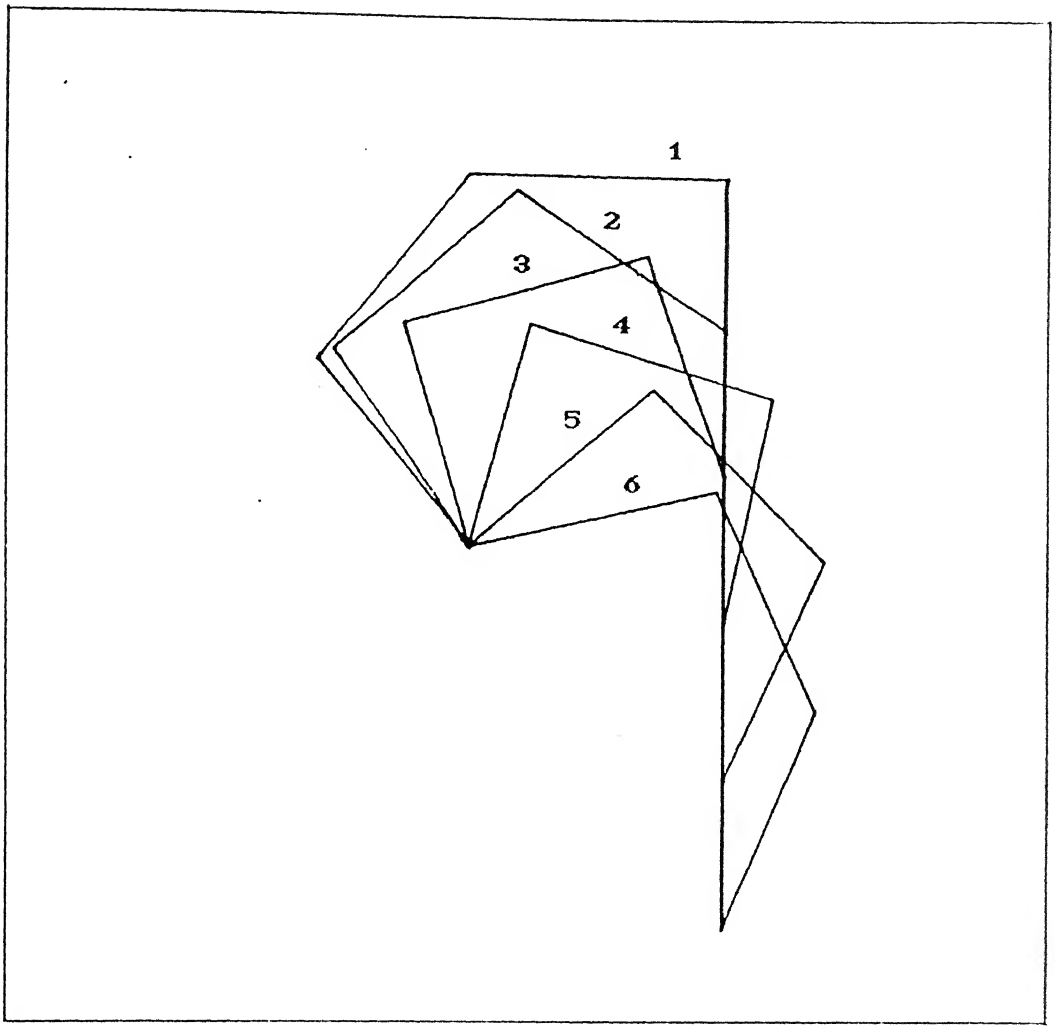

FIG. 4.10(a) MANIPULATOR CONFIGURATIONS IN OPTIMAL TRACKING WITH JOINT CONSTRAINT

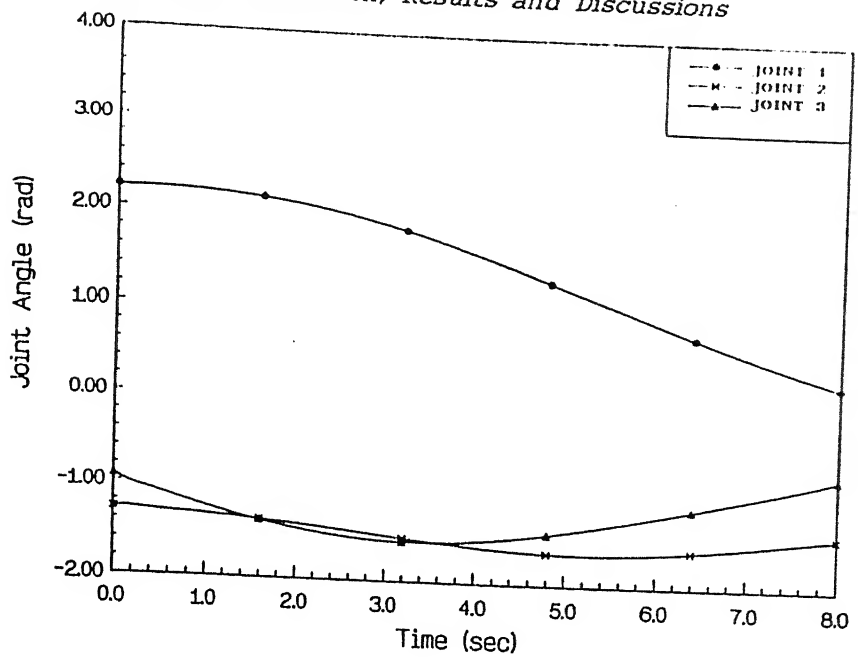

FIG. 4.10(b) VARIATION OF JOINT ANGLES WITH TIME IN OPTIMAL TRACKING WITH JOINT CONSTRAINT

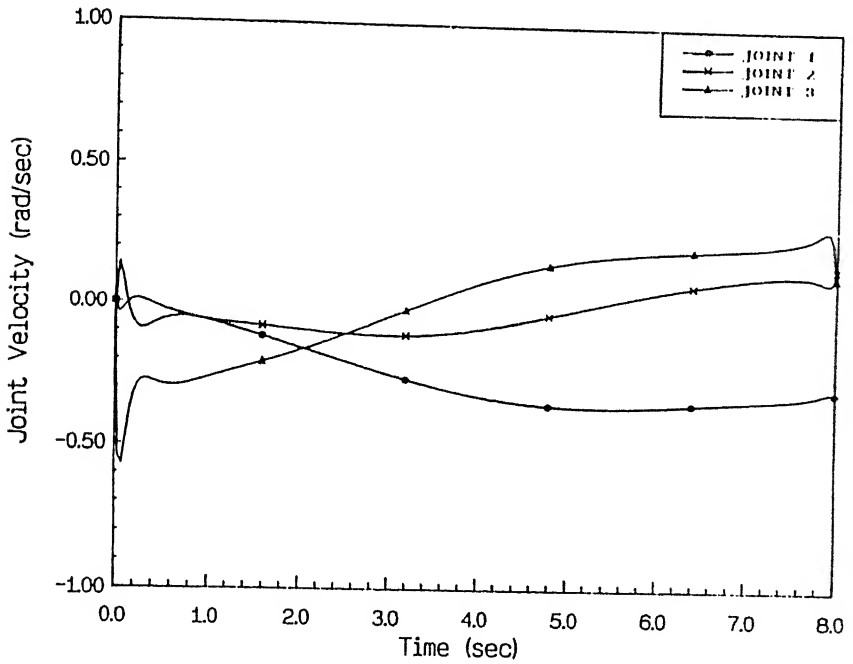

FIG. 4.10(c) VARIATION OF JOINT VELOCITIES WITH TIME IN OPTIMAL TRACKING WITH JOINT CONSTRAINT

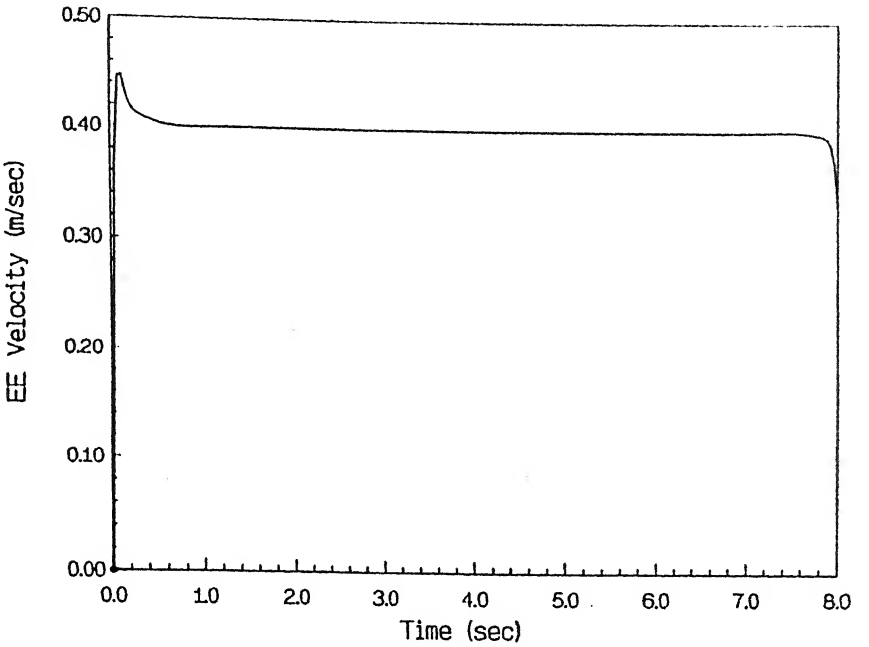

FIG. 4.10(d) VARIATION OF END-EFFECTOR VELOCITY WITH TIME IN OPTIMAL TRACKING WITH JOINT CONSTRAINT

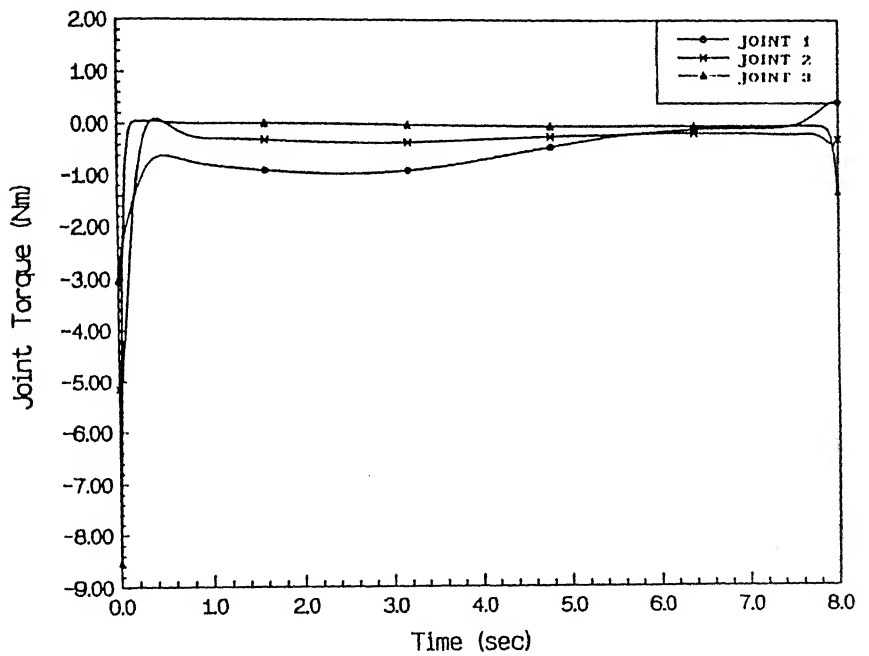

FIG. 4.10(e) VARIATION OF JOINT TORQUES WITH TIME IN OPTIMAL TRACKING WITH JOINT CONSTRAINT

4.3.3 Circular Trajectory Tracking with Bounds on Joint Torques and Joint Velocities

In the examples discussed above, no bound on the joint velocities or torques were prescribed. In all practical cases however, there are definite bounds on the joint velocities and torques from the design considerations and actuator ratings. In such cases, the joint torques obtained from the optimal control algorithm may be infeasible to achieve. This aspect has been taken care of by using a penalty approach as described below.

In this case the performance index was of the form

$$J = \frac{1}{2} z_f^T Q_f z_f + \frac{1}{2} \int_0^{t_f} (z^T Q z + u^T R u) dt \qquad (4.6)$$

where,

$z = [e \quad q']^T$,

e is the trajectory error vector,

$z_f = z\Big|_{t=t_f}$,

u is the joint torque vector,

t_f = 10.0 sec, is the time of travel,

Q_f, Q, R are the positive definite weighting matrices,

Q = diag $[Q_1 \quad Q_2]$ and

$Q_f = Q\Big|_{t=t_f}$.

The sub-matrix, Q_1 is of dimension 2×2 while, Q_2 is of dimension 3×3.

The observer equation (3.6),as mentioned in Sec. 3.4, in this case was defined to be same as in (4.2). The weight matrices, in this case, were defined as

$$R_{ii} = R^{0}_{ii} + \Delta R\ g(\tau_i, \tau_{lim}) \qquad i = 1, 3$$

$$Q_{2ii} = Q^{0}_{2ii} + \Delta Q_2\ g(q_i, q_{lim}) \qquad i = 1, 3$$

where,

R_{ii} is the element of the weight matrix on the joint torques,

Q_{2ii} is the element of the weight matrix on the joint velocities,

R^{0}_{ii}, Q^{0}_{2ii} are the nominal values of the weights and

ΔR, ΔQ_2 are the penalty weights.

The function $g(\cdot,\cdot)$ is defined as

$$g(a, b) = 0.0 \qquad a < b$$

$$= 1.0 \qquad a \geq b.$$

In the present case, the limiting values of the joint velocity and torque are set on the basis of the results obtained in the simple tracking in Case 1 of Sec. 4.3.1. The numerical values are taken as

$$R^{0}_{ii} = 1.0$$

$$\Delta R = 100.0$$

τ_{lim} = 4.0 Nm

Q^{0}_{2ii} = 0.0

ΔQ_{2ii} = 100.0

q_{lim} = 0.80 rad/sec.

The results of the simulation are presented in Figs. 4.11(a)-(e). In Fig. 4.11(a), the manipulator configurations are plotted at regular time intervals at six instants over the trajectory. The joint angle is plotted against time in Fig. 4.11(b). The variation of joint velocities, end-effector velocity and joint torques with time are presented in Figs. 4.11(c)-(e) respectively.

From the joint velocity plot (Fig. 4.11(c)) and the joint torque plot (Fig. 4.11(e)), it is observed that the bounds are indeed maintained by the algorithm.

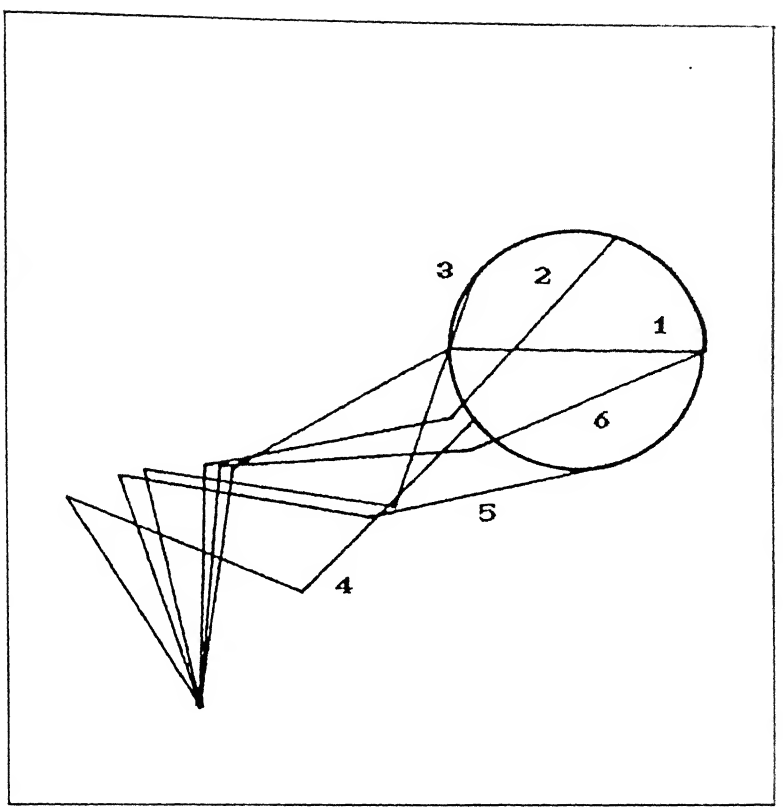

FIG. 4.11(a) MANIPULATOR CONFIGURATIONS IN OPTIMAL TRACKING WITH BOUNDS ON JOINT VELOCITIES AND JOINT TORQUES

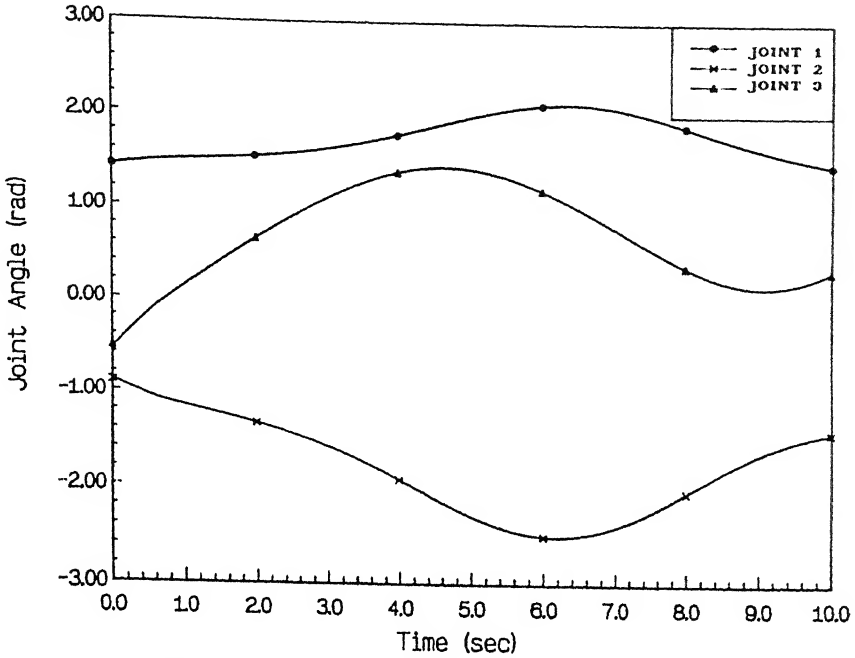

FIG. 4.11(b) VARIATION OF JOINT ANGLES WITH TIME IN OPTIMAL TRACKING WITH BOUNDS ON JOINT VELOCITIES AND JOINT TORQUES

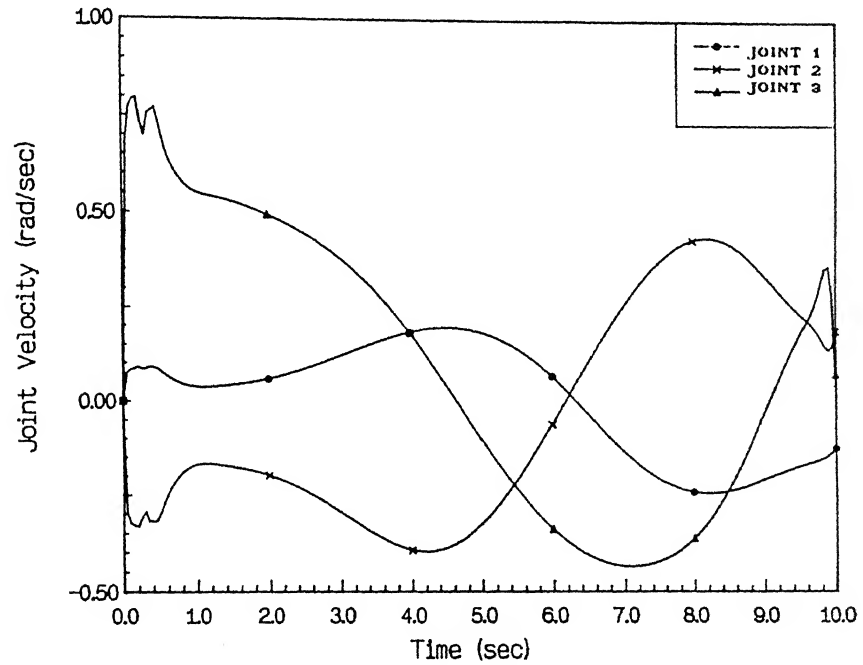

FIG. 4.11(c) VARIATION OF JOINT VELOCITIES WITH TIME IN OPTIMAL TRACKING WITH BOUNDS ON JOINT VELOCITIES AND JOINT TORQUES

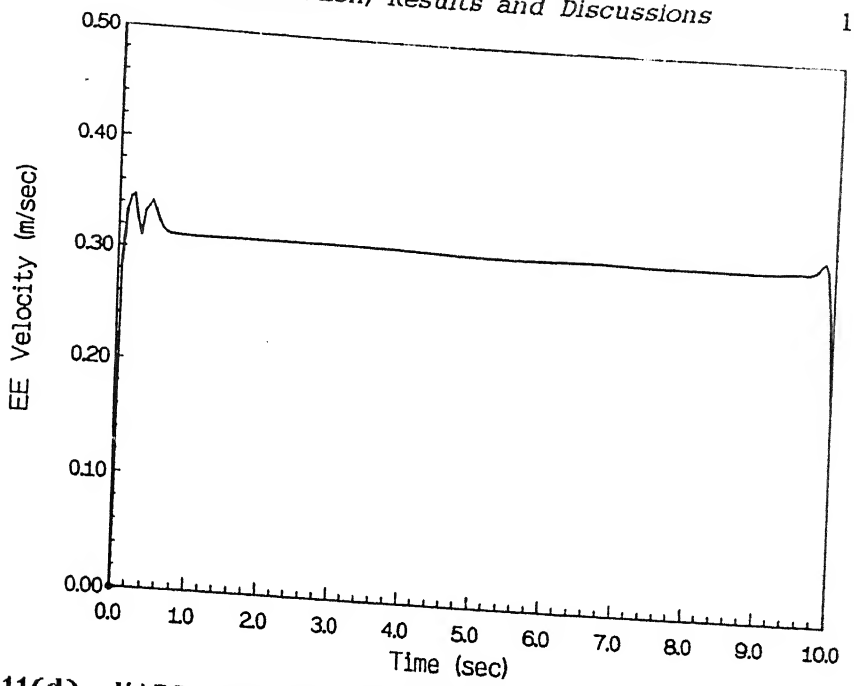

FIG. 4.11(d) VARIATION OF END-EFFECTOR VELOCITY WITH TIME IN OPTIMAL TRACKING WITH BOUNDS ON JOINT VELOCITIES AND TORQUES

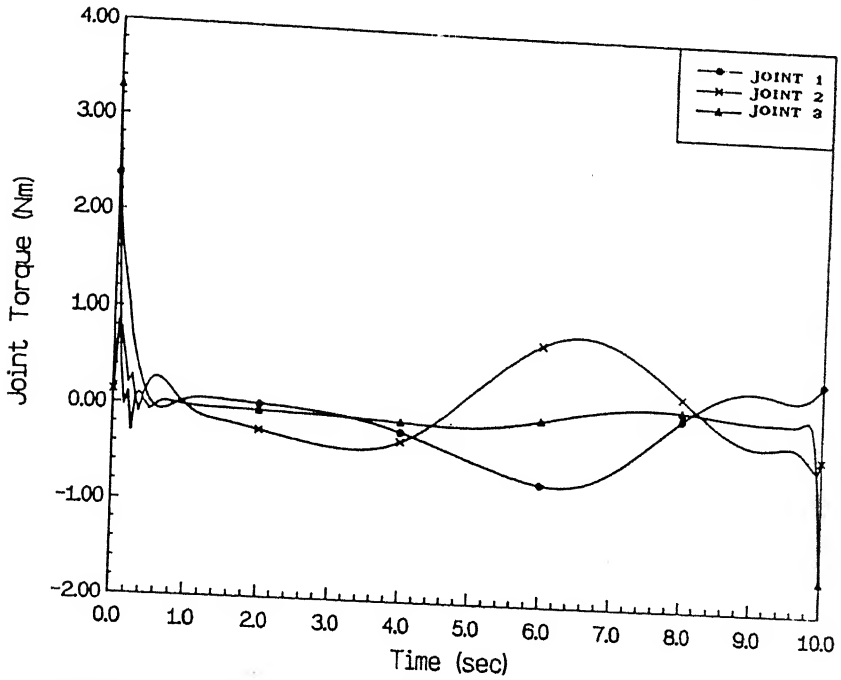

FIG. 4.11(e) VARIATION OF JOINT TORQUES WITH TIME IN OPTIMAL TRACKING WITH BOUNDS ON JOINT VELOCITIES AND TORQUES

CHAPTER 5

CONCLUSIONS AND SCOPE OF FUTURE WORK

5.1 CONCLUSIONS

In this work the trajectory tracking problem of redundant manipulators was investigated. The problem was posed as an Optimal Tracking Problem with fixed initial states, free terminal states and fixed terminal time. The redundancy was resolved by minimizing an integral performance index which was constructed using the weighted norms of the tracking error and the joint torques. The equations of motion of the manipulator were taken as the constraint equations. Using the Variational Principle, the problem was reduced to a NLTPBVP which was solved using an iterative numerical scheme.

The study was made on a three-link planar manipulator. Two types of trajectories, a circular and a linear, were considered. Various types of examples were considered and solved using the algorithm. Some of the results obtained using this approach were compared with the corresponding pseudo-inverse solutions.

In particular, the examples were classified in three broad categories. The conclusions drawn are as follows.

In the first category, the tracking of a circular trajectory

with no bounds on the joint torques or joint velocities was considered. It was observed, from the various cases considered, that the algorithm is suitable for tracking a trajectory as well as meeting additional requirements such as attaining a desired terminal configuration, kinetic energy minimization and satisfying the constraint on the range of joint motion. It was observed that the problem of drift in the configuration for cyclic tasks is present but is stable in nature unlike in the case of the pseudo-inverse solution where it is unstable. A stable starting configuration for such cyclic tasks could be obtained after a few cycles of the task. Another approach to prevent drift was also presented in which the terminal configuration was specified to be same as the starting configuration. The results obtained were quite satisfactory.

In the second category, the tracking of a linear trajectory was considered. In this case two sub-cases, a simple tracking without any constraint on the motion of the joints and tracking with joint motion range limits, were presented. The results obtained serve to confirm the conlusions drawn for the tracking of the circular trajectory.

In the third category, the circular trajectory tracking problem was considered with bounds on the joint torques and joint velocities. The results obtained indicate that the bounds were satisfied by the optimal solution obtained.

In all the cases considered, it was seen that the joint motion and the end-effector motion never ceased at the end of the trajectory. This was because of the fact that the terminal states were considered free in the optimal control solution procedure. Only a penalty was imposed at the terminal time on the norm on the joint velocities. In all the plots of joint torques, an initial non-zero value is observed in the optimal solution, the magnitude of which varied from case to case. This was unavoidable since the time history of the end-effector velocity was not prescribed in the tracking problem. The algorithm is essentially an off-line scheme as far as implementation is concerned.

5.2 SCOPE OF FUTURE WORK

The present work was limited to the numerical investigation of the fixed time optimal trajectory tracking problem for redundant manipulators. The problem may be extended for the minimum time case though, at present, no suggestion can be made as to how to tackle it. Some practical implementation issues can be investigated. As mentioned in the previous section, an initial non-zero joint torque was required in each case which is quite impractical to achieve due to finite response time of all practical actuators. It is expected that by presenting the end-effector velocity along the trajectory, in addition to the end-effector trajectory, and considering this velocity also in the

performance index, the sharp peaks can be reduced. Moreover, the problem was solved as a continuous time optimal control scheme with no attempt being made for discretization. In practical implementations involving a digital computer however, discretization is essential and the stability of the algorithm with sampling frequency has to be investigated. Since the scheme uses the equations of dynamics of the manipulator which are derived theoretically, there are many uncertainities that remain specially due to the flexibility of the links and joint friction. This is a big bottleneck in the practical implementation of the scheme which should be investigated.

APPENDIX A

A.1 THE MINIMUM NORM SOLUTION

Consider the motion rate equations of a redundant manipulator, as discussed in Sec. 2.2, of the form

$$y' = J\, q' \qquad \text{(A.1)}$$

where,

y' is the end-effector velocity vector,

J is the Jacobian matrix of the manipulator and

q' is the joint velocity vector.

The Jacobian matrix of a redundant manipulator is a rectangular matrix and hence is not ordinarily invertible. So, in order to determine the joint velocities when the end-effector velocity is specified, the following optimization problem is posed.

Minimize

$$J = q'^{T}\, W\, q'$$

subject to

$$y' = J\, q'$$

where,

W is a positive definite symmetric weighting matrix.

This constrained optimization problem is converted to an unconstrained optimization problem using Lagrange undetermined multiplier as

$$J = q'^{T} W q' + \lambda^{T} (J q' - y') \qquad (A.2)$$

where,

λ is the Lagrange undetermined multiplier.

The necessary condition for (A.2) to be minimum are given by

$$\frac{\partial J}{\partial q'} = 0 \quad \text{and}$$

$$\frac{\partial J}{\partial \lambda} = 0$$

The above conditions imply that

$$2 W q' + J^{T} \lambda = 0$$

or,
$$q' = \frac{1}{2} W^{-1} J \lambda \qquad (A.3a)$$

and

$$J q' - y' = 0 \qquad (A.3b)$$

Substituting the expression for q' from (A.3a) in (A.3b) yields

$$y' = \frac{1}{2} J W^{-1} J \lambda$$

or, $$\lambda = 2 [J W^{-1} J]^{-1} y'$$

Substituting this expression for λ in (A.3a), the joint velocity vector is expressed in terms of the end-effector veclocity vector as

$$q' = W^{-1} J [J W^{-1} J]^{-1} y'$$

or, $$\dot{q}' = J^{+} y'$$

where,

$J^{+} = W^{-1} J [J W^{-1} J]^{-1}$ is known as pseudo-inverse of the Jacobian matrix.

APPENDIX B

B.1 STATE-SPACE FORMULATION AND LINEARIZATION OF THE EQUATIONS OF MOTION OF A THREE-LINK PLANAR MANIPULATOR

The general representation of the equations of motion of the three-link planar manipulator, as derived in Sec. 3.2 is given by

$$[M(q)]q'' + C(q,q') + F(q') = u \qquad (B.1)$$

where,

$q = [\ \theta_1 \quad \theta_2 \quad \theta_3\ ]^T$ is the joint variable vector,

$q' = [\ \theta_1' \quad \theta_2' \quad \theta_3'\ ]^T$ is the joint velocity vector,

$q'' = [\ \theta_1'' \quad \theta_2'' \quad \theta_3''\ ]^T$ is the joint acceleration vector,

$u = [\ \tau_1 \quad \tau_2 \quad \tau_3\ ]^T$ is the joint torque vector,

$M(q)$ is the inertia matrix of size 3×3,

$C(q,q')$ is the Coriolis and centrepetal force vector of size 3×1,

$F(q')$ if the friction force vector of size 3×1.

The matrix elements are detailed below.

$$M_{11} = I_1 + I_2 + I_3 + m_3 l_1 \rho_3 \cos(\theta_{23}) + 2m_3 l_2 \rho_3 \cos(\theta_3) + m_3 \rho_3^2 + m_3 l_1 l_2 \cos(\theta_2) + m_2 l_1 \rho_2 \cos(\theta_2) + m_3 l_2^2 + m_2 \rho_2^2 + m_{23} l_1^2 + m_3 l_2 l_1 \cos(\theta_2) + m_2 \rho_2 l_1 \cos(\theta_2) + m_3 \rho_3 l_1 \cos(\theta_{23}) + m_1 \rho_1^2$$

$$M_{12} = I_2 + I_3 + 2m_3 l_2 \rho_3 \cos(\theta_3) + m_3 \rho_3^2 + m_3 l_2^2 + m_2 \rho_2^2 + m_3 l_2 l_1 \cos(\theta_2) + m_2 \rho_2 l_1 \cos(\theta_2) + m_3 \rho_3 l_1 \cos(\theta_{23})$$

$$M_{13} = I_{zz_3} + m_3 \rho_3^2 + m_3 \rho_3 l_2 \cos(\theta_3) + m_3 \rho_3 l_1 \cos(\theta_{23})$$

$$M_{21} = I_2 + I_3 + m_3 l_1 \rho_3 \cos(\theta_{23}) + 2m_3 l_2 \rho_3 \cos(\theta_3) + m_3 \rho_3^2 + m_3 l_1 l_2 \cos(\theta_2) + m_2 l_1 \rho_2 \cos(\theta_2) + m_3 l_2^2 + m_2 \rho_2^2$$

$$M_{22} = I_2 + I_3 + 2m_3 l_2 \rho_3 \cos(\theta_3) + m_3 \rho_3^2 + m_3 l_2^2 + m_2 \rho_2^2$$

$$M_{23} = I_3 + m_3 \rho_3^2 + m_3 l_3 \rho_2 \cos(\theta_3)$$

$$M_{31} = I_3 + m_3 l_1 \rho_3 \cos(\theta_{23}) + 2m_3 l_2 \rho_3 \cos(\theta_3) + m_3 \rho_3^2$$

$$M_{32} = I_3 + m_3 l_2 \rho_3 \cos(\theta_3) + m_3 \rho_3^2$$

$$M_{33} = I_3 + m_3 \rho_3^2$$

$$C_1 = m_3 l_1 \rho_3 \theta_1'^2 \sin(\theta_{23}) + m_3 l_2 \rho_3 \theta_{12}'^2 \sin(\theta_3) + m_{23} l_1 \rho_2 \theta_1'^2 \sin(\theta_2) - m_3 \rho_3 l_2 \theta_{123}'^2 \sin(\theta_3) - m_2 l_1 \bar{\rho}_2 \theta_1'^2 \sin(\theta_2) - m_3 l_2 l_1 \theta_{12}'^2 \sin(\theta_2) - m_2 \rho_2 l_1 \theta_{12}'^2 \sin(\theta_2) - m_3 \rho_3 l_1 \theta_{123}'^2 \sin(\theta_{23})$$

$$C_2 = m_3 l_1 \rho_3 \theta_1'^2 \sin(\theta_{23}) + m_3 l_2 \rho_3 \theta_{12}'^2 \sin(\theta_3) + m_{23} l_1 l_2 \theta_1'^2 \sin(\theta_2) - m_3 l_3 \rho_2 \theta_{123}'^2 \sin(\theta_3) - m_2 l_1 \bar{\rho}_2 \theta_2'^2 \sin(\theta_2)$$

$$C_3 = m_3 l_1 \rho_3 \theta_1'^2 \sin(\theta_{23}) + m_3 l_2 \rho_3 \theta_{12}'^2 \sin(\theta_3)$$

The conversion of the equations of motion of the manipulator to state space form has been presented in chapter three. The

state-space representation, as given by (3.11) in Sec. 3.4 is

$$\begin{aligned} q_1' &= q_2 \\ q_2' &= [M(q_1)]^{-1} [- C(q_1,q_2) - F(q_2) + u] \end{aligned} \qquad \text{(B.2)}$$

where,

$q_1 = [\theta_1 \quad \theta_2 \quad \theta_3]^T$ is the joint variable vector and

$q_2 = [\theta_1' \quad \theta_2' \quad \theta_2']^T$ is the joint velocity vector.

Let

$$\begin{aligned} x &= [\, q_1 \quad q_2 \,]^T \\ &= [\, \theta_1 \quad \theta_2 \quad \theta_3 \quad \theta_1' \quad \theta_2' \quad \theta_3' \,]^T \\ &= [\, x_1 \quad x_2 \quad x_3 \quad x_4 \quad x_5 \quad x_6 \,]^T. \end{aligned} \qquad \text{(B.3)}$$

Then (B.2) above can be written as

$$x' = f(x, u) \qquad \text{(B.4)}$$

where,

$$f(x,u) = [q_2 \quad [M(q_1)]^{-1}\{ - C(q_1,q_2) - F(q_2) + u \}]^T$$

$$= \begin{bmatrix} x_4 \\ x_5 \\ x_6 \\ [M(q_1)]^{-1} r(x,u) \end{bmatrix}$$

where,

$$r(x, u) = [\, r_1 \;\; r_2 \;\; r_3 \,]^T$$
$$= [-\, C(q_1, q_2) - F(q_2) + u]. \qquad (B.5)$$

The state equations above are linearized based on a nominal trajectory. The linearization scheme has been presented in Sec. 3.5. The linearized equations are represented as

$$x' = A\,x + B\,u + e \qquad (B.6)$$

where, the A and B matrices are defined over the i^{th} trajectory as

$$A = \frac{\partial f}{\partial x} \quad \text{and}$$

$$B = \frac{\partial f}{\partial u}\,.$$

Let

$$A = [\, A_1^T \;\; A_2^T \;\; A_3^T \;\; A_4^T \;\; A_5^T \;\; A_6^T \,]^T$$

where,

A_i represents the i^{th} row of A matrix.

The row elements of the matrices A and B can be derived from the definition above in (B.6) as described below.

The first three rows of the A matrix are given by

$$A_1 = \left(\frac{\partial}{\partial x} [f_1(x, u)] \right)^T = [\, 0 \quad 0 \quad 0 \quad 1 \quad 0 \quad 0 \,]$$

$$A_2 = \left(\frac{\partial}{\partial x} [f_2(x, u)] \right)^T = [\, 0 \quad 0 \quad 0 \quad 0 \quad 1 \quad 0 \,]$$

$$A_3 = \left(\frac{\partial}{\partial x} [f_3(x, u)] \right)^T = [\, 0 \quad 0 \quad 0 \quad 0 \quad 0 \quad 1 \,]$$

where,

$f_i(x, u)$ is the i^{th} element of $f(x, u)$ defined in (B.4).

The j^{th} element of the vectors A_4, A_5 and A_6 where j varies from 1 through 6 are given as follows.

$$\begin{aligned}
A_{4j} &= \left(\frac{\partial}{\partial x_j} [f_4(x, u)] \right) \\
&= \frac{1}{\Delta^2} \Bigg[\Delta \Bigg(B_{11} \frac{\partial}{\partial x_i}(r_1) + r_1 \Big\{ M_{22} \frac{\partial}{\partial x_i}(M_{33}) + M_{33} \frac{\partial}{\partial x_i}(M_{22}) \\
&\quad - M_{32} \frac{\partial}{\partial x_i}(M_{23}) - M_{23} \frac{\partial}{\partial x_i}(M_{32}) \Big\} + B_{12} \frac{\partial}{\partial x_i}(r_2) \\
&\quad + r_2 \Big\{ M_{32} \frac{\partial}{\partial x_i}(M_{13}) + M_{13} \frac{\partial}{\partial x_i}(M_{32}) - M_{12} \frac{\partial}{\partial x_i}(M_{33}) \\
&\quad - M_{33} \frac{\partial}{\partial x_i}(M_{12}) \Big\} + B_{13} \frac{\partial}{\partial x_i}(r_3) + r_3 \Big\{ M_{12} \frac{\partial}{\partial x_i}(M_{23}) \\
&\quad + M_{23} \frac{\partial}{\partial x_i}(M_{12}) - M_{22} \frac{\partial}{\partial x_i}(M_{13}) - M_{13} \frac{\partial}{\partial x_i}(M_{22}) \Big\} \Bigg) \\
&\quad - (B_{11}r_1 + B_{22}r_2 + B_{33}r_3) \Big(M_{11}(M_{22} \frac{\partial}{\partial x_i}(M_{33}) \\
&\quad + M_{33} \frac{\partial}{\partial x_i}(M_{22}) - M_{32} \frac{\partial}{\partial x_i}(M_{23}) - M_{23} \frac{\partial}{\partial x_i}(M_{32})) \\
&\quad + (M_{22}M_{33} - M_{32}M_{23}) + \frac{\partial}{\partial x_i}(M_{11}) - M_{12}(M_{21} \frac{\partial}{\partial x_i}(M_{33})
\end{aligned}$$

$$+ M_{33}\frac{\partial}{\partial x_i}(M_{21}) - M_{31}\frac{\partial}{\partial x_i}(M_{23}) - M_{23}\frac{\partial}{\partial x_i}(M_{31}))$$

$$- (M_{21}M_{33} - M_{31}M_{23}) + \frac{\partial}{\partial x_i}(M_{12}) - M_{13}(M_{21}\frac{\partial}{\partial x_i}(M_{32})$$

$$+ M_{32}\frac{\partial}{\partial x_i}(M_{21}) - M_{31}\frac{\partial}{\partial x_i}(M_{22}) - M_{22}\frac{\partial}{\partial x_i}(M_{31}))$$

$$+ (M_{21}M_{32} - M_{31}M_{22}) + \frac{\partial}{\partial x_i}(M_{13}) \Big) \Big]$$

$$A_{5j} = \left(\frac{\partial}{\partial x_j}[f_5(x, u)] \right)$$

$$= \frac{1}{\Delta^2}\Big[\Delta \Big(B_{21}\frac{\partial}{\partial x_i}(r_1) + r_1 \Big\{ M_{31}\frac{\partial}{\partial x_i}(M_{23}) + M_{23}\frac{\partial}{\partial x_i}(M_{31})$$

$$- M_{21}\frac{\partial}{\partial x_i}(M_{33}) - M_{33}\frac{\partial}{\partial x_i}(M_{21}) \Big\} + B_{22}\frac{\partial}{\partial x_i}(r_2)$$

$$+ r_2 \Big\{ M_{11}\frac{\partial}{\partial x_i}(M_{33}) + M_{33}\frac{\partial}{\partial x_i}(M_{11}) - M_{31}\frac{\partial}{\partial x_i}(M_{13})$$

$$- M_{13}\frac{\partial}{\partial x_i}(M_{31}) \Big\} + B_{23}\frac{\partial}{\partial x_i}(r_3) + r_3 \Big\{ M_{21}\frac{\partial}{\partial x_i}(M_{13})$$

$$+ M_{13}\frac{\partial}{\partial x_i}(M_{21}) - M_{11}\frac{\partial}{\partial x_i}(M_{23}) - M_{23}\frac{\partial}{\partial x_i}(M_{11}) \Big\} \Big)$$

$$- (B_{21}r_1 + B_{22}r_2 + B_{23}r_3) \Big(M_{11}(M_{22}\frac{\partial}{\partial x_i}(M_{33})$$

$$+ M_{33}\frac{\partial}{\partial x_i}(M_{22}) - M_{32}\frac{\partial}{\partial x_i}(M_{23}) - M_{23}\frac{\partial}{\partial x_i}(M_{32}))$$

$$+ (M_{22}M_{33} - M_{32}M_{23}) + \frac{\partial}{\partial x_i}(M_{11}) - M_{12}(M_{21}\frac{\partial}{\partial x_i}(M_{33})$$

$$+ M_{33}\frac{\partial}{\partial x_i}(M_{21}) - M_{31}\frac{\partial}{\partial x_i}(M_{23}) - M_{23}\frac{\partial}{\partial x_i}(M_{31}))$$

$$- (M_{21}M_{33} - M_{31}M_{23}) + \frac{\partial}{\partial x_i}(M_{12}) - M_{13}(M_{21}\frac{\partial}{\partial x_i}(M_{32})$$

$$+ M_{32}\frac{\partial}{\partial x_i}(M_{21}) - M_{31}\frac{\partial}{\partial x_i}(M_{22}) - M_{22}\frac{\partial}{\partial x_i}(M_{31}))$$

$$+ \left(M_{21}M_{32} - M_{31}M_{22} \right) + \frac{\partial}{\partial x_i}(M_{13}) \Big) \Big]$$

$$A_{6j} = \left(\frac{\partial}{\partial x_j}[f_6(x, u)] \right)$$

$$= \frac{1}{\Delta^2} \Big[\Delta \Big(B_{31} \frac{\partial}{\partial x_i}(r_1) + r_1 \Big\{ M_{21} \frac{\partial}{\partial x_i}(M_{32}) + M_{32} \frac{\partial}{\partial x_i}(M_{21})$$

$$- M_{31} \frac{\partial}{\partial x_i}(M_{22}) - M_{22} \frac{\partial}{\partial x_i}(M_{31}) \Big\} + B_{32} \frac{\partial}{\partial x_i}(r_2)$$

$$+ r_2 \Big\{ M_{31} \frac{\partial}{\partial x_i}(M_{12}) + M_{12} \frac{\partial}{\partial x_i}(M_{31}) - M_{11} \frac{\partial}{\partial x_i}(M_{31})$$

$$- M_{31} \frac{\partial}{\partial x_i}(M_{11}) \Big\} + B_{33} \frac{\partial}{\partial x_i}(r_3) + r_3 \Big\{ M_{11} \frac{\partial}{\partial x_i}(M_{22})$$

$$+ M_{22} \frac{\partial}{\partial x_i}(M_{11}) - M_{21} \frac{\partial}{\partial x_i}(M_{12}) - M_{12} \frac{\partial}{\partial x_i}(M_{21}) \Big\} \Big)$$

$$- (B_{31}r_1 + B_{32}r_2 + B_{33}r_3) \Big(M_{11}(M_{22} \frac{\partial}{\partial x_i}(M_{33})$$

$$+ M_{33} \frac{\partial}{\partial x_i}(M_{22}) - M_{32} \frac{\partial}{\partial x_i}(M_{23}) - M_{23} \frac{\partial}{\partial x_i}(M_{32}))$$

$$+ \left(M_{22}M_{33} - M_{32}M_{23} \right) + \frac{\partial}{\partial x_i}(M_{11}) - M_{12}(M_{21} \frac{\partial}{\partial x_i}(M_{33})$$

$$+ M_{33} \frac{\partial}{\partial x_i}(M_{21}) - M_{31} \frac{\partial}{\partial x_i}(M_{23}) - M_{23} \frac{\partial}{\partial x_i}(M_{31}))$$

$$- \left(M_{21}M_{33} - M_{31}M_{23} \right) + \frac{\partial}{\partial x_i}(M_{12}) - M_{13}(M_{21} \frac{\partial}{\partial x_i}(M_{32})$$

$$+ M_{32} \frac{\partial}{\partial x_i}(M_{21}) - M_{31} \frac{\partial}{\partial x_i}(M_{22}) - M_{22} \frac{\partial}{\partial x_i}(M_{31}))$$

$$+ \left(M_{21}M_{32} - M_{31}M_{22} \right) + \frac{\partial}{\partial x_i}(M_{13}) \Big) \Big]$$

The B matrix is defined as

$$B = \frac{\partial}{\partial u}[f(x, u)]$$

$$= \begin{bmatrix} 0 & 0 & 0 \\ 0 & 0 & 0 \\ 0 & 0 & 0 \\ M_{22}M_{33} - M_{32}M_{23} & -(M_{12}M_{33} - M_{32}M_{13}) & M_{12}M_{23} - M_{22}M_{13} \\ -(M_{21}M_{33} - M_{31}M_{23}) & M_{11}M_{33} - M_{31}M_{13} & -(M_{11}M_{23} - M_{21}M_{13}) \\ M_{21}M_{32} - M_{31}M_{22} & -(M_{11}M_{32} - M_{31}M_{12}) & M_{11}M_{22} - M_{21}M_{12} \end{bmatrix}$$

The various terms in the expressions above are expanded in terms of the quantities defined in the equations of motion in (B.1) above and are given below.

$$\frac{\partial}{\partial x_i}(M_{jk}) = 0 \qquad \text{for } i = 4, 5, 6,\ j = 1, 2, 3 \text{ and } k = 1, 2, 3$$

$$\frac{\partial}{\partial x_2}(M_{11}) = - m_3 l_1 \rho_3 S_{23} - m_3 l_1 l_2 S_2 - m_2 l_2 \rho_2 S_2 - m_3 l_2 l_1 S_2 - m_2 \rho_2 l_1 S_2 - m_3 \rho_3 l_1 S_{23}$$

$$\frac{\partial}{\partial x_2}(M_{12}) = - 2m_3 l_2 l_1 S_2 - m_2 \rho_2 l_1 S_2 - m_3 \rho_3 l_1 S_{23}$$

$$\frac{\partial}{\partial x_2}(M_{13}) = - m_3 \rho_3 l_1 S_{23}$$

$$\frac{\partial}{\partial x_3}(M_{11}) = - m_3 \rho_3 l_1 S_{23} - m_3 l_2 \rho_3 S_3 - m_3 \rho_3 l_1 S_{23}$$

$$\frac{\partial}{\partial x_3}(M_{12}) = - 2m_3 l_2 \rho_3 S_3 - m_3 \rho_3 l_1 S_{23}$$

$$\frac{\partial}{\partial x_3}(M_{13}) = - m_3 \rho_3 l_2 S_3 - m_3 \rho_3 l_1 S_{23}$$

$$\frac{\partial}{\partial x_2}(M_{21}) = - m_3 l_1 \rho_3 S_{23} - m_{23} l_1 l_2 W_2 + m_2 l_1 \rho_2 S_2$$

$$\frac{\partial}{\partial x_2}(M_{22}) = 0$$

$$\frac{\partial}{\partial x_2}(M_{23}) = 0$$

$$\frac{\partial}{\partial x_3}(M_{21}) = - m_3 l_1 \rho_3 S_{23} - 2 m_3 l_2 l_3 S_3$$

$$\frac{\partial}{\partial x_3}(M_{22}) = - m_3 l_2 \rho_3 S_3 - m_3 \rho_3 l_2 S_3$$

$$\frac{\partial}{\partial x_3}(M_{23}) = - m_3 \rho_3 l_2 S_3$$

$$\frac{\partial}{\partial x_2}(M_{31}) = - m_3 l_1 \rho_3 S_{23}$$

$$\frac{\partial}{\partial x_2}(M_{32}) = 0$$

$$\frac{\partial}{\partial x_2}(M_{33}) = 0$$

$$\frac{\partial}{\partial x_3}(M_{31}) = - m_3 l_1 \rho_3 S_{23} - m_3 l_2 \rho_3 S_3$$

$$\frac{\partial}{\partial x_3}(M_{32}) = - m_3 l_2 \rho_3 S_3$$

$$\frac{\partial}{\partial x_3}(M_{33}) = 0$$

$$\frac{\partial}{\partial x_1}(r_1) = 0$$

$$\frac{\partial}{\partial x_2}(r_1) = - m_3 l_1 \rho_3 x_4 C_{23} - m_{23} l_1 l_2 x_4 C_2 + m_2 l_1 \bar{\rho}_2 x_4 C_2 + m_3 l_2 l_1 x_{45} C_2 + m_2 \rho_2 l_1 C_2 x_{45} + m_3 \rho_3 l_1 C_{23} x_{456}$$

$$\frac{\partial}{\partial x_3}(r_1) = - m_3 l_1 \rho_3 x_4 C_{23} - m_3 l_2 \rho_3 x_{45} C_3$$

$$- m_3\rho_3 l_2 x_{456} C_3 + m_3\rho_3 l_1 x_{345} C_{23}$$

$$\frac{\partial}{\partial x_4}(r_1) = -2\,(m_3 l_1 \rho_3 x_4 S_{23} + m_3 l_2 \rho_3 x_{45} S_3 + m_{23} l_1 l_2 x_4 S_2 -$$

$$m_3\rho_3 l_2 x_{456} S_3 - m_2 l_1 \bar{\rho}_2 x_4 S_2 - m_3 l_2 l_1 x_{45} - m_2\rho_2 l_1 x_{45} S_2$$

$$- m_3\rho_3 l_1 x_{456}$$

$$\frac{\partial}{\partial x_5}(r_1) = -2\,(m_3 l_2 \rho_3 x_{45} S_3 - m_3\rho_3 l_2 x_{456} S_3 - m_3 l_3 l_2 x_{45} S_2$$

$$- m_2\rho_2 l_1 x_{45} S_2 - m_3\rho_3 l_1 x_{456} S_{23})$$

$$\frac{\partial}{\partial x_6}(r_1) = -2\,(-m_3\rho_3 l_2 x_{456} S_3 - m_3\rho_3 l_1 x_{456} S_{23})$$

$$\frac{\partial}{\partial x_1}(r_2) = 0$$

$$\frac{\partial}{\partial x_2}(r_2) = - m_3 l_1 \rho_3 x_4 C_{23} - m_{23} l_2 l_1 x_4 C_2$$

$$- m_2 l_1 \bar{\rho}_2 x_4 C_2$$

$$\frac{\partial}{\partial x_3}(r_2) = - m_3 l_1 \rho_3 x_4 C_{23} + m_3 l_2 \rho_3 x_{45} C_3$$

$$- m_3\rho_3 l_2 x_{456} C_3$$

$$\frac{\partial}{\partial x_4}(r_2) = -2\,(m_3 l_1 \rho_3 x_4 S_{23} + m_3 l_2 \rho_3 x_{45} S_3 + m_{23} l_1 l_2 x_4 S_2 -$$

$$m_3\rho_3 l_2 x_{456} S_3 - m_3 l_2 \rho_2 x_4 S_2)$$

$$\frac{\partial}{\partial x_5}(r_2) = -2\,(m_3 l_2 \rho_3 x_{45} S_3 - m_3\rho_3 l_2 x_{456} S_3)$$

$$\frac{\partial}{\partial x_6}(r_2) = 2 m_3\rho_3 l_2 x_{456} S_3$$

$$\frac{\partial}{\partial x_1}(r_3) = 0$$

$$\frac{\partial}{\partial x_2}(r_3) = - m_3 l_1 x_4 \rho_3 C_{23}$$

$$\frac{\partial}{\partial x_3}(r_3) = -m_3 l_1 \rho_3 x_4 C_{23} - m_3 l_2 \rho_3 x_{45} C_3$$

$$\frac{\partial}{\partial x_4}(r_3) = -2\,(m_3 l_1 \rho_3 x_4 S_{23} + m_3 l_2 \rho_3 x_{45} S_3)$$

$$\frac{\partial}{\partial x_5}(r_3) = -2 m_3 l_2 \rho_3 x_{45} S_3$$

$$\frac{\partial}{\partial x_6}(r_3) = 0$$

where,

M_{ij} represents the elements of the inertia matrix as defined in (B.1),

x_i is the i^{th} state vector as defined in (B.3),

r_i is a function of the state vectors as defined in (B.5),

$x_{1..n} = x_1 + \ldots + x_n$,

$S_{1..n} = \sin(x_1 + \ldots + x_n)$,

$C_{1..n} = \cos(x_1 + \ldots + x_n)$ and

$\Delta = \det [M(q)]$.

REFERENCES

Anderson, K., Angeles, J., [1989], "*Kinematic Inversion of Robotic Manipulators in the Presence of Redundancies*", International Journal of Robotics Research, Vol. 8, No. 6, pp 80-97.

Baillieul, J., [1985], "*Kinematic Programming Alternatives for Redundant Manipulators*", Proceedings of the IEEE International Conference on Robotics and Automation, pp 722-728.

Dubey, R. V., Euler, J. A., Babcock, S. M., [1988], "*An Efficient Gradient Projection Optimization Scheme for seven DOF Redundant Robot with Spherical Wrist*", Proceedings of the IEEE International Conference on Robotics and Automation, pp 28-36.

Dubey, R. V., Euler, J. A., Babcock, S. M., [1991], "*Real Time Implementation of an Optimization Scheme for seven DOF Redundant Manipulators*", IEEE Transactions on Robotics and Automation, Vol. 7, No. 5, pp 579-588.

Dubey, R. V., Luh, J. Y. S., [1987], "*Redundant Robot Control for higher Flexibility*", Proceedings of the IEEE International Conference on Robotics and Automation, pp 1066-1072.

Fu, K. S., Gonzalez, R. C., Lee, C. S. G., [1987], "*Robotics: Control, Sensing, Vision and Intelligence*", McGraw-Hill Book Company.

Gupta, S., Luh, J. Y. S., [1991], "*Closed-Loop Control of Manipulators with Redundant Joints Using the Hamilton-Jacobi-Bellman Equation*", Proceedings of the IEEE International Journal on Robotics and Automation,pp 472-477.

Hollerbach, J. M., Suh, K. C., [1985], "*Redundancy Resolution of Manipulators through Torque Optimization*", Proceedings of IEEE International Conference on Robotics and Automation, pp 1016-1021.

Hollerbach, J. M., Suh, K. C., [1987(a)], "*Redundancy Resolution of Manipulators through Torque Optimization*", IEEE Journal of Robotics and Automation, Vol RA-3, No. 4, pp 308-316.

Hollerbach, J. M., Suh, K. C., [1987(b)], "*Local versus Global Torque Optimization of Redundant Manipulators*" , Proceedings of IEEE International Journal of Robotics and Automation, pp 619-624.

Hsu, P., Hauser, J., Sastry, S., [1988], "*Dynamic Control of Redundant Manipulators*", Proceedings of IEEE International Conference on Robotics and Automation, pp 183-187.

Kazerounian, K., Nedungadi, A., [1987], "*An Alternative Method for Minimization of the Driving Forces in Redundant Manipulators*", Proceedings of the IEEE International Conference on Robotics and Automation, pp 1701-1705.

Kazerounian, K., Wang, Z., [1988] "*Global Versus Local Optimization in Redundancy Resulution of Robotic Manipulators*", International Journal of Robotics Research, Vol. 7, No. 5, pp 3-12.

Kirk, D. E., [1970], "*Optimal Control Theory*", Englewood Cliffs, New Jersey, Prentice-Hall, Inc.

Klein, C. A., Huang, C. H., [1983], "*Review of Pseudo-Inverse Control for use with Kinematically Redundant Manipulators*", IEEE Transactions on System Man Cybernetics, Vol. 13, No. 3, pp 245-250.

Klein, C. A., Kee, Koh-Bon, [1989] "*The Nature of Drift in Pseudo-Inverse Control of Kinematically Redundant Manipulators*", IEEE Transactions on Robotics and Automation, Vol 5, No. 2, pp 231-234.

Liegeois, A., [1977], "*Automatic Supervisory Control of the Configuration and Behaviour of Multibody Mechanisms*", IEEE Transactions on System, Man and Cybernetics, Vol. SMC-7, No. 12, pp. 868-871.

Maciejewski, Klein, C. A., [1985], "*Obstacle Avoidance for Kinematically Redundant Manipulators in Dynamically Varying Environments*", International Journal of Robotics Research, Vol. 4, No. 3, pp. 109-117.

Martin, D. P., Baillieul, J., Hollerbach, J. M., [1989], "*Resolution of Kinematic Redundancy using Optimization Techniques*", IEEE Transactions on Robotics and Automation, Vol. 5, No. 4, pp 529-533

Nakamura, Y., Hanafusa, H., [1986], "*Control of Articulated robots with Redundancy*", Theory of Robots - Selected Papers from IFAC Symposium, Vienna, Austria, pp 15-22.

Nakamura, Y., Hanafusa, H., [1987], "*Optimal Redundancy Control of Robot Manipulators*", International Journal of Robotics Research, Vol. 6, No. 1, pp 32-42.

Nakamura, Y., Hanafusa, H., Yoshikawa, T., [1987], "*Task Priority based Redundancy Control of Robot Manipulators*", International Journal of Robotics Research, Vol. 6, No. 2, pp 3-15.

Nedeljkovic, N., [1981], "*New Algorithms for Unconstrained Nonlinear Optimal Control Problems*", IEEE Transactions on Automatic Control, Vol. AC-26, No. 4, pp 868-884.

Sage, A. P., White, C. C., [1978], "*Optimum Systems Control*", Englewood Cliffs, New Jersey, Prentice-Hall, Inc.

Sheraji, H., [1989], "*Configuration Control of Redundant Manipulators: Theory and Implementation*", IEEE Transactions on Robotics and Automation, Vol. 5, No. 4, pp 472-490.

Whitney, D. E., [1969], "*Resolved Motion Rate Control of Manipulators and Prostheses*", IEEE Transactions on Man Machine System, MMS-10, pp 47-53.

Whitney, D. E., [1972], "*The Mathematics of Coordinated Control of Prosthetic Arms and Manipulators*", Transactions of ASME, Journal of Dynamic Systems Measurement and Control, 94 (14), pp 303-309.

Won, J. H., Choi, B. W., Chung, M. J., [1993], "*A Unified Approach to the Inverse Kinematic Solution for a Redundant Manipulator*", Robotica, Vol. 11, Part 2, pp 159-165.

Yoshikawa, T., [1985(a)], "*Manipulability and Redundancy Control of Robotic Mechanisms*", Proceedings of IEEE International Conference on Robotics and Automation, pp 1004-1009.

Yoshikawa, T., [1985(b)], "*Manipulability of Robotic Mechanisms*", International Journal of Robotics Research, Vol. 4, No. 2, pp 3-9.

Yoshikawa, T., [1990], "*Foundations of Robotics: Analysis and Control*", The MIT Press, Cambridge, Massachusetts.